Interference of transcription on H-NS mediated repression in *Escherichia coli*

I n a u g u r a l - D i s s e r t a t i o n

zur

Erlangung des Doktorgrades

der Mathematisch-Naturwissenschaftlichen Fakultät

der Universität zu Köln

vorgelegt von

Aathmaja Anandhi Rangarajan

aus Arakkonam, Indien

Berichterstatter:	Prof. Dr. Karin Schnetz
(Gutachter)	Prof. Dr. Jürgen Dohmen
Tag der mündlichen Prüfung:	08.01.2018

“I am among those who think that science has great beauty. A scientist in his laboratory is not only a technician: he is also a child placed before natural phenomena which impress him like a fairy tale’’

Marie Curie

Contents

Zusammenfassung

Das hitzestabile Nukleoid-assoziierte Protein H-NS ist ein globaler Transkriptionsrepressor in *Escherichia coli* und anderen enterobakteriellen Spezies. H-NS bindet an AT-reiche DNA-Regionen und reprimiert Gene welche für verschiedene Stressantworten und Pathogenitätsdeterminanten kodieren und durch horizontalen Gentransfer erworben wurden. Die Repression der Transkription durch H-NS erfolgt durch die Bildung eines repressiven Nukleoproteinkomplexes durch DNA-Versteifen (stiffening) oder DNA-Brückenbildung (bridging). H-NS blockiert die Bindung der RNA-Polymerase an den Promotor oder setzt sie am Promotor fest. StpA, ist ein Paralog von H-NS, welches ähnlich wie H-NS wirkt und einen heteromeren Komplex mit H-NS bildet. Einige Gene werden durch H-NS und StpA reprimiert. Die Repression der Transkription durch H-NS kann durch die Bindung spezifischer Transkriptionsregulatoren oder durch Änderung der DNA-Struktur aufgehoben werden.

Die Transkriptionselongation und die Repression durch H-NS können möglicherweise interferieren. *In vitro* kann H-NS das Pausieren der RNA-Polymerase verstärken und die Rho-abhängige Termination fördern. *In vivo* ist die H-NS-DNA Bindung reduziert, wenn die Transkription durch Hemmung Rho-vermittelter Termination gesteigert wird.

In dieser Arbeit wurde die Wirkung der Transkriptionselongation auf H-NS- und H-NS/StpA-reprimierte Promotoren analysiert. Die Ergebnisse zeigen, dass die Elongation der Transkription über eine von H-NS- und H-NS/StpA-gebundene Promotor-DNA-Region (*bgl*, *proU*, *pdeL* und *appY*) hinweg die Repression der Promotoren vermindert. Zum Beispiel bewirkt eine in das bgl_{DRE} (*bgl* downstream regulatory element) hinein gerichtete Transkription die Derepression eines H-NS reprimierten Promoters $P3_{bgl}$ innerhalb des $bgl_{DRE.}$ Darüber hinaus verringert die Induktion eines stromaufwärts von *bgl* liegenden Operons (*pst-phoU*) die Repression der *bgl*-Promotoren durch H-NS/StpA. Zusätzlich wurde eine inverse Korrelation zwischen der Transkriptionsrate und H-NS-Repression beobachtet. Die Daten legen nahe, dass die transkribierende RNA-Polymerase in der Lage ist, den H-NS (und StpA) Komplex umzustrukturieren. Durch diese Umstrukturierung während der Transkription kommt es vermutlich zur Dislokation von H-NS (und StpA) von der DNA und damit zur verminderten Repression, während bei niedrigen Transkriptionsraten der H-NS-Repressionskomplex stabil ist. Dies impliziert die wechselseitige Interferenz zwischen Transkription und H-NS-Repression. Daher werden gering transkribierte AT-reiche Regionen

eher durch H-NS reprimiert werden, wohingegen eine effizient transkribierte Region die Bildung eines Repressionskomplexes nicht erlauben sollte. Im Kontext des Genoms kann das Durchlesen der Transkription von einem stromaufwärts gelegenen Locus, den H-NS-Komplex von stromabwärts gelegenen Genen verdrängen, und die Expression dieser Gene modifizieren.

Summary

The heat-stable nucleoid-associated protein H-NS is a global transcriptional repressor in *Escherichia coli* and other Enterobacterial species. H-NS binds to AT-rich DNA regions repressing several stress response genes, pathogenic genes, horizontally acquired DNA and is also indicated to play a role in genome organization. Transcriptional repression by H-NS is mediated by the formation of nucleoprotein complex that stiffens or bridges DNA. H-NS represses transcription at the level of initiation by excluding or trapping the RNA polymerase at promoters. StpA is a H-NS paralogue that presumably acts similarly as H-NS and forms heteromeric complex with H-NS and some genes are repressed by H-NS and StpA. H-NS mediated repression can be relieved by binding of gene specific transcription factors or by perturbations of DNA structure.

H-NS repression and transcription elongation may also interfere with each other. *In vitro*, H-NS enhances RNA polymerase pausing and promotes Rho-dependent termination. Complementarily, inhibition of Rho-mediated termination resulting in increased transcription reduced H-NS binding.

In this work, the effect of transcription elongation into H-NS and H-NS/StpA repressed promoters were analyzed. The results show that transcription elongation across the H-NS and H-NS/StpA bound DNA region of *bgl*, *proU*, *pdeL* and *appY* relieves the repression of promoter by H-NS and H-NS/StpA. For example, analysis of transcripts from bgl_{DRE} (*bgl* downstream regulatory element) revealed the presence of additional H-NS repressed promoter $P3_{bgl}$ which was de-repressed upon increase in transcription. Moreover, in the native context, transcription from upstream *pst-phoU* operon decreases H-NS/StpA repression of *bgl* promoters. Additionally, an inverse correlation between the transcription rate and H-NS repression was observed. The data suggest that the transcribing RNA polymerase is able to remodel the H-NS (and StpA) complex and/or dislodge H-NS (and StpA) from the DNA and thus relieve repression, while at low transcription rates the H-NS repression complex is stable. This implies mutual interference between transcription and H-NS repression. Poorly transcribed AT-rich regions are prone to be repressed by H-NS, whereas efficiently transcribed region do not allow the formation of repression complex. Furthermore, the transcriptional read-through from an upstream locus can concurrently dislodge the H-NS complex of downstream genes and modify their expression.

1. Introduction

Escherichia coli possess an approximately 5 Mb circular genome which has to be compacted several thousand folds to be accommodated within the dimensions of the cells. Concurrently, the genome must be available for processes including but not limited to replication, segregation and gene regulation. Nucleoid compaction in *E. coli* is aided by several nucleoid-associated proteins such as H-NS, HU, StpA and Fis. These proteins bind non-specifically across the genome, enabling wrapping, bending and bridging the DNA and many of them also acts as gene-regulators (Dillon & Dorman, 2010, Badrinarayanan *et al.*, 2015). H-NS (Heat-stable Nucleoid Structuring protein) is an abundant nucleoid-associated protein in *E. coli* and other *Enterobacteriaceae* which performs dual role in genome organization and transcriptional repression (Dorman, 2014a). Transcriptional repression by H-NS is enabled by the formation of nucleoprotein complex by bridging or stiffening DNA (Maurer *et al.*, 2009). H-NS represses transcription at the level of initiation by excluding the RNA polymerase or by trapping the RNA polymerase at the promoter (Grainger, 2016). H-NS repression at the level of transcription initiation can be relieved by specific transcription regulators (Stoebel *et al.*, 2008, Will *et al.*, 2015). However, whether H-NS also modulates later stages of transcription such as transcription elongation and termination has not been studied in detail. Conversely, the influence of transcription on H-NS repression has not been addressed yet. In this work, the interference of transcriptional elongation by RNA polymerase on H-NS repression was analyzed.

1.1 H-NS, global repressor in *E. coli*

H-NS is a pleiotropic regulator, which is highly conserved in Gammaproteobacteria (Tendeng & Bertin, 2003). H-NS plays a dual role in global transcriptional repression and genome organization (Dorman, 2004, Luijsterburg *et al.*, 2006, Dorman, 2014a). H-NS protein is highly abundant, present at around 20,000 molecules per genome equivalent and controls the expression of 5% of the genes in *E. coli* (Ali Azam *et al.*, 1999, Hommais *et al.*, 2001). H-NS binds non-specifically to any DNA sequence with higher AT-content (Navarre *et al.*, 2007). The T-A base step which forms the minor groove of the DNA is critical for H-NS binding (Gordon *et al.*, 2011). A poor consensus motif has been defined for high affinity H-NS binding (Lang *et al.*, 2007) (Figure 1C). H-NS first nucleates in AT-rich high affinity sites dispersed across the genome and subsequently polymerizes into the low affinity sites forming repressive nucleoprotein complex (Rimsky *et al.*, 2001, Kahramanoglou *et al.*, 2011, Bouffartigues *et al.*, 2007). Genome wide H-NS binding determined using Chromatin

Immunoprecipitation-on-chip (ChIP-on-chip) studies have revealed H-NS binding to ~ 350 loci spread across the *E. coli* genome (Lucchini *et al.*, 2006, Grainger *et al.*, 2006, Kahramanoglou *et al*., 2011). H-NS binds AT-rich DNA, a characteristic of xenogeneic DNA hence, H-NS plays a significant role in silencing horizontally acquired DNA including several virulence factors and pathogenicity islands (Navarre *et al*., 2007, Lucchini *et al*., 2006, Dorman, 2014b). H-NS also affects major DNA transactions such as conjugation, replication, transposition and recombination (Dorman, 2004, Dorman, 2014b, Helgesen *et al.*, 2016).

1.2 Regulation of the *hns* gene

Ths *hns* gene is regulated at the level of transcription and post-transcription. The *hns* gene is negatively autoregulated, with Fis antagonizing H-NS mediated repression (Falconi *et al.*, 1993, Falconi *et al.*, 1996). Iron regulator Fur and cold shock protein CspA also influences *hns* transcription (Brandi *et al.*, 1994, Troxell *et al.*, 2011). Moreover, auto repression of *hns* is exerted tightly when the replication fork is arrested, suggesting *hns* transcription is sensitive to the progression of cell cycle (Free & Dorman, 1995). Additionally H-NS expression is negatively at the post transcriptional level by DsrA (sRNA), which is induced upon stress (Brescia *et al.*, 2004).

1.3 Structure and binding modes of H-NS

H-NS is a 15 kDa protein consisting of 137 amino acids (Falconi *et al.*, 1988). It possess a N-terminal oligomerization domain with two dimerization interfaces, followed by a short linker domain and C-terminal DNA- binding domain (Esposito *et al.*, 2002, Grainger, 2016) (Figure 1A). The N-terminal domain (1-83 residues) consists of four α-helices (α1-α4) which permits self-association by 'head-to-head' and 'tail-to-tail' contacts, thus enabling the formation of higher order H-NS oligomers (Esposito *et al*., 2002, Arold *et al.*, 2010). The C-terminal domain (91-137 residues) consists of two β-sheets (β1 and β2), an α-helix (α5) and a 3_{10} helix which forms a hydrophobic core stabilizing the C-terminal domain (Gordon *et al*., 2011) (Figure 1A). Conserved residues '(Q/R)GR' in the C-terminal domain forms AT-hook motif in which the first (Q/R) and the last (R) side chain extend in opposite direction and docks into the AT-rich DNA minor groove (Gordon *et al*., 2011). H-NS thus binds to AT-rich DNA sequences forming repressive nucleoprotein complex. This nucleoprotein complex can bind to DNA in two modes, it can form linear complex by stiffening the DNA or form bridged complex by binding to two strands of DNA (Figure 1B) (Dame *et al.*, 2005, Maurer *et al*., 2009). However, the formation of stiffening or bridged complexes depends on the Mg^{2+}

concentration *in vitro*, with higher Mg^{2+} concentration favoring the bridged H-NS DNA complex (Liu *et al.*, 2010).

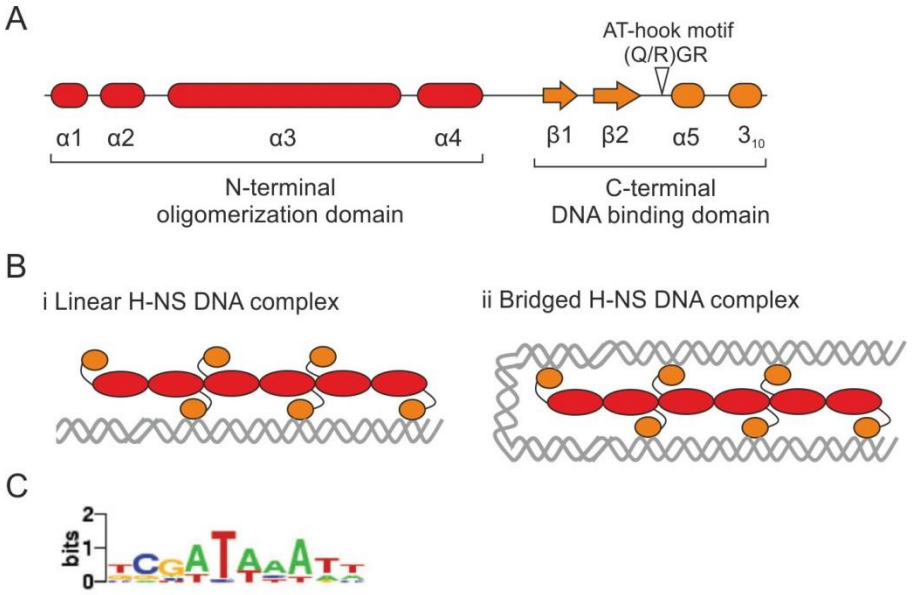

Figure 1: Domain organization and binding modes of H-NS. (A) Schematic illustration of structural components and domain organization of H-NS protein. The N-terminal oligomerization domain (red) consists of four α-helices (α1-α4) and the C-terminal DNA-binding domain (orange) which comprises of two β-sheets (β1 and β2), an α-helix (α5) and 3_{10} helix. The AT-hook motif consisting of residues (Q/R)GR is indicated (Arold *et al.*, 2010, Gordon *et al.*, 2011). (B) Schematic representation of binding modes of H-NS DNA complex. (i) In a linear H-NS DNA complex, H-NS binds to the adjacent DNA sites in linear arrangement and stiffens the DNA. (ii) In a bridged H-NS DNA complex, H-NS binds and bridges two strands of DNA. (C) Logo representation of experimentally determined H-NS binding motif taken from Lang *et al.*, 2007.

1.4 Mechanisms of repression and de-repression of H-NS at the level of transcription initiation

H-NS repression predominantly occurs by counteraction of transcription at the level of initiation. Several mechanisms have been described for H-NS repressing transcription initiation. H-NS occludes the RNA polymerase from binding, traps the RNA polymerase or directly interacts with RNA polymerase to modulate its activity at the promoter regions (Grainger, 2016). Occlusion of RNA polymerase is the most common mechanism by which H-NS represses transcription initiation (Figure 2A). As stated earlier, H-NS preferentially binds to AT-rich DNA binding regions which is also characteristic of promoter region, hence H-NS binding coincides with the binding of RNA polymerase (Grainger *et al.*, 2006, Panyukov & Ozoline, 2013, Singh *et al.*, 2014). Thus, binding of H-NS in the promoter regions occludes the RNA polymerase binding (Yoshida *et al.*, 1993). In some cases H-NS

forms a repressive loop by bridging distal H-NS binding sites in which RNA polymerase is trapped (Figure 2B). Trapping of RNA polymerase in such repressive loop has been shown for *rrnB* and *hdeAB* promoters (Dame *et al.*, 2002, Shin *et al.*, 2005). Further, H-NS can also directly interact with RNA polymerase and inhibit promoter escape by RNA polymerase activity (Figure 2C). In the Enteropathogenic *E. coli LEE5* promoter region, H-NS was shown to directly interact with the alpha-subunit of RNA polymerase and prevent RNA polymerase isomerization to form an open promoter complex (Shin *et al.*, 2012).

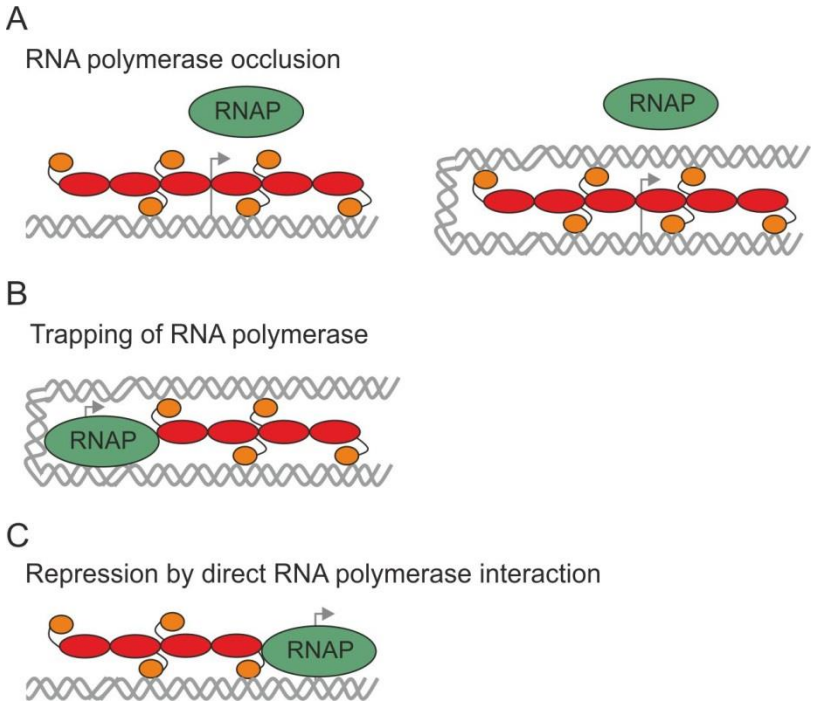

Figure 2: Mechanisms of H-NS repression at the level of transcription initiation. (A) RNA polymerase occlusion. H-NS complex can occlude binding of RNA polymerase to the promoter (arrow) in linear or bridged conformation to repress transcription (Yoshida *et al.*, 1993). (B) Trapping of RNA polymerase. H-NS can allow the formation of repression loops by bridging which may entrap the bound RNA polymerase and prevents translocation of RNA polymerase (Dame *et al.*, 2002, Shin *et al.*, 2005). (C) Repression by direct RNA polymerase interaction. H-NS can directly interact with alpha C-terminal domain of RNA polymerase and prevents isomerization of RNA polymerase at the promoter (Shin *et al.*, 2012).

In most of the cases studied, de-repression by H-NS at the level of transcription initiation is facilitated by trans-acting factors. These trans-acting factors can be canonical transcription factors which acts gene specifically or H-NS like proteins which disrupts the oligomerization state of H-NS and causes de-repression non-specifically. Gene-specific transcription factors competes with H-NS for binding sites and displaces H-NS or changes DNA topology to drive-

off H-NS binding (Navarre *et al*., 2007, Stoebel *et al*., 2008, Will *et al*., 2015, Winardhi *et al.*, 2015). Ler and SsrB were shown to displace H-NS from promoter region (Desai *et al.*, 2016, Winardhi *et al.*, 2014, Walthers *et al.*, 2011). Binding of VirB induces a conformational change which bends and remodels the DNA disrupting the H-NS DNA complex (Gao *et al.*, 2013). SlyA inhibits H-NS binding and alters the confirmation of DNA to enable initiation of transcription (Lithgow *et al.*, 2007). In *hdeAB* and *dps* promoter, DNA bending by σ^{70} associated RNA polymerase allows the formation of repression loop by H-NS, which is circumvented when σ^{38} associated RNA polymerase is bound (Shin *et al*., 2005, Grainger *et al.*, 2008). Truncated protein orthologs of H-NS interact with H-NS and alter the oligomerization of H-NS preventing the formation of a repressive complex. Proteins such as gp 5.5 from bacteriophage T7 and H-NST from Enteropathogenic *E. coli*, bind to the N-terminal region of H-NS thereby disrupting oligomerization by H-NS which is critical for silencing activity (Liu & Richardson, 1993, Williamson & Free, 2005, Levine *et al.*, 2014).

Apart from trans-acting factors environmental factors such as temperature and osmolarity can affect degree of curvature by increasing or decreasing bend angles in DNA, which eventually cause H-NS de-repression (Sinden *et al.*, 1998, Amit *et al.*, 2003, Prosseda *et al.*, 2004). In *virF* promoter, H-NS repression is favored at lower temperature whereas at higher temperature DNA bending is reduced which displaces H-NS (Di Martino *et al.*, 2016). Further, several pathogenic genes have been reported to be repressed by H-NS at lower temperature (25°C) which is alleviated at a higher temperature (37°C) (Trachman & Yasmin, 2004, Yang *et al.*, 2005, Ono *et al.*, 2005). Moreover, *in vitro* analysis has shown that DNA bridging complex formation is inhibited at 37°C (Kotlajich *et al.*, 2015). However, the mechanism by which these environmental factors influence H-NS activity and the DNA structure remains elusive.

1.5 H-NS modulating transcription elongation and vice-versa

In many gene loci H-NS binding extends several hundred base pairs into the coding region downstream of the promoter (Singh *et al*., 2014). H-NS complex bound in the coding region could encounter active elongation complex and can act as a road block for the transcribing RNA polymerase. H-NS road block can facilitate RNA polymerase pausing and termination of the elongation complex. On the other hand, transcribing RNA polymerase can also disrupt the bound H-NS complex. Thus, H-NS repression complex and the transcribing RNA polymerase could counteract each other (Landick *et al.*, 2015). Recent evidences suggest both the phenomena may occur.

H-NS could interfere with transcription elongation and enable Rho dependent transcription termination. The *bgl* downstream regulatory element (DRE) which extends up to 700 bp downstream of the *bgl* promoter is repressed by H-NS (Nagarajavel *et al.*, 2007). Efficient H-NS repression by bgl_{DRE} requires the Rho terminator protein (Dole *et al.*, 2004a). Furthermore, an *in vitro* transcription experiment with inverse bgl_{DRE} as template showed that bridged H-NS complex enhances RNA polymerase pausing thereby facilitating Rho dependent termination (Kotlajich *et al*., 2015). These results posit a model in which, H-NS complex increases the dwelling time of RNA polymerase at pause sites, enabling Rho to catch up with RNA polymerase to cause termination (Figure 3A). Moreover, genome wide ChIP analysis has also shown that H-NS binding sites coincide with Rho termination sites (Peters *et al.*, 2012). Thus, this phenomenon of H-NS enabled pausing and termination by Rho might be true for many genes that are bound by H-NS.

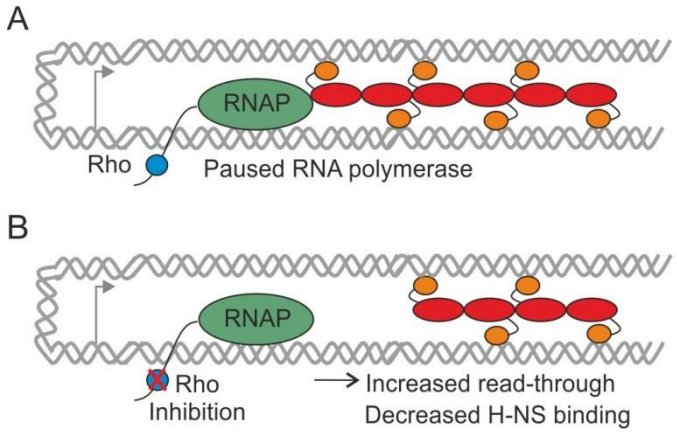

Figure 3: H-NS modulating transcription elongation and vice-versa (A) H-NS interfers with transcription elongation. Bridged H-NS complex causes pausing of RNA polymerase enabling Rho mediated termination (Kotlajich *et al*., 2015). (B) Transcription elongation decreases H-NS binding. Increased read-through of the RNA polymerase by inhibition of Rho or by other factors decreases H-NS binding. H-NS, RNA polymerase and Rho are depicted in red, green and blue circles respectively (Chandraprakash & Seshasayee, 2014).

While the H-NS complex could interfere with transcription, the converse phenomena of transcription elongation interferring with H-NS could also occur. Transcription elongation interfering with H-NS is supported by a genome wide ChIP experiment, showing decreased H-NS binding in several loci upon inhibition of transcription termination factor Rho. This decreased H-NS binding is probably due to increased read through of RNA polymerase into the H-NS bound region (Chandraprakash & Seshasayee, 2014) (Figure 3B). Moreover, single

molecule studies with optical tweezers have shown that a force of 7 pN is sufficient to dislodge DNA binding by a H-NS dimer, while the elongating RNA polymerase exerts a force of about 25 pN (Wang *et al.*, 1998, Dame *et al.*, 2006). These suggest that transcription elongation complex could dislodge H-NS complex, although experimental evidence for this is still lacking.

1.6 Association of H-NS with other proteins

H-NS does not act independently in all cases, but is often associated with other modulator proteins such as StpA and Hha. StpA is a paralogue of H-NS, which shares 59% sequence identity on amino acid level with H-NS (Zhang & Belfort, 1992). StpA also shares functional properties of H-NS by binding to AT-rich DNA sequences, forming bridged and linear filaments and silences gene expression (Sonnenfield *et al.*, 2001, Lim *et al.*, 2012, Muller *et al.*, 2006). In *hns* mutants StpA binds to high affinity H-NS binding sites and silences the expression of horizontally acquired genes that are otherwise bound by H-NS (Srinivasan *et al.*, 2013). Biochemical and genetic analysis have shown that StpA forms heteromeric complex with H-NS (Williams *et al.*, 1996, Johansson *et al.*, 2001). StpA levels are low in the exponential growth phase because *stpA* gene is repressed by H-NS at the transcriptional level and StpA is degraded post-translationally by Lon protease when it is not associated with H-NS (Zhang *et al.*, 1996, Johansson *et al.*, 2001). A subset of genes in *E. coli* is bound and regulated by H-NS and StpA (Uyar *et al.*, 2009, Srinivasan *et al.*, 2013). In *E. coli*, *bgl* and *leuO* promoters are regulated by both H-NS and StpA (Wolf *et al.*, 2006, Stratmann *et al.*, 2012). It is still an open question how StpA modulates the H-NS complex.

Hha is a small basic protein that interacts with the N-terminal domain of H-NS providing an additional DNA-binding surface as it is positively charged (Ali *et al.*, 2013, Wang *et al.*, 2014). The additional positive charge provided by Hha presumably stabilizes the H-NS-Hha DNA bridging complex (Ali *et al.*, 2013, van der Valk *et al.*, 2017) (Figure 4). Thus, H-NS/Hha complex presumably enhances H-NS repression by forming a stable bridged repressive complex at a subset of H-NS regulated genes. In *E. coli*, Hha binds to a subset of genes that is bound by H-NS in the coding part of the genome (Ueda *et al.*, 2013). In *Salmonella*, H-NS/Hha complex specifically affect horizontally acquired genes and does not affect housekeeping genes that are repressed by H-NS (Vivero *et al.*, 2008, Banos *et al.*, 2009). Very few genes have been reported in *E. coli* and *Salmonella* which are regulated by Hha/H-NS complex. The H-NS/Hha complex represses haemolysin (*hlyCABD*) operon, *htrA* gene and *esc* operon of *E. coli* O157:H7 (Nieto *et al.*, 2000, Forns *et al.*, 2005, Sharma &

Zuerner, 2004). In *Salmonella* H-NS/Hha complex negatively regulates Salmonella pathogenicity island SPI-2 (Coombes *et al.*, 2005, Silphaduang *et al.*, 2007).

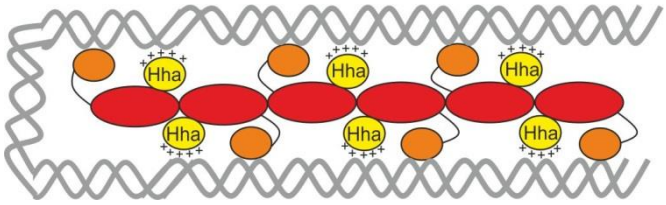

Figure 4: Binding of Hha protein in H-NS complex. Hha (yellow) binds to the N-terminal domain of H-NS (red) providing an additional contact surface with a positive charge for DNA binding. Figure adapted and modified from Ali *et al*., 2013.

1.7 Role of H-NS in genome organization

H-NS is indicated to be involved in nucleoid organization because of its bridging property which could bridge distance DNA fragments enabling DNA compaction (Luijsterburg *et al*., 2006, Dorman, 2014a). On a broad scale, *E. coli* genome is divided into four major macrodomains; Ori, Ter, Right, Left and two non-structured domains (Valens *et al.*, 2004). Superimposed on the macrodomain structure is the chromosome organization as looped microdomains which are highly dynamic. *E. coli* chromosome possess approximately 400 looped microdomains with 10-12 kb in length (Postow *et al.*, 2004, Deng *et al.*, 2005). The distribution of H-NS binding sites in the genome is consistent with the likely locations of the domain loop boundaries, and the bridging property of H-NS indicates the role of H-NS in stabilizing the microdomain loops (Noom *et al.*, 2007, Dillon & Dorman, 2010). Additionally, insights from atomic force microscopy and single molecule experiments revealed condensation of large domains by H-NS suggesting a role for DNA condensation by H-NS (Dame *et al.*, 2000, Ohniwa *et al.*, 2013, Thacker *et al.*, 2014). Moreover, H-NS, when overproduced lead to a highly condensed nucleoid which is lethal (Spurio *et al.*, 1992, McGovern *et al.*, 1994). The precise role of H-NS in the genome organization is yet to be determined.

1.8 H-NS repression of *proU* and *bgl* operons

The *bgl* and *proU* operon are classical genetic loci for studying H-NS repression. The *hns* gene was first discovered as a part of *bgl* and *proU* operon and was named as *osmZ* and *bglY*, whose mutation lead to high expression levels of *bgl* and *proU* operon, respectively. Further

studies on *proU* and *bgl* operon enabled to elucidate the mechanism of repression and de-repression of H-NS complex.

The *proU* operon encodes ABC transporter for the transport of compatible solutes such as proline and glycine betaine (Lucht & Bremer, 1994, Gowrishankar & Manna, 1996). The *proU* operon consists of genes *proV*, *proW* and *proX* (Figure 5A). The *proU* operon is osmoregulated, at low osmolarity conditions it is repressed by H-NS and at high osmolarity concentrations the expression is high (Gowrishankar, 1985, Ueguchi & Mizuno, 1993, Lucht *et al.*, 1994). The binding of H-NS complex to regulatory elements upstream and downstream of the promoter (URE and DRE) which is critical for nucleoprotein complex formation by H-NS was first elucidated in *proU* operon (Overdier & Csonka, 1992). Later, this binding of H-NS in upstream and downstream regulatory elements was discovered in other H-NS repressed genes such as *bgl* and *hilA* (Schnetz, 1995, Olekhnovich & Kadner, 2006). In *proU*, the nucleoprotein complex spreads from -230 nt upstream to +270 nt downstream of the promoter (Lucht *et al.*, 1994, Badaut *et al.*, 2002). H-NS binds to the 10 bp high affinity H-NS binding sites at +25 and +130 relative to the transcription start site and laterally oligomerizes along the DNA to the low affinity sites forming a repressive nucleoprotein complex (Bouffartigues *et al.*, 2007). Although, the H-NS repression is well studied in *proU*, the mechanism by which the H-NS repression is relieved at high osmolarity remains a puzzle.

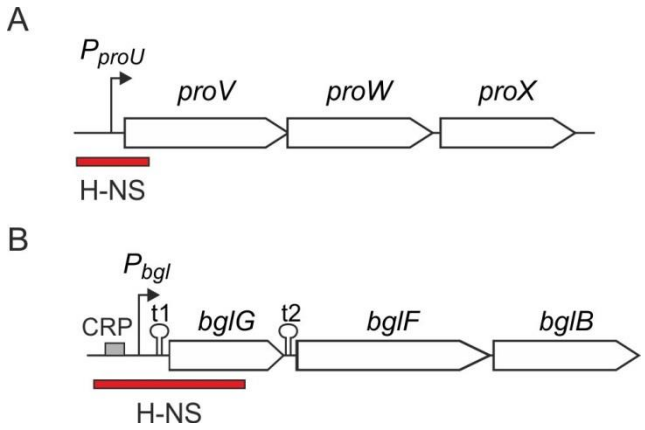

Figure 5: *E. coli proU* and *bgl* operons. (A) Schematic representation of *proU* operon consisting of P_{proU} promoter and *proV, proW, proX* genes. H-NS was shown to bind between -230 bp upstream to +270 bp downstream relative to the transcription start site from P_{proU} (Lucht *et al.*, 1994, Badaut *et al.*, 2002). (B) Schematic representation of *bgl* operon consisting of P_{proU} and structural genes *bglG, bglF, bglB*. Two rho independent terminators t1 and t2 are present flanking *bglG* gene. CRP binding site is shown in grey. H-NS was shown to bind *bgl* atleast between -160 bp upstream to +700 bp downstream of the transcription start site (Schnetz, 1995, Dole *et al.*, 2004b).

The *bgl* operon encodes for the proteins that enable uptake and utilization of aryl-β, D-glucosides. The *bgl* operon consists of *bglGFB* genes and two rho independent terminators flanking *bglG* gene (Mahadevan *et al.*, 1987, Schnetz *et al.*, 1987, Schnetz & Rak, 1988) (Figure 5B). H-NS binds to upstream and downstream regulatory region of *bgl* promoter causing 100-fold repression (Schnetz, 1995). It was first shown in *bgl* that any trans-acting factor binding to the upstream AT-rich regulatory region can relieve the H-NS repression. Interestingly, binding of classical repressors such as λ repressor and LacI were shown to increase the transcription from *bgl* promoter by relieving repression by H-NS complex (Caramel & Schnetz, 1998). Repression by H-NS can also be overcome by spontaneous mutations, including the deletion of an AT-rich regulatory region upstream of the promoter, integration of insertion elements, and point mutations in the CRP-binding site (Schnetz & Rak, 1992, Mukerji & Mahadevan, 1997). Additionally, repression of *bgl* can also be abrogated by transcriptional factors LeuO and BglJ-RcsB, both of which counteract H-NS repression of *bgl* upstream regulatory element (Madhusudan *et al.*, 2005, Salscheider *et al.*, 2014). Binding of H-NS at the *bgl* promoter with upstream and downstream elements, was shown to inhibit transcription initiation by targeting a step before open complex formation of RNA polymerase (Nagarajavel *et al.*, 2007). Furthermore, repression by H-NS via *bgl* downstream regulatory element requires transcription termination factor Rho (Dole *et al.*, 2004b). Recent *in vitro* evidences also show enhancement of Rho mediated termination in *bgl* downstream element under the conditions where H-NS forms bridged complex by enabling pausing of RNA polymerase (Kotlajich *et al.*, 2015). These suggest that H-NS complex could also modulate transcription elongation and termination in *bgl* and other genes.

1.9 Objectives of the thesis

H-NS, as a global repressor controls the expression of several pathogenic, stress response and horizontally acquired genes and it also plays a role in genome organization. Most of the studies to unravel the mechanism of H-NS repression and de-repression have been focussed at the level of transcription initiation. In most of the genes, H-NS represses transcription initiation by binding to the promoter region which is relieved by gene specific trans-acting factors (Stoebel *et al.*, 2008, Will *et al.*, 2015). In many genes H-NS binds several hundred bases downstream of promoter into the coding region (Singh *et al.*, 2014), suggesting a role of H-NS in affecting transcription elongation. Recent evidences also suggest that transcription elongation could interfere with H-NS repression and vice versa (Chandraprakash & Seshasayee, 2014, Landick *et al.*, 2015). In this thesis, I addressed the following objectives:

I studied whether transcription into H-NS and H-NS/StpA bound promoter regions relieves H-NS and H-NS/StpA mediated repression.

I addressed whether the change in processivity and speed of RNA polymerase modulates the H-NS repression complex.

I determined the role of Hha in H-NS/Hha complex and studied whether transcription into the H-NS/Hha complex modulates the repression.

I studied whether transcription into the H-NS repressed gene relieves its long range chromosomal interaction with other H-NS repressed genes.

2. Results

Recent studies on H-NS repression indicate that transcription elongation and H-NS repression could counteract each other (Landick *et al*., 2015, Chandraprakash & Seshasayee, 2014). However, the effect of transcription elongation on specific H-NS repressed genes has not been studied so far. In this work, I studied the effect of transcription elongation on selected H-NS repressed loci across the genome. Transcription directed towards the H-NS repressed gene was modulated by two inducible promoter modules. In one module, a constitutive P_{UV5} promoter was combined with conditional terminator (P_{UV5}*tR1*) and the second module is based on the arabinose inducible P_{BAD} promoter. These experimental modules were inserted upstream of H-NS repressed gene to direct transcription into the specific H-NS repressed locus. The effect of transcription elongation was tested on classical H-NS repressed loci bgl_{DRE} and *proU* and also other H-NS and H-NS/StpA loci such as *pdeL* and *appY*, respectively.

Additionally, I analyzed whether the speed of transcription is relevant for modulation of H-NS repression using slow moving and fast moving RNA polymerase mutants. Furthermore, the regulatory role of Hha protein, a modulator of the H-NS complex was analyzed at three loci (*yciF*, *ycdT*, *appY*) in order to determine whether transcription into H-NS/Hha repressed loci relieves their repression. Further, H-NS role has been implicated in nucleoid structuring and it was reported that H-NS repressed loci that are located at distant sites on the chromosome co-localize into foci (Wang *et al.*, 2011). Therefore, I wanted to test whether transcription into H-NS repressed gene in such foci affects their cellular localization.

2.1 Experimental system for modulating transcription elongation

In this work, I determined whether transcription elongation interferes with H-NS repression of selected genes. To modulate the rate of transcription elongation and to direct transcription into specific H-NS repressed locus, two different experimental systems were designed. The first system consisted of a constitutive variant of the P_{UV5} promoter and the conditional transcriptional terminator *tR1*. The second system consisted of an arabinose inducible P_{BAD} promoter.

In the P_{UV5}*tR1* system, the constitutive promoter P_{UV5} with terminator and anti-terminator complex (*λtR1*-N) from phage lambda is used to modulate transcription elongation. The *λtR1* is a Rho-dependent transcriptional terminator. The λN protein binds to *nutR* RNA region upstream of *λtR1*, and then further interacts with RNA polymerase along with host factors. Association of λN to the RNA polymerase increases the processivity and enables read-

through at transcriptional terminators (Nudler & Gottesman, 2002, Roberts *et al.*, 2008). To test whether the P_{UV5}*tR1* is suitable for modulating transcription elongation, P_{UV5}*tR1* module was fused to *lacZ* reporter and the expression was determined by β-galactosidase assay. As a control, P_{UV5} promoter is used without the *tR1* (Figure 6A). These modules, P_{UV5}*tR1-lacZ* (plasmid pKES269) and P_{UV5}-*lacZ* (plasmid pKES268) were previously constructed in the laboratory (Brühl, 2011). I inserted these constructs, in the chromosome, which allows the expression analysis in single copy. λN was provided plasmidically with low-medium copy plasmid pKES219 that possess λN gene under the control of the IPTG inducible P_{tac} promoter (Muhr, 2008). In strain carrying P_{UV5}*tR1-lacZ* construct, the β-galactosidase activity increases 6-fold in the presence of λN protein both in wild-type (110 units to 640 units) and *hns* mutant (145 units to 941 units) (Figure 6A, left). This 6-fold increase in the presence of λN protein was also observed in an independent P_{UV5}*tR1-lacZ* construct (plasmid pKEIB19) as determined previously in the laboratory (Bouchara, 2009). However, in the control P_{UV5}-*lacZ* construct no increase in expression was observed in the presence and absence of λN protein both in wild-type and *hns* mutant (Figure 6A, right). This 6-fold increase in P_{UV5}*tR1-lacZ* construct is in accordance with previously determined 80% termination at *λtR1* (Rosenberg *et al*., 1978). Moreover, this 6-fold increase is observed both in wild-type and *hns* mutant, indicating H-NS has no effect on P_{UV5}*tR1* module. Thus, the P_{UV5}*tR1* module with λN protein can be used to modulate transcription to be further directed into H-NS repressed genes.

The advantage of using the *λtR1*-N system is that the rate of transcription is modulated by λN which is a RNA binding protein, which will not influence DNA binding activity of H-NS. However, using this module the rate of transcription cannot be gradually increased. Moreover λN, along with other host factors modulates RNA polymerase and increases its processivity (Nudler & Gottesman, 2002, Roberts *et al*., 2008, Parks *et al.*, 2014). In order to circumvent these limitations, in the second system, the arabinose inducible P_{BAD} promoter was used to direct transcription into H-NS repressed regions. The P_{BAD} promoter is known to possess stochastic behavior in the presence of arabinose due to negative and positive feedback regulation of genes involved in arabinose utilization. Negative feedback is caused by fermentation of arabinose by intracellular enzymes encoded by *araBAD* (Siegele & Hu, 1997). Positive feedback is enabled by induction of transporters encoded by *araFGH* and *araE* enabling high uptake of arabinose (Siegele & Hu, 1997, Megerle *et al.*, 2008). In order to avoid this feedback regulation and to allow the gradual induction by arabinose, the *araC*-P_{BAD} module was chromosomally inserted in strain U65 which carries deletions of *araBAD* and *araFGH* and low affinity transporter *araE* under control of a constitutive promoter (P_{cp8})

(Kogenaru & Tans, 2014) (Breddermann & Schnetz, 2016). As the P_{BAD} promoter is under catabolite regulation, cultures were grown in tryptone medium lacking glucose. Gradual induction of *araC*-P_{BAD} construct with increasing concentration of arabinose was confirmed

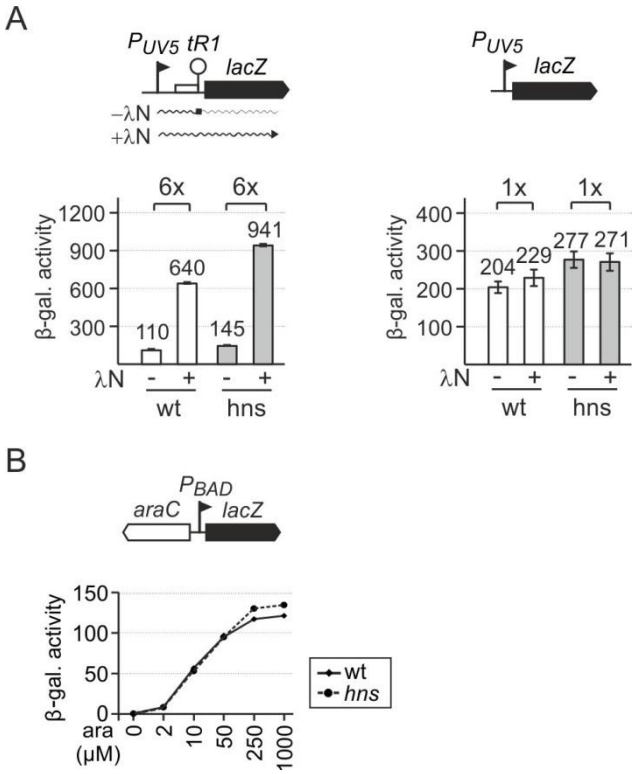

Figure 6: Experimental systems for modulating transcription elongation. (A) Schematic representation of P_{UV5} *lacZ* constructs with λ phage terminator tR1 and the control P_{UV5} *lacZ* construct integrated chromosomally. Expression levels given as β-galactosidase activities were determined in derivatives of Δ(*lacI-lacZYA*) strain S4084 (white bars) and isogenic *hns* mutant (grey bars). Anti-terminator protein λN was provided plasmidically using transformants of plasmid pKES219 (+λN). Cultures were inoculated from fresh overnight cultures in LB medium to OD_{600} 0.05 and grown to OD_{600} 0.5. For transformants with plasmid pKES219, the LB medium was supplemented with kanamycin and 1 mM IPTG. Error bars represent standard deviation of three biological replicates (B) Schematic representation of *araC*-P_{BAD}-*lacZ* construct integrated chromosomally. Expression level given as β-galactosidase activities were determined in derivative of Δ*ara*, Δ*lac* strain U65 and isogenic *hns* mutant. Cultures were inoculated from fresh overnight cultures in tryptone medium to an OD_{600} of 0.05 and induced with 0, 2, 10, 50, 250 and 1000 µM arabinose. The expression levels of wild-type and *hns* mutant are indicated as solid and dashed lines, respectively. Average values of three biological replicates are shown. Standard deviation is less than 20%. The following strains were used (A) T2316 (*attB::*P_{UV5}*-λtR1-lacZ*/pKES269), T2318 (*attB::*P_{UV5}*-λtR1-lacZ hns*/pKES269), T2261 (*attB::*P_{UV5}*-lacZ*/pKES268), T2279 (*attB::*P_{UV5}*-lacZ hns*/pKES268) (B) U115 (*attB::araC-*P_{BAD}*-lacZ*/pKEAR19), U127 (*attB::ara-*P_{BAD}*-lacZ hns*/pKEAR19).

using a *lacZ* reporter fusion (Figure 6B). As the concentration of arabinose increased, the level of β-galactosidase activity increased in both wild-type and in the *hns* mutant similarly (Figure 6B). This shows that H-NS has no effect on *araC*-P_{BAD} module. Taken together, these

data show that *araC-P_{BAD}* allows gradual increase of transcription with increasing concentrations of arabinose and *araC-P_{BAD}* module can be used to direct transcription into the H-NS repressed loci.

2.2 Transcription into H-NS repressed *proU* abrogates repression

The *proU* operon consisting of *proVWX* genes is osmoregulated. At low osmolarity, the *proU* promoter is repressed by H-NS, whereas the expression is strongly increased at high osmolarity conditions (Gowrishankar, 1985, Lucht *et al*., 1994, Ueguchi & Mizuno, 1993). H-NS binds to upstream and downstream regulatory elements of *proU* promoter enabling repression at low osmolarity (Dattananda *et al.*, 1991, Overdier & Csonka, 1992, Bouffartigues *et al*., 2007). To investigate whether transcription into the H-NS repressed *proU* promoter abrogates the repression by H-NS, I inserted the *P_{UV5}tR1* module upstream of the *proU* promoter region within the native chromosomal context using λ-Red mediated homologous recombination (Figure 7A). Transcription initiated at *P_{UV5}* promoter can be directed into the H-NS repressed *proU* promoter region by providing anti-termination protein λN. The relative expression levels of *proU* were determined using qRT-PCR using primer specific to *proV*, the first gene of the *proU* operon. For qRT-PCR, RNA was isolated from bacteria grown in LB at low osmolarity (10 mM NaCl) and high osmolarity (300 mM NaCl) conditions. The wild-type *proU* locus was used as control. In strain containing *P_{UV5}tR1-P_{proU}*, the relative expression level was tested in the absence and presence of λN provided plasmidically. The expression levels, given in arbitrary units were determined relative to the expression level of wild-type *proU* at high osmolarity (300 mM NaCl).

For wild-type *proU*, the relative expression level increased 500-fold from 0.22 at low osmolarity (10mM NaCl) to 100 at high osmolarity (300 mM NaCl) (Figure 7B). This 500-fold increase at high osmolarity is in accordance with the previously determined several hundred fold osmoregulation of *proU* operon (Gowrishankar, 1985, Dattananda *et al*., 1991). Similarly, osmoregulation of *P_{UV5} tR1-P_{proU}* was 600-fold in the absence of λN (Figure 2B, compare 0.25 and 154 units grown at 10 and 300 mM NaCl, respectively). This shows that the insertion of *P_{UV5}tR1* module does not affect *proU* osmoregulation. However, in the presence of λN protein, the relative expression of *P_{UV5}tR1-P_{proU}* increased from 0.25 to 22 at low osmolarity (10 mM NaCl) (Figure 7B, *P_{UV5}tR1-P_{proU}*). At high osmolarity, no difference in expression was observed in the presence and absence of λN protein (300 mM NaCl) (Figure 2B, compare expression levels 154 and 158, *P_{UV5}tR1-P_{proU}*). These data show that the

expression of P_{UV5}*tR1*-P_{proU} increases at low osmolarity (10 mM NaCl) upon expression of λN.

This increase in expression of P_{UV5}*tR1*-P_{proU} at low osmolarity might be due to the transcriptional read through from upstream P_{UV5}*tR1* promoter into the *proV* region. However, transcription directed from the upstream P_{UV5}*tR1* module might also de-repress the native *proU* promoter. In order to differentiate these possibilities, I performed 5'RACE analysis of RNA isolated from P_{UV5}*tR1*-P_{proU} grown at low osmolarity (10 mM NaCl) in the presence and absence of λN protein. For 5'RACE, primary transcripts were ligated to a RNA adapter and the transcription start site was determined by PCR using adapter specific and *proV* specific primer (Figure 7A, indicated by an arrow). In the absence of λN protein no products corresponding to P_{proU} and P_{UV5} promoter were observed (Figure 7C). However, in the presence of λN products corresponding to transcripts initiated at P_{UV5} and the P_{proU} promoters were detected (Figure 7C). These products were cloned and at least four clones of each were sequenced. The assemblies of the sequenced clones are shown in Figure 6C. In case of P_{UV5}, all the four clones mapped to the known transcription start site of P_{UV5} promoter. In case of P_{UV5} three out of four clones mapped to the known transcription start site of P_{proU} promoter and one clone mapped 3 bp upstream of the P_{proU} promoter. Taken together, these data suggest that transcription into the H-NS repressed *proU* promoter region de-represses P_{proU} promoter.

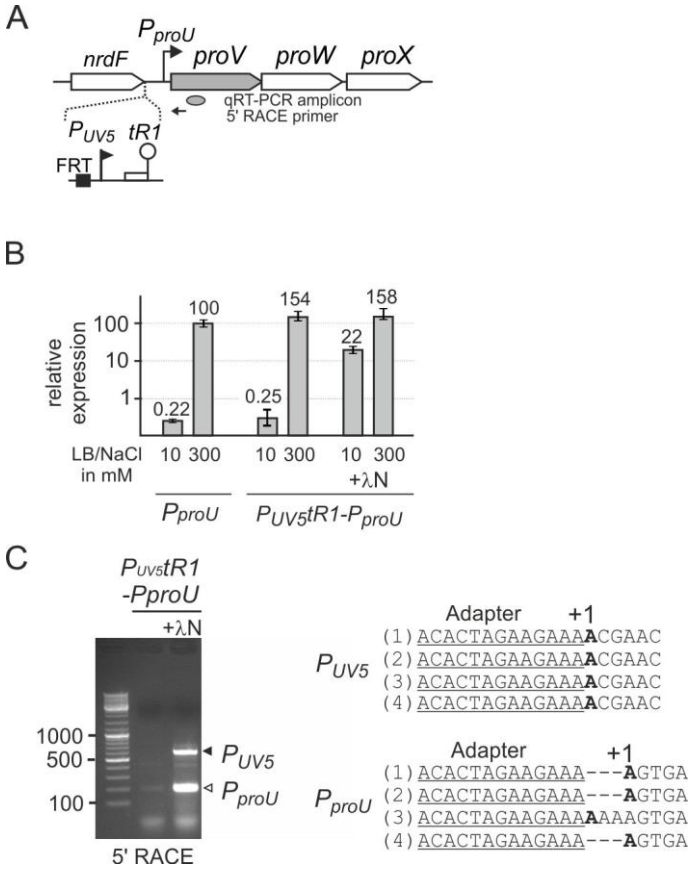

Figure 7: Transcription into the H-NS repressed *proU* promoter relieves its repression. (A) Schematic representation of *proU* operon consisting of P_{proU} promoter and *proV*, *proW*, *proX* genes. Allele P_{UV5}*tR1-PproU* was generated by insertion of P_{UV5}*tR1* cassette 292 bp upstream of *PproU* promoter. Arrow indicates the position of *proV* specific primer (S728) used for 5ˈRACE.The qRT-PCR amplicon is indicated. (B) Relative expression of *proU* operon (wild-type strain T1241) and allele P_{UV5}*tR1-PproU* (strain T1642) was determined by qRT-PCR. RNA was isolated from cells grown at low and high osmolarity, in LB with 10 mM and 300 mM NaCl, respectively. Anti-terminator protein λN was provided by transformation of strain T1642 with plasmid pKES219 (+λN), which was grown in medium supplemented with kanamycin and 1 mM IPTG. For qRT-PCR *proV* specific primers T520 and T521 were used. Ct values are normalized to expression levels of 16s rRNA determined by primers T528 and T529. The expression level (in arbitrary units) is determined relative to the expression level of wild-type *proV* (strain T1241) grown in high osmolarity (LB with 300 mM NaCl). Error bars represent standard deviation of three biological replicates. (C) Mapping of the 5ˈend of the transcript by 5ˈRACE of P_{UV5}*tR1-PproU* (strain T1642) grown in LB medium with 10 mM NaCl. Adapter specific primer OA9 and *proV* specific primer S728 were used for PCR amplification. PCR was done for 30 cycles. 5ˈRACE products marked in black and white triangles were cloned and at least four clones of each were sequenced. The assemblies of the sequenced clone are shown. Transcription start sites (+1) are marked in bold and the RNA adapter is underlined. 5ˈend of the transcript mapped to known transcription start site (+1) of P_{UV5} in 4 out of 4 clones and P_{proU} in 3 out of 4 clones.

2.3 De-repression of *proU* is directly proportional to the transcription rate

My above results suggest that transcription into the H-NS repressed *proU* promoter region de-represses the P_{proU} promoter. In order to determine the correlation between the transcription rate and de-repression of P_{proU} promoter, I inserted the *araC*-P_{BAD} cassette upstream of the *proU* promoter region in the native chromosomal context (Figure 8A). The *araC*-P_{BAD} module allows increasing the transcription rate gradually by inducing with increasing concentration of arabinose (0, 0.01, 0.05, 0.26, 1.3 mM). The strain containing *araC*-P_{BAD}-P_{proU} was grown in low osmolarity medium, under which P_{proU} is repressed by H-NS (10 mM NaCl). The expression levels were determined using primer pairs that map upstream and downstream of P_{proU} by qRT-PCR. The upstream primer pair measures the transcripts directed by P_{BAD} promoter and the downstream primer pair measures the transcripts in the *proV* region directed by P_{BAD} and P_{proU} (Figure 8A). As expected, the transcript directed from P_{BAD} promoter, increased with the increase in concentration of arabinose (Figure 8B, dashed line). Moreover, the level of *proV*, measured by downstream primers pair also increased with the increase in concentration of arabinose (Figure 8B, solid line). Additionally, the ratio between the transcription rate and the *proV* expression, measured by the upstream and downstream primer pairs respectively, was calculated to be constant across different arabinose concentrations (Figure 8B, grey line). This result shows that increasing the transcription rate from P_{BAD} increases the expression of *proV* at low osmolarity and the ratio of transcripts between upstream and downstream of P_{proU} is constant.

To differentiate between the read through from P_{BAD} promoter and P_{proU}, 5' RACE analysis was performed using *proV* specific primer (Figure 8A, indicated by arrow). As a control, wild-type *proU* was grown in LB at low and high osmolarity medium (10 and 300 mM NaCl). In wild-type *proU*, no product corresponding to P_{proU} was observed at 10 mM NaCl, whereas P_{proU} was detected at 300 mM NaCl (Figure 8C). In *araC*-P_{BAD}-P_{proU}, to determine the transcripts directed from P_{BAD} and P_{proU}, RNA was isolated from bacteria grown at low osmolarity medium (10 mM NaCl) with increasing concentrations of arabinose (0, 0.01, 0.05, 0.26, 1.3 mM). In *araC*-P_{BAD}-P_{proU}, the amount of 5'RACE product corresponding to P_{BAD} promoter increased with the increase in concentration of arabinose (Figure 8C). Additionally, with the induction of $P_{BAD,}$ a P_{proU} specific 5'RACE product was apparent and its amount increased similar to the level of induction of P_{BAD} (Figure 8C). These data validate the finding that transcription into H-NS repressed *proU* promoter region de-represses P_{proU} and the transcription rate is proportional to the de-repression.

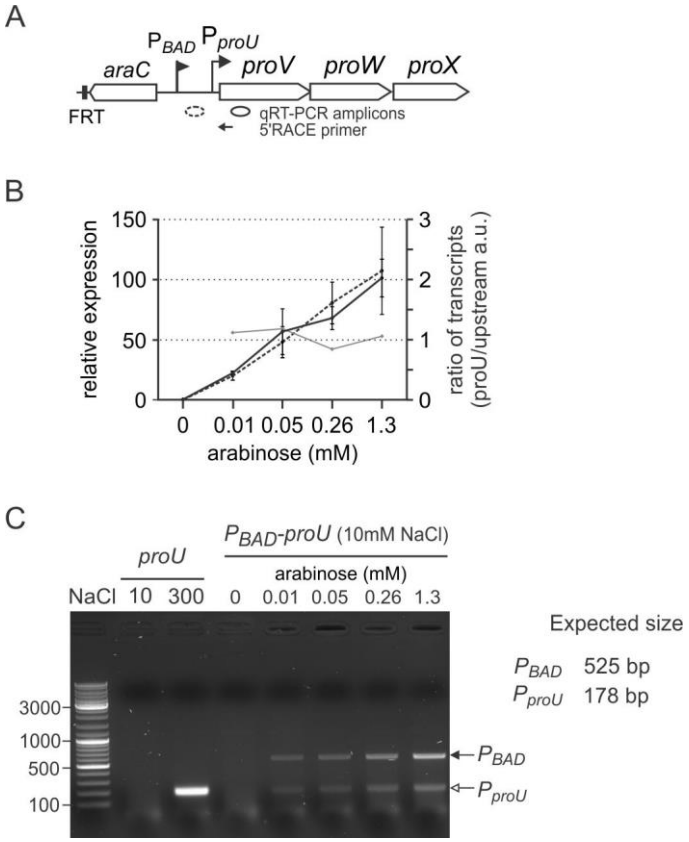

Figure 8: De-repression of P_{proU} is directly proportional to rate of transcription into the promoter region. (A) Schematic representation of the allele *araC*-P_{BAD}-P_{proU} which was generated by inserting *araC* P_{BAD} cassette 282 bp upstream of P_{proU} promoter. Arrow indicates the position of *proV* specific primer used for 5'RACE. qRT-PCR amplicons upstream and downstream of P_{proU} are indicated. (B) Expression levels were determined by qRT-PCR in allele *araC*-P_{BAD}-P_{proU} (strain U86). RNA was isolated from cells grown in LB medium at low osmolarity (10 mM NaCl) and induced with 0, 0.01, 0.05, 0.26 and 1.3 mM arabinose in exponential culture. Transcript levels upstream of P_{proU} (dashed line) were determined with primers OA94 and OA95 and transcript levels downstream of P_{proU} (solid line) were determined with T520 and T521. Ct values are normalized to the expression levels of 16S rRNA determined with primers T528 and T529. The expression levels (in arbitrary units) are determined relative to the expression level of cells grown with 1.3 mM arabinose. The grey line indicates the ratio of transcripts between downstream and upstream regions of P_{proU}. Error bars represent standard deviation of three biological replicates. (C) 5' RACE analysis was done using *proU* specific primer S728 in wild-type (strain U65) grown in LB with 10 mM and 300 mM NaCl and *araC*-P_{BAD}-P_{proU} (strain U86) grown in LB with 10 mM NaCl induced with 0, 0.01, 0.05, 0.26 and 1.3 mM arabinose. Bands corresponding to P_{BAD} and P_{proU} are indicated by closed and open arrow, respectively. PCR was done for 30 cycles.

2.4 Transcription into H-NS and H-NS/StpA repressed *pdeL* and *appY* abrogates repression

StpA is a paralogue of H-NS protein which forms heteromeric complexes with H-NS (Zhang *et al*., 1996, Johansson *et al*., 2001). I wanted to determine whether transcription into other H-NS and H-NS/StpA repressed genes abrogates repression similar to *proU*. In order to study this, *pdeL* and *appY* were chosen which were found to be bound by H-NS and H-NS/StpA, respectively, in a ChIP-Microarray (Uyar *et al*., 2009). The *pdeL* gene encodes for cyclic-di-GMP phosphodiesterase and transcriptional regulator (Schmidt *et al.*, 2005, Sundriyal *et al.*, 2014). The promoter of *pdeL* is repressed 15-fold by H-NS (Yilmaz, 2014). The *appY* gene encodes for an AraC type transcriptional regulator which is induced during anaerobiosis, phosphate starvation and stationary phase (Brondsted & Atlung, 1996, Atlung & Brondsted, 1994). The promoter of *appY* gene is repressed by H-NS and bound by H-NS and StpA (Atlung *et al.*, 1996, Uyar *et al*., 2009).

In order to test whether transcription into *pdeL* abrogates repression, I inserted the P_{UV5}*tR1* module upstream of *pdeL* promoter region at the native chromosomal locus (Figure 9A, left). The relative expression levels of wild-type *pdeL* and P_{UV5}*tR1-*P_{pdeL} were determined by qRT-PCR using *pdeL* specific primers. For wild-type *pdeL*, the relative expression increased from 5 units in the wild-type to 111 units in the *hns* mutant (Figure 9B left, P_{pdeL}). This result shows a 22-fold H-NS repression of P_{pdeL}. Next, the relative expression level of P_{UV5}*tR1-*P_{pdeL} was tested in wild-type and *hns* background in the presence and absence of λN protein. In the absence of λN, P_{UV5}*tR1-*P_{pdeL} was repressed 44-fold by H-NS (Figure 9B left, compare expression levels 1.5 and 66 in P_{UV5}*tR1-*P_{pdeL}). However, in the presence of λN protein, the relative expression increased from to 145 units in wild-type and to 180 units in *hns* mutant (Figure 9B left, P_{UV5}*tR1-*P_{pdeL}). These data show that the expression of P_{UV5}*tR1-*P_{pdeL} increases upon increasing the transcription elongation by λN. To distinguish read-through from the upstream P_{UV5} promoter and de-repression of P_{pdeL}, 5ˈRACE analysis was performed with primer specific to *pdeL*. As control, 5ˈRACE product of the native *pdeL* locus was analyzed in wild-type and *hns* mutant. No product corresponding to P_{pdeL} was observed for RNA isolated from wild-type, but a product corresponding to P_{pdeL} transcript was observed for RNA isolated from *hns* mutant (Figure 9C, left, P_{pdeL}). In case of P_{UV5}*tR1-*P_{pdeL}, in the absence of λN protein, no product corresponding to P_{UV5} and P_{pdeL} transcripts were observed. However, in the presence of λN protein, bands corresponding to P_{UV5} and P_{pdeL} were detected (Figure 9C, left, P_{UV5}*tR1-*P_{pdeL}). Cloning and sequencing of these bands showed that the

product of P_{UV5} mapped to the known transcription start site of P_{UV5} and the band corresponding to P_{pdeL} mapped to 4 nucleotides downstream of the previously predicted P_{pdeL} transcription start site (Shimada *et al.*, 2005).The mapped transcription start site of P_{pdeL} possesses a typical -10 region (TATAAT) which is the characteristic of most of the promoters in *E. coli* (Figure 9C). This indicates that the newly mapped transcription start site represents the actual transcription start site of P_{pdeL}. Taken together, these data suggest that the transcription into the *pdeL* promoter region counteracts its repression by H-NS.

Next, I studied whether transcription into *appY* abrogates its repression. For this, I inserted the P_{UV5}*tR1* module upstream of the *appY* promoter region in chromosomal context (Figure 9A, right). The relative expression levels were determined in wild-type, *hns* and *hns stpA* background, by qRT-PCR using primers mapping in *appY* gene. In wild-type background, P_{appY} is repressed 75 fold by H-NS (Figure 9B right, compare expression levels 0.08 and 6 in P_{appY}) and 1250 fold by H-NS/StpA (Figure 9B right, compare expression levels 0.08. and 100 in P_{appY}). This shows that *appY* promoter is strongly repressed by H-NS/StpA heteromeric complex. Next, the P_{UV5}*tR1*-P_{appY} expression was tested in wild-type, *hns*, and *hns stpA* background in the presence and absence of λN protein. In the presence of λN protein, the relative expression increased from 0.11 to 10 in wild-type (Figure 9B right, P_{UV5}tR1-P_{appY}). In *hns* mutant, the relative expression level increased from 9 to 46 units (Figure 9B right, P_{UV5}tR1-P_{appY}) and in *hns stpA* mutant the expression level remained the same (Figure 9B right, compare expression levels 116 and 109 in P_{UV5}tR1-P_{appY}). These data suggest that the relative expression level of P_{UV5}*tR1*-P_{appY} increases when transcription is directed into P_{appY} by λN. In order to differentiate between the read-through from upstream P_{UV5} promoter and de-repression of P_{appY} promoter, 5'RACE was performed. As control, RNA isolated from wild-type, *hns* and *hns stpA* background were used. In wild-type, P_{appY} promoter is strongly repressed by StpA and weakly by H-NS, as the products corresponding to P_{appY} were observed in *hns stpA* mutant, while they were weak in *hns* mutant, and not detected in wild-type (Figure 9C right, P_{appY}). Likewise, for P_{UV5}*tR1*-P_{appY} in the absence of λN protein, the products corresponding to P_{appY} was seen weakly in *hns* and strongly in *hns stpA* mutant. However, in the presence of λN protein, in P_{UV5}*tR1*-P_{appY} the bands corresponding to P_{UV5} and P_{appY} transcripts were detected in wild-type and it was also apparent in *hns* and *hns stpA* mutant background (Figure 9C right, P_{UV5}tR1-P_{appY}). Since the transcription start site of P_{appY} is unknown, the P_{appY} specific transcripts ($P_{appY\text{-}1}$ and *appY-2*) from *hns stpA* mutant were cloned and sequenced. Products corresponding to $P_{appY\text{-}1}$ transcripts mapped to 101 bp upstream of the translational start site of *appY* preceded by an ideal -10 region. Products corresponding to

appY-2 transcripts mapped within *appY* gene, 7 bp downstream of translation start site (Figure 9C, $P_{appY\text{-}1}$ and *appY-2*). Since all the transcripts analyzed are from TAP (Tobacco acid pyrophosphatase) treated samples, processed and the primary transcript could not be differentiated. Therefore, it remains to be analyzed whether *appY-2* is a processed or primary transcript. For P_{UV5}*tR1*-P_{appY}, cloning and sequencing of the band corresponding to P_{UV5} mapped to the known transcription start site of P_{UV5}, and the bands corresponding to P_{appY} transcripts mapped to $P_{appY\text{-}1}$ and *appY-2* transcripts. Collectively, these data suggest that the transcription into *appY* promoter region relieves repression by H-NS and StpA.

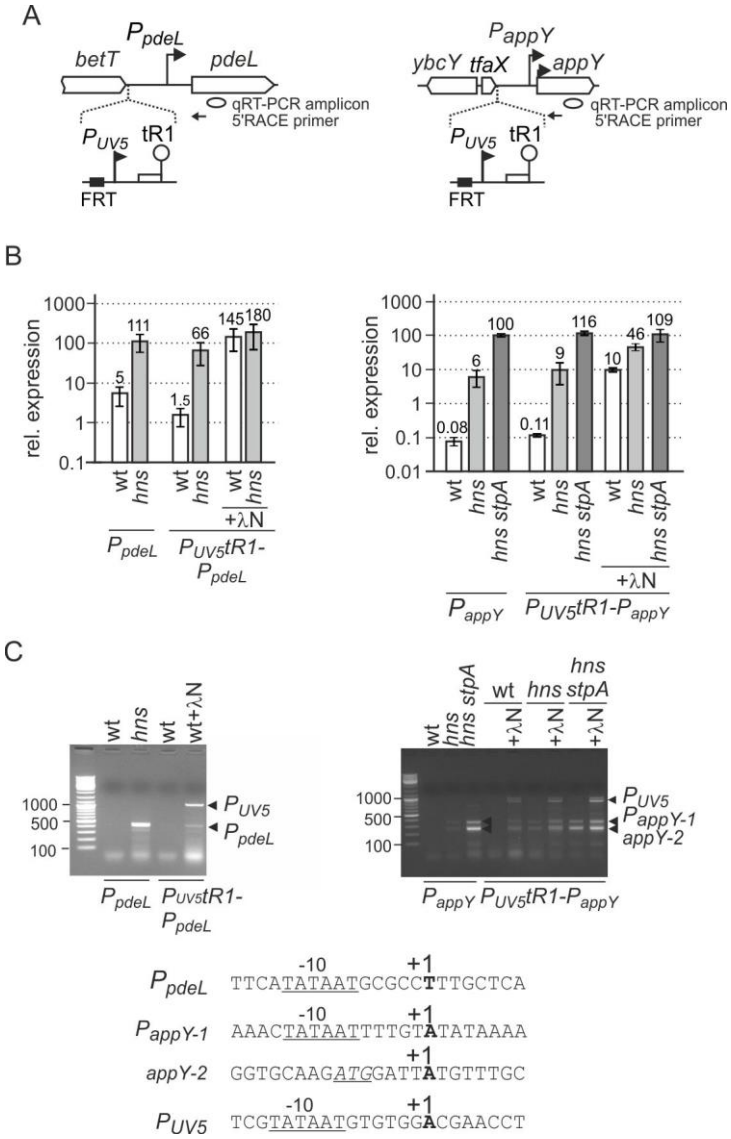

Figure 9: Transcription into *pdeL* and *appY* relieves repression by H-NS and H-NS/StpA respectively. (A) Schematic representation of P_{UV5}*tR1-pdeL* (left) and P_{UV5}*tR1-appY* (right) alleles in which P_{UV5} *tR1* cassette was inserted 838 bp and 463 bp upstream of *pdeL* and *appY* start codon respectively. Arrow indicates the position of primers used for 5'RACE. qRT-PCR amplicons are indicated. (B) Expression levels of *pdeL*, P_{UV5}*tR1-pdeL* (left) and expression levels of *appY*, P_{UV5}*tR1-pdeL* in wild-type (white bars), *hns* (grey bars) and *hns stpA* (dark grey bars) strain background, as indicated. The λN provided was provided by transformation with plasmid pKES219 (+λN), grown in a medium supplemented with kanamycin and 1 mM IPTG. For expression analyses of *pdeL* and *appY* wild-type strain T1241, *hns* mutant U72, and *hns stpA* mutant U73 were used, as indicated. Allele P_{UV5}*tR1-pdeL* was analyzed in strains T1647 (wt) and T1713 (*hns*). Allele P_{UV5}*tR1-appY* was analyzed in strains T1646 (wt), T1712 (*hns*), and T1949 (*hns stpA*). qRT-PCR was performed using *pdeL* specific primers T892, T893 and *appY* specific primers T910, T911 and the data were normalized to *rpoD* expression, determined with primers T247 and T248. For *pdeL*, the expression levels are determined relative to the expression level in *hns* mutant U72 (left). For *appY*, the expression levels are determined relative to the expression level in *hns stpA* mutant U73 (right). Error bars represent standard deviation of three biological replicates. (C) 5' RACE was performed with *pdeL* and *appY* specific primers T930 and OA24. PCR was done for 30 cycles. Bands indicated with triangles were cloned and at least four clones were sequenced. Mapped 5' mRNA ends (marked in bold) correspond to the known start site of the P_{UV5} promoter and the presumptive transcription start sites of P_{pdeL} and P_{appY} promoters each preceded by a -10 region (underlined). The mapped RNA 5' end labelled *appY-2* maps within the *appY* coding region and may correspond to a promoter or processed transcript.

2.5 Transcription into bgl_{DRE} relieves H-NS repression and activates transcription from H-NS repressed promoter $P3_{bgl}$ within bgl_{DRE}

The *bgl* operon encoding gene products for the uptake and utilization of aryl-β-glucosides is repressed ~100-fold by H-NS (Schnetz, 1995). Repression of *bgl* by H-NS requires upstream (URE) and downstream regulatory elements (DRE) (Schnetz, 1995, Dole *et al*., 2004a). The bgl_{DRE} region extends up to 700 bp downstream of the transcription start site of *bgl* and the presence of bgl_{DRE} itself causes 8-fold repression by H-NS (Nagarajavel *et al*., 2007). I wanted to determine whether transcription directed into the H-NS repressed bgl_{DRE} relieves H-NS repression. To modulate transcription, arabinose inducible *araC*-P_{BAD} module was used. This *araC*-P_{BAD} cassette was inserted upstream of H-NS bound bgl_{DRE} to direct transcription into the bgl_{DRE}. Additionally, *mVenus* gene which is presumably not bound by H-NS was used as a control.

Control constructs *araC*-P_{BAD}-*lacZ*, *araC*-P_{BAD}-*mVenus-lacZ* as well as the bgl_{DRE} containing constructs *araC*-P_{BAD}-bgl_{DRE}-*lacZ*, *araC*-P_{BAD}-*mVenus*-bgl_{DRE}-*lacZ* were integrated at the *attB* integration site in the chromosome (Figure 10A). The expression levels of these *lacZ* reported fusions were determined by β-galactosidase assay. First, I wanted to determine the expression levels of strains carrying control constructs P_{BAD}-*lacZ* and P_{BAD}-*mVenus-lacZ* with increasing concentrations of arabinose. For both reporter constructs, the expression increased with the increase in the arabinose concentrations, both in the wild-type and in the *hns* mutant background (Figure 10B). These data show that H-NS has no effect on P_{BAD}-*lacZ* and P_{BAD}-*mVenus-lacZ* constructs. However, the absolute expression levels of P_{BAD}-*lacZ* reporter was10-fold lower than of P_{BAD}-*mVenus-lacZ* in both wild-type and *hns* mutant background (Figure 10B).

To elucidate the reason for this decreased expression level, I used m-fold to predict the mRNA secondary structure of P_{BAD}-*lacZ* (Zuker, 2003). For the prediction of mRNA secondary structure nucleotides from P_{BAD} +1 transcription start site to the eighth codon of *lacZ* was used. The predicted secondary structure of P_{BAD}-*lacZ* revealed a prominent stem-loop structure with ΔG of -18.60 (Figure 11C (i)). I further modified *araC*-P_{BAD}-*lacZ* which contains *Eco*RI, *Spe*I, *Xba*I sites and constructed P_{BAD}-$lacZ_{26}$ in which the *Spe*I site is deleted and the *Eco*RI and *Xba*I sites are combined (Figure 11A (ii)). The absolute expression level of P_{BAD}-$lacZ_{26}$ was ~2-fold decreased when compared to P_{BAD}-*lacZ* in both wild-type and *hns* mutant (Figure 11B (ii)). The predicted m-fold structure of P_{BAD}-$lacZ_{26}$ also contained stem-loop with ΔG of -16.10 (Figure 11C (ii)). Moreover, upon deletion of all the restriction sites,

in P_{BAD}-*lacZ*$_{27}$ construct, the absolute expression level increased 10-fold in both wild-type and *hns* mutant (Figure 11A (iii), Figure 11B (iii)). In accordance with the expression analysis, the predicted secondary structure possess ΔG of -13.10 (Figure 11C (iii)). It is evident from the secondary structures of P_{BAD}-*lacZ* alleles, that first few nucleotides of *lacZ* ORF with the nucleotides in the P_{BAD} transcription start site enabled the formation of stem-loop structure. Hence, in P_{BAD}-*lacZ*$_{28}$, silent mutations were made in the 2nd, 5th and 8th codon of *lacZ* (Figure 11A (iv)). The absolute expression level of P_{BAD}-*lacZ*$_{28}$ increased 100-fold when compared to the P_{BAD}-*lacZ* in both wild-type and *hns* mutant (compare Figure 11B, (i) and (iv)) and the predicted m-fold structure with ΔG of -13.10 (Figure 11C (iv)). Thus, the decrease in expression level of P_{BAD}-*lacZ* is due to the stem-loop structures formed in mRNA which affects the translation of the constructs.

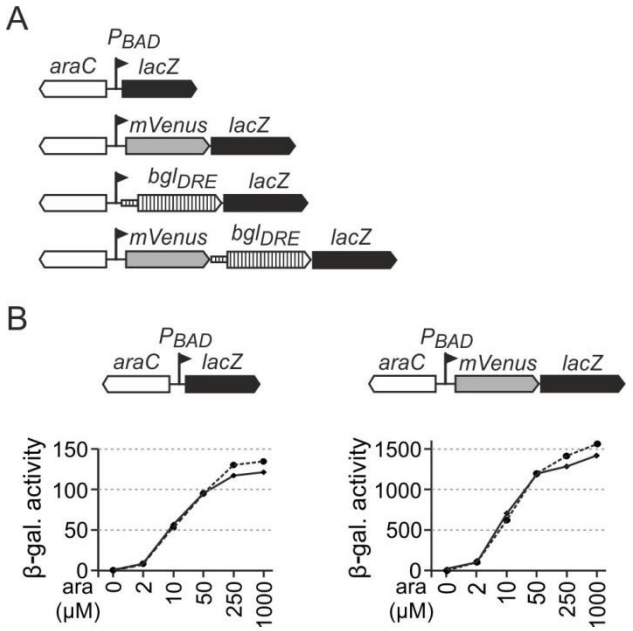

Fig 10: Expression analysis of *araC-P$_{BAD}$-lacZ* and *araC-P$_{BAD}$-mVenus-lacZ* constructs. (A) Schematic representation of *araC-P$_{BAD}$-lacZ* constructs that carry *mVenus* and H-NS repressed *bgl* downstream regulatory element (*bgl$_{DRE}$*), as indicated. (B) Expression level given as β-galactosidase activities were determined in derivatives of Δ*ara*, Δ*lac* strain U65 and isogenic *hns* mutant. Overnight cultures were inoculated in tryptone medium to an OD_{600} 0.05, induced with 0, 2, 10, 50, 250 and 1000 µM arabinose and grown to OD_{600} 0.5. Expression levels of wild-type and *hns* mutant were indicated in solid line and dashed line respectively. Expression level indicated is the average of three biological replicates. Standard deviation is less than 20%. The following strains were used (i) U115 (*attB::araC-P$_{BAD}$-lacZ*/pKEAR19), U127 (*attB::araC-P$_{BAD}$-lacZ hns*/pKEAR19) (ii) U123 (*attB::araC-P$_{BAD}$-mVenus-lacZ*/pKEAR22), U130 (*attB::araC-P$_{BAD}$-mVenus-lacZ hns*/pKEAR22).

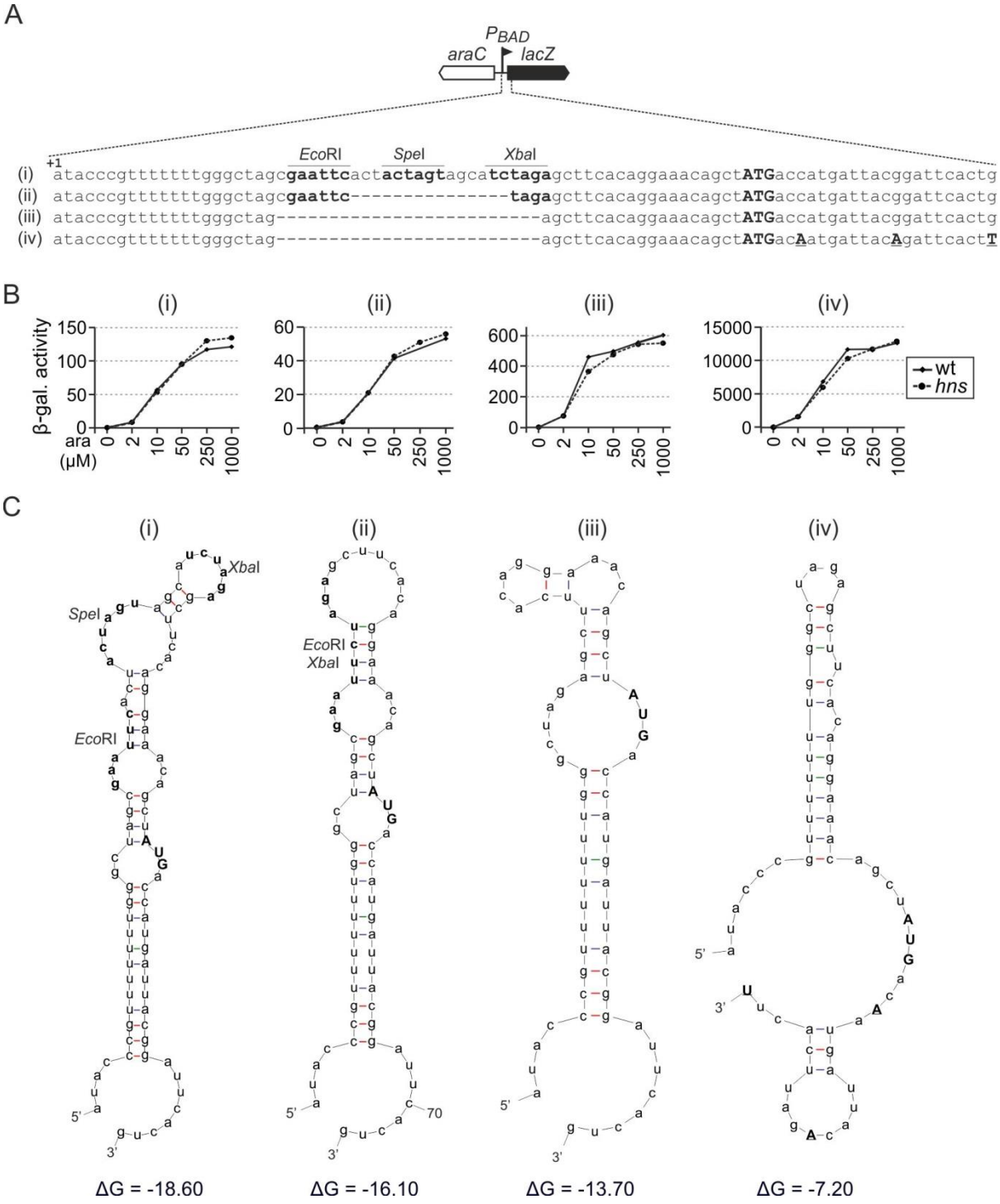

Figure 11: Expression analysis of *araC-P_{BAD}-lacZ* constructs. (A) Schematic representation of *araC-P_{BAD}-lacZ* constructs. Nucleotide sequence from transcription start (+1) of P_{BAD} promoter to the eighth codon of *lacZ* were indicated for all the constructs and the mutations are marked in bold and underlined. Restriction sites are indicated in the sequence. (i) *araC-P_{BAD}-lacZ*, (ii) *araC-P_{BAD}-lacZ$_{26}$*, (iii) *araC-P_{BAD}-lacZ$_{27}$*, (iv) *araC-P_{BAD}-lacZ$_{28}$*. (B) Expression level given as β-galactosidase activities were determined in derivatives of Δ*ara*, Δ*lac* strain U65 and isogenic *hns* mutant. Overnight cultures were inoculated in tryptone medium to an OD_{600} 0.05, induced with 0, 2, 10, 50, 250 and 1000 µM arabinose and grown to OD_{600} 0.5. The expression levels of wild-type and *hns* mutant were indicated in solid line and dashed line respectively. Expression level indicated is the average of three biological replicates. Standard deviation is less than 20%. (C) Secondary mRNA structures of *araC-P_{BAD}-lacZ*

constructs predicted using *mfold* software (Zuker, 2003). The predicted structure contains sequence from (+1) transcription start site of P_{BAD} promoter until eighth codon in *lacZ* ORF. The restriction sites are marked in bold. Translation start (AUG) is given in bold capital letters. Predicted ΔG values are given. The following strains were used (i) U115 (*attB::araC-*P_{BAD}*-lacZ/*pKEAR19), U127 (*attB::araC-*P_{BAD}*-lacZ hns/*pKEAR19) (ii) U134 (*attB::araC-*P_{BAD}*-*$lacZ_{26}$*/*pKEAR26), U138 (*attB::araC-*P_{BAD}*-*$lacZ_{26}$ *hns/*pKEAR26) (iii) U141 (*attB::araC-*P_{BAD}*-*$lacZ_{27}$*/*pKEAR27), U145 (*attB::araC-*P_{BAD}*-*$lacZ_{27}$ *hns/*pKEAR27) (iv) U142 (*attB::araC-*P_{BAD}*-*$lacZ_{28}$*/*pKEAR28), U146 (*attB::araC-*P_{BAD}*-*$lacZ_{28}$ *hns/*pKEAR28).

Next, I wanted to test whether H-NS repression via bgl_{DRE} is relieved by transcription from the upstream P_{BAD} promoter. In order to study the effect of transcription on bgl_{DRE}, control constructs with P_{BAD}-$lacZ_{28}$, P_{BAD}-*mVenus-lacZ* and constructs containing bgl_{DRE}, P_{BAD}-bgl_{DRE}-*lacZ* and P_{BAD}-*mVenus*-bgl_{DRE}-*lacZ* were integrated in the chromosome (Figure 12A). The expression levels of these *lacZ* reporter fusions were determined by β-galatosidase assays. In the control constructs, P_{BAD}-$lacZ_{28}$ and P_{BAD}-*mVenus-lacZ,* the expression increased with the increase in the arabinose concentration in both wild-type and *hns* mutant background. However, the absolute expression level of P_{BAD}-*mVenus*-bgl_{DRE}-*lacZ* was ~10 fold lower than of P_{BAD}-$lacZ_{28}$ (Figure 12B, compare P_{BAD} and P_{BAD}-*mVenus*). Expression of P_{BAD}-bgl_{DRE}-*lacZ,* in wild-type, was low at 0 µM arabinose and increased with increasing arabinose concentration. However, in the *hns* mutant background, expression was high at 0 µM and further increased with increase in arabinose concentration (Figure 12B). Likewise expression of P_{BAD}-*mVenus*-bgl_{DRE}-*lacZ*, in wild-type, also increased with the increase in the arabinose concentration, but possessed ~10 fold lower expression when compared to P_{BAD}-bgl_{DRE}-*lacZ* from 10 µM to 1000 µM arabinose concentrations. Expression of P_{BAD}-*mVenus*-bgl_{DRE}-*lacZ,* in *hns* mutant background, was high at 0 µM and increased at higher arabinose concentrations (10 µM to 1000 µM) (Figure 12B). However, the expression of P_{BAD}-*mVenus*-bgl_{DRE}-*lacZ* was ~10 fold lower when compared to P_{BAD}-bgl_{DRE}-*lacZ* from 10 µM to 1000 µM arabinose concentrations (Figure 12B, compare P_{BAD}-bgl_{DRE}-*lacZ* and P_{BAD}-*mVenus*-bgl_{DRE}-*lacZ*). These data show that upon induction of P_{BAD}, the expression of bgl_{DRE} increase and constructs with *mVenus* have lower expression compared with isogenic constructs without *mVenus*.

Since the *mVenus* constructs have ~10 fold lower expressions in both wild-type and *hns* mutant background compared to the isogenic construct without *mVenus*, the secondary structure formed by the *mVenus* mRNA was predicted using m-fold software. The predicted secondary structure of the *mVenus* mRNA shows a strong stem-loop structure with high ΔG of -16.30 (Figure 13). Thus, this stem-loop structure of *mVenus* mRNA may inhibit translation of *mVenus* constructs. Interestingly, in P_{BAD}-bgl_{DRE}-*lacZ and* P_{BAD}-*mVenus*-bgl_{DRE}-

lacZ even without induction of P_{BAD} at 0 µM arabinose, high expression was observed in *hns* mutant (Figure 12B, P_{BAD} bgl_{DRE} and P_{BAD} *mVenus* bgl_{DRE}). This indicates the presence of an H-NS repressed internal promoter within bgl_{DRE}.

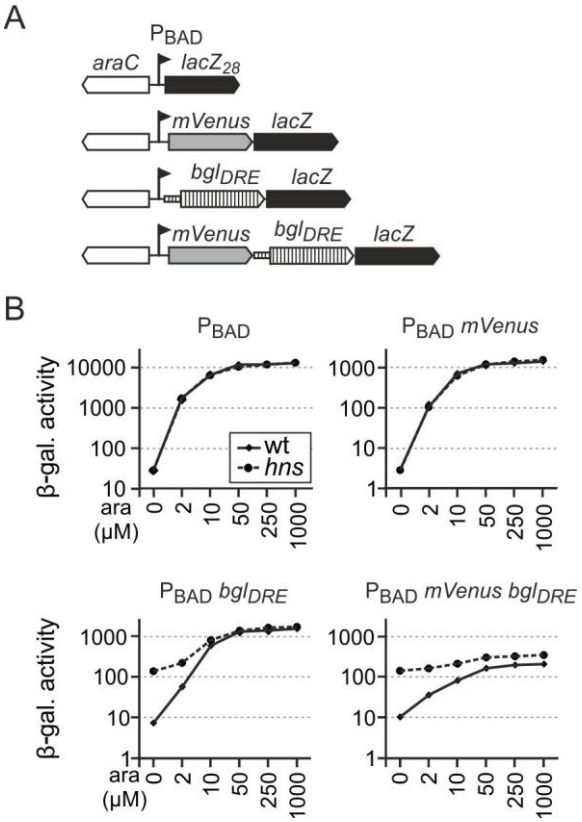

Figure 12: Transcription from upstream P_{BAD} promoter decreases H-NS repression of bgl_{DRE}. (A) Schematic representation of *araC*-P_{BAD}-*lacZ* constructs that carry *mVenus* and the H-NS repressed *bgl* downstream regulatory element (bgl_{DRE}), as indicated. (B) Expression level given as β-galactosidase activities were determined in derivatives of Δ*ara*, Δ*lac* strain U65 and isogenic *hns* mutant. Overnight cultures were inoculated in tryptone medium to an OD_{600} 0.05, induced with 0, 2, 10, 50, 250 and 1000 µM arabinose and grown to OD_{600} 0.5. The expression levels of wild-type and *hns* mutant were indicated in solid line and dashed line respectively. Expression level indicated is the average of three biological replicates. Standard deviation is less than 20%. The following strains were used (i) U142 (*attB::araC-*P_{BAD}*-lacZ*/pKEAR28), U146 (*attB::araC-*P_{BAD}*-lacZ hns*/pKEAR28) (ii) U123 (*attB::araC-*P_{BAD}*-mVenus-lacZ*/pKEAR22), U130 (*attB::araC-*P_{BAD}*-mVenus-lacZ hns*/pKEAR28) (iii) U124 (*attB::araC-*P_{BAD}*-*bgl_{DRE}*-lacZ*/pKEAR23), U131 (*attB::araC-*P_{BAD}*-*bgl_{DRE}*-lacZ hns*/pKEAR23) (iv) U126 (*attB::araC-*P_{BAD}*-mVenus-*bgl_{DRE}*-lacZ*/pKEAR25), U133 (*attB::araC-*P_{BAD}*-mVenus-*bgl_{DRE}*-lacZ hns*/pKEAR25).

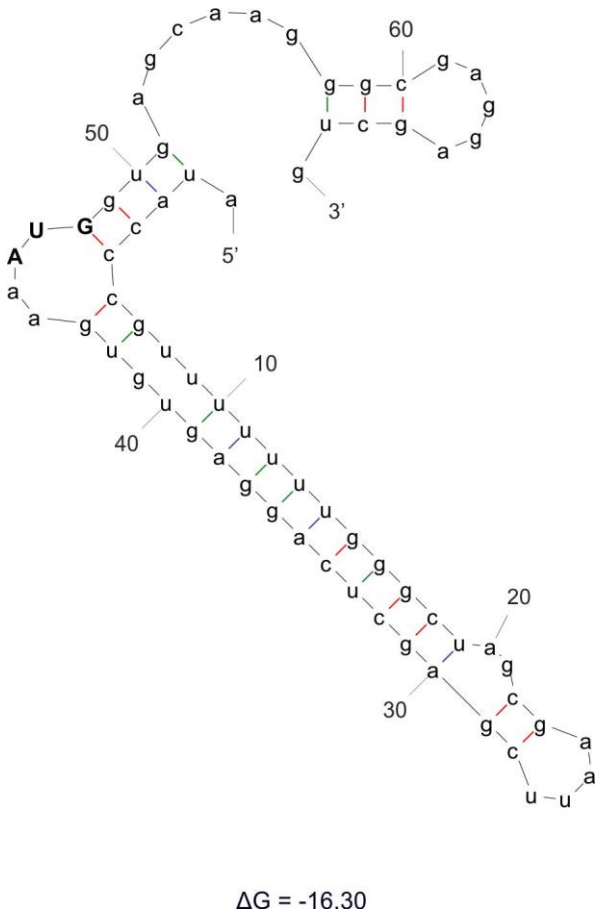

Figure 13: Secondary structure of P_{BAD}-*mVenus* mRNA. Secondary mRNA structure of P_{BAD}-*mVenus* mRNA predicted using *mfold* software (Zuker, 2003). The predicted structure contains sequence from (+1) transcription start site of P_{BAD} promoter until eighth codon in *mVenus* ORF. Translation start (AUG) is given in bold capital letters.

To locate the locus of the putative H-NS repressed internal promoter qRT-PCR and 5ˈRACE was performed. RNA was isolated from wild-type and *hns* mutant strains carrying P_{BAD}-*mVenus*-bgl_{DRE}-*lacZ* construct grown with 0, 10, and 250 µM arabinose. For qRT-PCR, primer pairs specific for *mVenus*, bgl_{DRE}, and *lacZ* locus were used respectively (Figure 14A). For *mVenus*, in both wild-type and *hns* mutant background, expression level was low at 0 µM arabinose and increased at 10 µM and 250 µM arabinose (Figure 14A, *mVenus*). These data show that transcript levels in *mVenus* locus depend on P_{BAD} induction and are not repressed by H-NS. For bgl_{DRE}, expression level was lower at 0 µM arabinose in wild-type and the expression level increased at 10 µM and 250 µM arabinose. Interestingly, bgl_{DRE} transcript levels in *hns* mutant background were high at 0 µM arabinose, while further increase in transcript levels were observed at 10 µM and 250 µM arabinose (Figure 14A, bgl_{DRE}). Similarly, for *lacZ* transcripts, in wild-type, the expression level was low at 0 µM arabinose

and increased at 10 µM and 250 µM arabinose, while in *hns* mutant background, the expression level was high at 0 µM arabinose, and further increased at 10 µM and 250 µM arabinose. High transcript levels observed at 0 µM arabinose, in *hns* mutant for bgl_{DRE} and *lacZ*, is in accordance with my above result, which indicates the presence of H-NS repressed internal promoter within bgl_{DRE} transcribing bgl_{DRE} and *lacZ*.

In order to precisely map the internal promoter within bgl_{DRE}, in P_{BAD}-*mVenus*-bgl_{DRE}-*lacZ* construct, 5'RACE was performed. RNA was isolated from wild-type and *hns* mutant strain carrying *araC*-P_{BAD}-*mVenus*-bgl_{DRE}-*lacZ* grown with 0, 10 and 250 µM arabinose. RNA was treated with or without RppH (RNA 5'Pyrophosphohydrolase) in order to differentiate primary and processed transcripts, respectively. For 5'RACE analysis, primers specific to *mVenus* and bgl_{DRE} were used, in order to determine the transcription from upstream P_{BAD} and the internal promoter in bgl_{DRE}. With *mVenus* specific primer, P_{BAD} specific primary transcript were observed at 10 µM and 250 µM arabinose in wild-type and *hns* mutant background whereas no product was seen at 0 µM arabinose (Figure 14B, *mVenus*). With bgl_{DRE} specific primer, at 0 µM arabinose no product is observed, whereas at 10 µM and 250 µM arabinose, $P3_{bgl}$ primary transcript and the *bgl*-4 processed transcript were observed. Moreover, in *hns* mutant at 0 µM arabinose, $P3_{bgl}$ primary transcript is observed and in 10 µM and 250 µM arabinose concentration both $P3_{bgl}$ and *bgl*-4 were detected. The presence of processed transcript *bgl*-4, in wild-type and *hns* mutant is observed only at 10 µM and 250 µM arabinose concentrations which suggests that the *bgl*-4 processed transcript could arise from the processed product of upstream P_{BAD} transcript. Cloning and sequencing of the product corresponding to P_{BAD}, mapped to 2 bp upstream of previously determined P_{BAD} transcription start site (Lee & Carbon, 1977) (Figure 14C). Cloning and sequencing of product corresponding to $P3_{bgl,}$ mapped to 8 bp upstream of the translation start of bgl_{DRE} with the apparent -10 region (TATAAA) (Figure 14C). Cloning and sequencing of the product corresponding to processed transcript *bgl*-4, mapped to 121 bp downstream of the translation start of bgl_{DRE} (Figure 14C). These data show the presence of H-NS repressed promoter $P3_{bgl}$ within bgl_{DRE}. The data further show that the transcription from upstream P_{BAD} promoter activates transcription from $P3_{bgl}$ and relieves repression of bgl_{DRE} by H-NS.

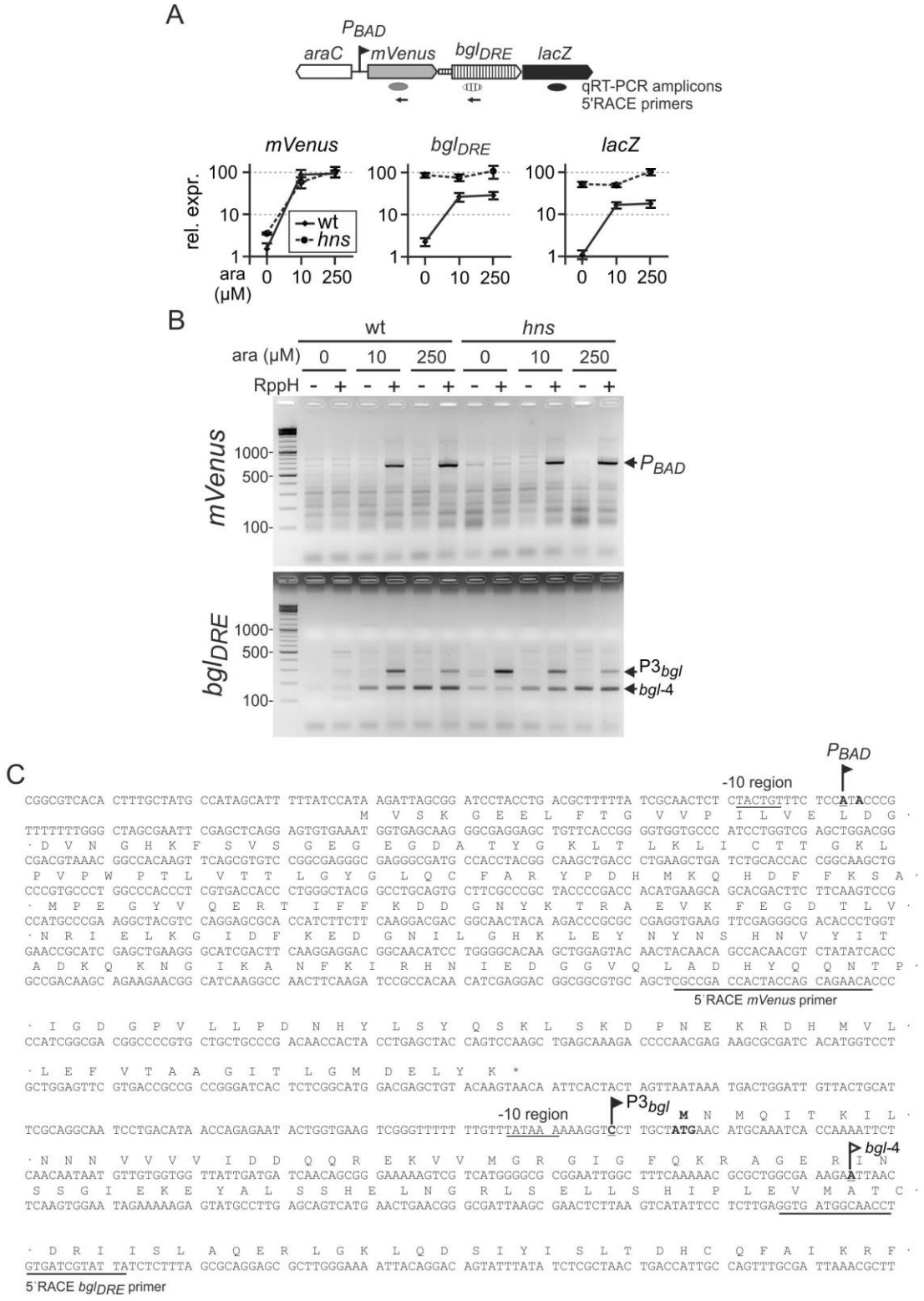

Figure 14: **Transcription from upstream P_{BAD} promoter into bgl_{DRE} activates transcription from $P3_{bgl}$.** (A) Schematic representation of *araC-*P_{BAD}*-mVenus-*bgl_{DRE}*-lacZ* construct. The qRT-PCR amplicons are indicated for the respective locus. Arrows indicate the position of 5ˈRACE primers used. (B) Expression levels of *mVenus*, bgl_{DRE} and *lacZ* were determined by qRT-PCR of RNA isolated from bacteria grown in tryptone medium with 0, 10 and 250 µM arabinose in wild-type (strain U137) and *hns* mutant (strain U140). For qRT-PCR *mVenus* specific primers OA443 and OA444, bgl_{DRE} specific primers OA457 and OA458, *lacZ* specific primers T888 and T889 were used. The Ct values were normalized to *rpoD* levels as determined by qRT-PCR, using primers T247 and T248.

The relative expression levels are determined relative to the expression level in *hns* mutant at 250 µM arabinose for each locus. The relative expression level of the wild-type and *hns* mutant is indicated in solid line and dashed line, respectively. Relative expression level indicated is the average of three biological replicates and error bars indicates standard deviation. (B) 5ˈRACE analysis of the RNA was isolated from wild-type (strain U137) and *hns* mutant (strain U140) with 0, 10, 250 µM arabinose induction in exponential phase. The samples were treated with or without RppH and the transcripts were analyzed using adapter specific primer OA9 and gene specific primer OA493 (*mVenus*) or OA489 (bgl_{DRE}). PCR was done for 30 cycles. Indicated bands were cloned and at-least two clones of each were sequenced. (C) The sequence of pKEAR25 (*araC-*P_{BAD}*-mVenus-*bgl_{DRE}*-lacZ)* plasmid is shown and the 5ˈRACE primer binding sites are indicated. 5ˈend of transcripts P_{BAD}, $P3_{bgl}$ and *bgl*-4 transcripts mapped to the sites that are marked in bold and underlined and the -10 region are underlined. P_{BAD} transcript mapped to 2 bp upstream of the previously mapped P_{BAD} promoter (marked in bold). $P3_{bgl}$ mapped to 8 bp upstream of the translation start ATG (marked in bold) of bgl_{DRE} and *bgl*-4 was mapped 121 bp downstream of the translation start of bgl_{DRE} in the coding region.

H-NS repression via bgl_{DRE} is facilitated by Rho terminator protein (Dole *et al*., 2004b). Further *in vitro* assays have shown that H-NS binding using an antisense template of bgl_{DRE} facilitates RNA polymerase pausing and enhances Rho mediated termination (Kotlajich *et al*., 2015). Thus, H-NS complex bound to bgl_{DRE} could interfere with transcription elongation or termination. In order to analyze whether H-NS interferes with transcription elongation or termination in bgl_{DRE}, conditional terminator anti-terminator module (*λtR1*-N) from phage lambda was used under the control of constitutive promoter P_{UV5}. This P_{UV5}*tR1* module was further used to modulate transcription elongation into H-NS repressed bgl_{DRE} and *lacZ* was used as reporter gene to determine the expression. Additionally *mVenus* gene, which is not repressed by H-NS was used as control.

First I addressed whether transcription elongation into the H-NS bound $bgl_{DRE,}$ activates $P3_{bgl}$ in P_{UV5}*tR1-*bgl_{DRE}*-lacZ.* To this end, 5ˈRACE analysis was performed of RNA isolated from the wild-type and *hns* mutant strains carrying constructs P_{UV5}*tR1-*bgl_{DRE}*-lacZ* in the presence and absence of λN protein. In wild-type, without the presence of λN protein, no transcript was observed, whereas in the presence of λN protein, bands corresponding to primary transcript P_{UV5} and $P3_{bgl}$ were observed. However, the intensity of the product corresponding to $P3_{bgl}$ is lower than P_{UV5} (Figure 15A). In the *hns* mutant, in the absence of λN protein, the band corresponding to primary transcript $P3_{bgl}$ was observed, whereas in the presence of λN protein the primary transcripts corresponding to P_{UV5} and $P3_{bgl}$ were observed similar to wild-type (Figure 15A). Cloning and sequencing of the indicated bands revealed that the transcripts mapped to known transcription start site of P_{UV5} and $P3_{bgl}$. This shows that the transcription from upstream P_{UV5} promoter activates the internal promoter $P3_{bgl}$.

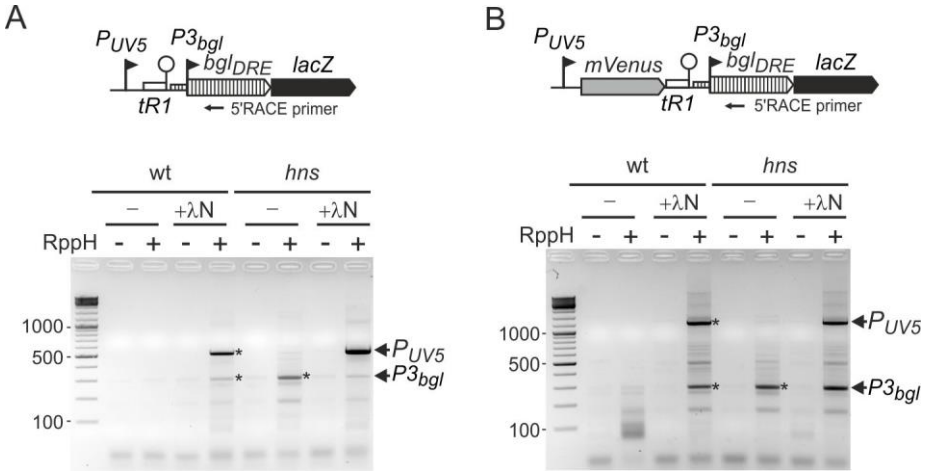

Figure 15: Transcription from the upstream P_{UV5} activates transcription from $P3_{bgl}$. (A) 5ˈRACE was performed in strain carrying P_{UV5}*tR1- bgl*$_{DRE}$*-lacZ* using *bgl*$_{DRE}$ specific primer OA489 (indicated with arrow). PCR was done for 30 cycles. Bands marked with asterisk were cloned and atleast two clones were sequenced. P_{UV5} and $P3_{bgl}$ transcripts mapped to known transcription start site (+1) of P_{UV5} and $P3_{bgl}$ respectively. The following strains were used, T204 (*attB::*P_{UV5}*tR1-bgl*$_{DRE}$*-lacZ/*pKEIB14), T233 (*attB::*P_{UV5}*tR1-bgl*$_{DRE}$*-lacZ hns/*pKEIB14). (B) 5ˈ RACE was performed in strain carrying P_{UV5}*-mVenus-tR1-bgl*$_{DRE}$*-lacZ* using *bgl*$_{DRE}$ specific primer OA489 (indicated with arrow). PCR was done for 30 cycles. Bands marked with asterisk were cloned and atleast two clones were sequenced. P_{UV5} and $P3_{bgl}$ transcripts mapped to known transcription start site (+1) of P_{UV5} and $P3_{bgl}$ respectively. The following strains were used, T2255 (*attB::*P_{UV5}*-mVenus-tR1-bgl*$_{DRE}$*-lacZ/*pKEAR14), T2273 (*attB::*P_{UV5}*-mVenus-tR1-bgl*$_{DRE}$*-lacZ hns/*pKEAR14).

In the construct P_{UV5}*tR1-bgl*$_{DRE}$*-lacZ,* the P_{UV5} promoter is in close proximity to the H-NS repressed $P3_{bgl}$ and *bgl*$_{DRE}$. Thus, the H-NS may polymerize into P_{UV5} promoter and also repress P_{UV5} promoter. In order to increase the distance of the upstream P_{UV5} promoter from *bgl*$_{DRE}$*, mVenus* which is not bound by H-NS was inserted between P_{UV5} and *bgl*$_{DRE}$. 5ˈRACE analysis was performed with the RNA isolated from the strains carrying constructs P_{UV5}*-mVenus-tR1-bgl*$_{DRE}$*-lacZ* in wild-type and *hns* mutant background in the presence and absence of λN protein. In wild-type without the presence of λN protein, no transcript was observed, whereas in the presence of λN protein, bands corresponding to primary transcript P_{UV5} and $P3_{bgl}$ were observed with similar band intensity. In the *hns* mutant, in the absence of λN protein, the band corresponding to primary transcript $P3_{bgl}$ was seen, whereas in the presence of λN protein the primary transcripts corresponding to P_{UV5} *bgl* and $P3_{bgl}$ were seen similar to wild-type (Figure 15B). Cloning and sequencing of the indicated bands revealed that the transcripts mapped to known transcription start of P_{UV5} and $P3_{bgl}$. This result suggests that in P_{UV5}*-tR1-bgl*$_{DRE}$*-lacZ,* H-NS might have polymerized into the proximal P_{UV5} promoter from *bgl*$_{DRE}$ which is de-repressed upon induction of λN protein (compare $P3_{bgl}$ in Figure 15A and 15B). However, in P_{UV5}*-mVenus-tR1-bgl*$_{DRE}$*-lacZ,* since *bgl*$_{DRE}$ is distal to the P_{UV5} promoter with the presence of *mVenus* between P_{UV5} and *bgl*$_{DRE}$, H-NS might not have polymerized into

the P_{UV5} promoter and the transcription directed by P_{UV5} promoter activated internal promoter $P3_{bgl}$.

In order to analyze whether H-NS interferes with transcription elongation or termination in bgl_{DRE}, β-galactosidase assay was performed in strains carrying constructs P_{UV5}*tR1-*bgl_{DRE}*-lacZ*, P_{UV5}*-mVenus-tR1-*bgl_{DRE}*-lacZ* and control constructs P_{UV5}*tR1-*bgl_{DRE}*-lacZ*, P_{UV5}*-mVenus-tR1-lacZ.* The expression levels determined by β-galactosidase assay could not be interpreted because of the high variations in the *lacZ* read out caused due to the context dependent termination of *λtR1*. Moreover, because of the presence of H-NS repressed internal promoter $P3_{bgl}$ upstream of bgl_{DRE}, whether bgl_{DRE} affects elongation or termination could not be determined.

2.6 Induction of *pst-phoU* operon located upstream of *bgl* decreases H-NS repression of *bgl*

To test whether transcription into the H-NS repressed promoter relieves repression in the native context, I chose H-NS repressed *bgl* operon which is preceeded by the *pst-phoU* operon. The *bgl* operon is repressed ~100 fold by H-NS and efficient repression requires upstream and downstream elements extending from -160 bp to +700 bp from the P_{bgl} promoter (Schnetz, 1995, Dole *et al*., 2004b). The *pst-phoU* operon is located immediately upstream of the *bgl* operon. I addressed whether transcription of the upstream *pst-phoU* operon relieves H-NS repression of *bgl* in the native context (Figure 16A). The *pst-phoU* operon belongs to the Pho regulon and *pst-phoU* operon is activated under low phosphate conditions (Hsieh & Wanner, 2010). To test whether transcription from the upstream *pst-proU* operon decreases repression of *bgl*, the expression of *bgl* was analyzed under low and high phosphate conditions. The wild-type *E.coli* K-12 strain BW30270 and the *hns* mutant strain U72 were grown in MOPS minimal medium at high and low phosphate concentrations (2 mM and 0.1 M K_2HPO_4, respectively). Since the *bgl* promoter is catabolite regulated by cAMP-CRP, the strains were grown with 2% glycerol as a carbon source. The relative expression of *bgl* was determined by qRT-PCR using primers located upstream of the *bgl* terminator t1. The expression level given in arbitrary units, were determined relative to the expression of *bgl* in *hns* mutant U72 grown at high phosphate (2mM K_2HPO_4). In wild-type, the expression level of *bgl* was 6 under high phosphate condition (2 mM K_2HPO_4) and the expression level increased to 28 under low phosphate condition (0.1 mM K_2HPO_4) (Figure 16B). However, in *hns* mutant, the expression of *bgl* is significantly higher than the wild-type, as expected, and no difference in expression level was observed in low and high phosphate

conditions (Figure 16B, compare 109 and 94 grown at 2 and 0.1 mM phosphate, respectively). These data show that the expression of *bgl* increases under low phosphate conditions. However, this increase in expression of *bgl* might be due to the read-through from upstream *pst-phoU* operon.

In order to investigate whether the transcription from the upstream *pst-phoU* operon at low phosphate condition, activates the native *bgl* promoters, 5ˈRACE analysis was performed. RNA was isolated of the wild-type and *hns* mutant strains grown in MOPS minimal medium with 2% glycerol at low and high phosphate conditions (0.1 mM and 2 mM K_2HPO_4). For 5ˈRACE analysis, primer OA442 mapping upstream of *bgl* terminator t1 and primer OA489 mapping to *bglG* gene were used. For the wild-type, at high phosphate condition (2 mM K_2HPO_4), no transcript was observed with primer OA442 (Figure 16C, OA442). However, at low phosphate condition (0.1 mM K_2HPO_4), a product corresponding to the P_{bgl} transcript was detected, which was also evident in *hns* mutant at low and high phosphate conditions (0.1 mM and 2 mM K_2HPO_4) (Figure 16C, OA442). Cloning and sequencing of the indicated bands revealed that the transcripts mapped to the known transcription start site of P_{bgl}. In order to determine whether $P3_{bgl}$ is also activated, 5ˈRACE analysis was performed with primer OA489 mapping to *bglG* gene. For wild-type, grown at high phosphate conditions (2 mM K_2HPO_4), no transcript was observed with primer OA489 (Figure 16C, OA489). However, at low phosphate condition (0.1 mM K_2HPO_4), products corresponding to P_{bgl}, $P3_{bgl}$ and *bgl*-4 transcript were detected. The same was apparent in *hns* mutant grown at low and high phosphate conditions (0.1 mM and 2 mM K_2HPO_4) (Figure 16C, OA489). Cloning and sequencing of the indicated bands revealed that the products corresponding to P_{bgl}, $P3_{bgl}$ and *bgl*-4 mapped to the known transcription start of P_{bgl}, $P3_{bgl}$ and *bgl*-4, respectively. These results show that the transcription from the upstream *pst-phoU* operon, decreases H-NS repression of *bgl* and activates the native P_{bgl} and $P3_{bgl}$ promoters.

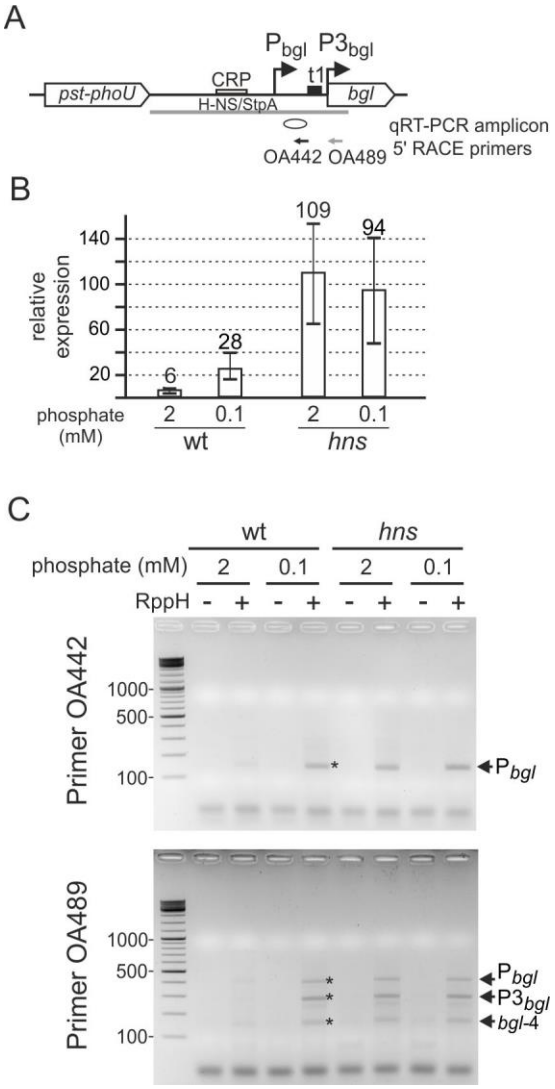

Figure 16: Induction of the *pst-phoU* operon reduces repression of the *bgl* operon by H-NS. (A) Schematic of the intergenic region between the *pst-phoU* and the *bgl* operon. H-NS/StpA binding region (grey bar), the *bgl* promoters P_{bgl} and $P3_{bgl}$, the CRP-binding site (CRP), *bgl* terminator t1, which is the target of substrate-specific regulation of *bgl* are indicated. qRT-PCR amplicon and the primers used for 5'RACE analysis are indicated. (B) Relative *bgl* transcript levels determined by qRT-PCR with primers OA98 and OA99, values normalized to 16srRNA levels determined with primers T528 and T529. Strains BW30270 (wild-type) and U72 (Δ*hns*) were grown in MOPS minimal medium with 2% glycerol at high (2mM K_2HPO_4) and low phosphate concentrations (0.1mM K_2HPO_4). (C) 5' RACE analysis of strains BW30270 (wild-type) and U72 (Δ*hns*) grown in MOPS minimal medium with 2% glycerol at high (2mM K_2HPO_4) and low phosphate concentrations (0.1mM K_2HPO_4) using bgl_{DRE} primers OA442 and OA489 and adapter specific primer T265. PCR is done for 30 cycles. The bands marked with asterisk were cloned and atleast 2 clones were sequenced. P_{UV5} and $P3_{bgl}$, *bgl*-4 transcripts mapped to known transcription start site (+1) of P_{UV5}, $P3_{bgl}$ and *bgl*-4 respectively.

2.7 Slow and fast moving RNA polymerase mutants did not affect the H-NS repression in bgl_{DRE} and *proU*

My above results show that transcription rate is inversely proportional to H-NS repression. In my above results, transcription rate into the H-NS bound region was modulated by using conditional terminator anti-terminator complex (*λtR1-N*) and arabinose inducible P_{BAD} promoter. I further wanted to test whether the speed of transcription is relevant for modulation of H-NS repression. I tested whether slow and fast moving RNA polymerase, modulates H-NS repression differently. The *rpoB* gene encodes for β-subunit of RNA polymerase which interacts with DNA template during the transcription process (Chenchik *et al.*, 1982). To test the effect of speed of transcription, I used slow moving RNA polymerase mutants *rpoB8* and *rpoB**35 and the fast moving RNA polymerase mutant *rpoB2*. The *rpoB2* possess less pausing and low termination efficiency and accelerated elongation rate (Jin *et al.*, 1988, McDowell *et al.*, 1994, Kogoma, 1994), the *rpoB8* possess high termination efficiency and defective elongation (Jin & Gross, 1991, Jin *et al.*, 1992, Yarnell & Roberts, 1999) and the *rpoB**35 is defective in open complex formation (Trautinger & Lloyd, 2002). The *bgl* downstream element (DRE) and *proU* upstream and downstream element (URE and DRE) which are repressed by H-NS were used as reporters to test H-NS repression. The alleles *rpoB8*, *rpoB2* and *rpoB**35 were transduced in strain containing constructs P_{UV5}*tR1-*$P3_{bgl}$-bgl_{DRE}-*lacZ* and $proU_{URE}$-P_{proU}-*proV-lacZ*. In P_{UV5}*tR1-*$P3_{bgl}$-bgl_{DRE}-*lacZ*, the transcription can be increased by the presence of λN protein. Since *proU* is osmoregulated and repressed by H-NS at low osmolarity conditions, the strain containing $proU_{URE}$-P_{proU}-*proV-lacZ* was tested in low osmolarity (10 mM NaCl) and high osmolarity (300 mM NaCl) medium. The expression levels of the *lacZ* reporter fusions were determined by β-galactosidase assays.

For the strain containing P_{UV5}*tR1-*bgl_{DRE}-*lacZ* construct, in wild-type background, the expression level was 6 units and increased to 360 units in the presence of λN protein. In *rpoB2*, *rpoB8* and *rpoB*35* mutant background no difference in expression level was observed in the absence and presence of λN protein compared to the wild-type (Figure 17A, compare wt, *rpoB8*, *rpoB2*, *rpoB*35*). Therefore, RNA polymerase mutants did not significantly affect H-NS repression of bgl_{DRE}. In a strain containing the $proU_{URE}$-P_{proU}-*proV-lacZ* construct, in wild-type background at low osmolarity (10 mM NaCl), the expression level was 2.3 units which increased to 684 units at high osmolarity conditions (300 mM NaCl) (Figure 17B). In the *rpoB2*, *rpoB8* and *rpoB*35* mutant background no significant difference in expression level is observed under low and high osmolarity conditions when compared to the wild-type (Figure 17B, compare wt, *rpoB8*, *rpoB2*, *rpoB*35* grown at 10 mM NaCl and

300 mM NaCl). These data show that slow moving RNA polymerase mutants *rpoB8* and *rpoB*35* and fast moving RNA polymerase mutant *rpoB2* do not significantly modulate the H-NS repression of bgl_{DRE} and *proU*.

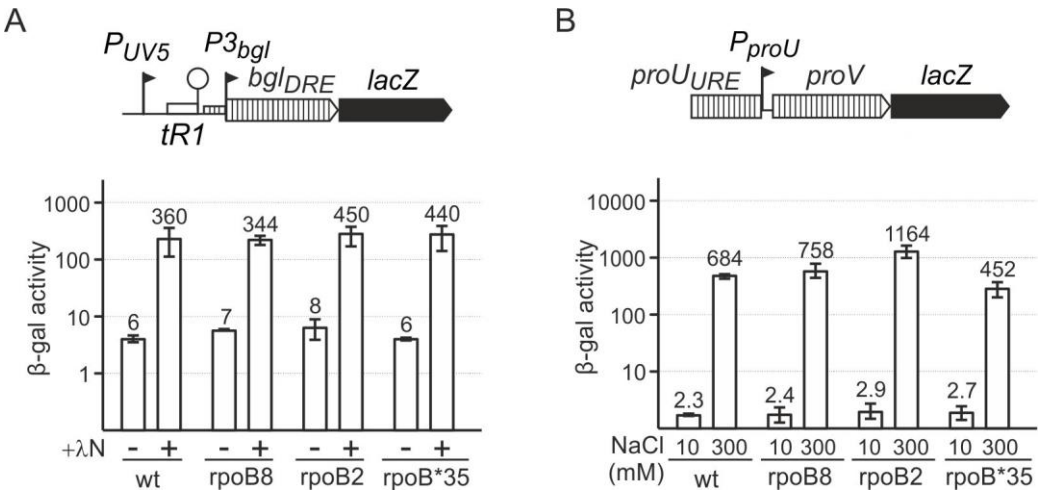

Figure 17: Slow moving and fast moving RNA polymerase mutants did not affect the H-NS repression in bgl_{DRE} and *proU*. (A) Schematic representation of P_{UV5}-*tR1-bglDRE-lacZ* construct integrated chromosomally. Expression levels given as β-galactosidase activities were determined in derivatives of Δ(*lacI-lacZYA*) strain S4084. Anti-terminator protein λN was provided plasmidically using transformants of plasmid pKES219 (+λN). Overnight cultures were inoculated in LB medium to OD_{600} 0.05 and grown to OD_{600} 0.5. For transformants with plasmid pKES219, LB medium was supplemented with kanamycin and 1mM IPTG. Average value of three biological replicates is shown as bars and error bars indicate standard deviation. The following strains were used, T204 (wt), T2165 (*rpoB8*), T2162 (*rpoB2*), T2149 (*rpoB*35*). (B) Schematic representation of $proU_{URE}$-P_{proU}-*proV-lacZ* construct integrated chromosomally. Expression levels given as β-galactosidase activities were determined in derivatives of Δ(*lacI-lacZYA*) Δ*proU* strain S541. Overnight cultures were inoculated in LB medium containing 10mM or 300 mM NaCl to OD_{600} 0.05 and grown to OD_{600} 0.5. Average value of three biological replicates is shown as bars and error bars indicate standard deviation. The following strains were used, S4066 (wt), T2154 (*rpoB8*), T2159 (*rpoB2*), T1815 (*rpoB*35*).

2.8 Hha plays a minor role in repression of *yciF*, *ycdT* and *appY* genes

Hha is a small basic protein which provides an additional binding surface to H-NS complex and stabilizes the bridging complex of H-NS (Ali et al., 2013, Wang et al., 2014, van der Valk et al., 2017). I wanted to determine whether the transcription into Hha/H-NS genes relieves repression. In order to address this *yciF*, *ycdT* and *appY* genes were chosen. The *ycidT*, *ycdT* and *appY* genes were shown to be bound by Hha and H-NS in ChIP analysis (Ueda *et al*., 2013). Hence, *ycidT*, *ycdT* and *appY* genes are likely to be regulated by Hha along with H-NS and H-NS/StpA.

First, I wanted to evaluate whether Hha indeed plays a significant role in the repression of *yciF*, *ycdT* and *appY* along with H-NS and H-NS/StpA. To this end, the relative expression of *yciF*, *ycdT* and *appY* are determined by qRT-PCR in wild-type, *hns*, *hns stpA, hha, hha hns and hha hns stpA* mutant backgrounds. RNA was isolated from strains grown in LB medium with 300 mM NaCl, since Hha regulated the expression of proteins at high salt conditions and similar growth conditions were used for ChIP analysis of Hha (Balsalobre *et al.*, 1999, Ueda *et al*., 2013). The relative expression level is given in arbitrary units with respect to the expression level of *hns stpA* mutant. The *yciF* gene expression is 0.2 in wild-type which increased to 92 in *hns* and 102 in *hns stpA* mutant background. This shows that *yciF* gene is repressed 460-fold by H-NS and that StpA does not contribute significantly to repression. In *hha* mutant background the expression increased 2-fold when compared to wild-type (Figure 18, *yciF*, compare 0.2 and 0.5 of wt and *hha*). But there was no significant change in expression level of *yciF* between *hns, hns stpA* and isogenic *hha* mutant background (Figure 18, *yciF*, compare 92 and 88 in *hns* and *hha hns*, compare 102 and 100 in *hns stpA* and *hha hns stpA*). In *ycdT*, the expression is 1.1 in wild-type and 15 in *hns* mutant and 111 in *hns stpA* mutant. This shows that *ycdT* is repressed 14 fold by H-NS and 100 fold by H-NS/StpA complex. In *ycdT*, the expression in *hha* mutant increased ~2 fold in *hha* and *hha* hns mutant when compared to the isogenic wild-type and hns mutant (Figure 18, *ycdT*, compare 1.1 to 2.1 in wt and *hha* and 15 to 27 in *hha hns* and *hns stpA*). No significant difference is seen in expression between *hns stpA* and *hha hns stpA* mutant (Figure 18, compare 111 and 109 in *hns stpA* and *hha hns stpA*). The *appY* gene is 14-fold regulated by H-NS (Figure 19, compare 0.7 and 10 in wt and *hns*) and 155-fold regulated by H-NS/StpA (Figure 18, compare 0.7 and 109 in wt and *hns stpA*). The *appY* gene is ~2 fold repressed by Hha (Figure 18, *appY*, compare 0.7 and 1.6 in wt and *hha*) and there is no significant change in expression in *hha hns* and *hha hns stpA* when compared to the isogenic *hns* and *hns stpA* mutant background (Figure 18, *appY*, compare 10 and 16 in *hns* and *hha hns*, compare 109 and 100 in *hns stpA* and *hha hns stpA*). These results suggest that *yciF*, *ycdT* and *appY* genes are only 2 fold regulated by Hha, while the regulation by H-NS and H-NS/StpA complex is much more significant. Since *yciF*, *ycdT* and *appY* are merely 2 fold regulated by Hha it was not tested further to address whether transcription into these genes relieves the Hha/H-NS repression.

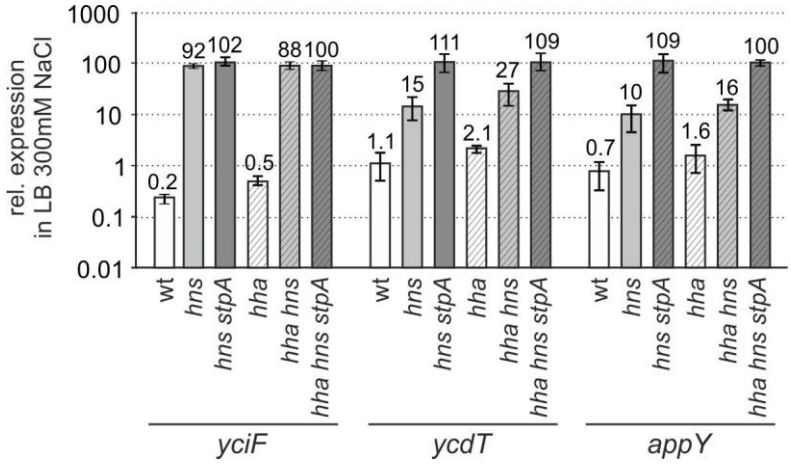

Figure 18: Hha does not have significant effect on *yciF*, y*cdT* and *appY* genes. Relative expression levels of *yciF*, *ycdT*, and *appY* were determined in RNA isolated from strains T1241 (wild-type), U72 (*hns*), U73 (*hns stpA*), U110 *(hha*), U111 (*hha hns*), U112 (*hha hns stpA*) using qRT-PCR. RNA was isolated from strains grown in LB with 300mM NaCl. qRT-PCR was performed using *yciF* specific primers OA161 and OA162, *ycdT* specific primers OA163 and OA164, *appY* specific primers T910 and T911 and the data were normalized to *rpoD* expression, determined with primers T247 and T248. The expression levels (in arbitrary units) are determined relative to the expression level in U112 (*hha hns stpA*) for each locus. Average value of three biological replicates is shown as bars and error bars indicate standard deviation.

3. Discussion

H-NS causes transcriptional repression by forming extended nucleoprotein complex on DNA which is also considered relevant for genome organization. H-NS complex silences transcription at the stage of transcription initiation and specific trans-acting proteins are required for relieving H-NS repression at specific loci (Stoebel *et al*., 2008, Will *et al*., 2015). H-NS binding to longer tracts of DNA into the coding part of gene suggests that it could impede transcription elongation and vice versa (Landick *et al*., 2015). Although there are indications of transcription elongation and H-NS repression negatively influencing each other, it is still unclear how transcription elongation and H-NS repression modulate each other (Chandraprakash & Seshasayee, 2014, Kotlajich *et al*., 2015). In this study, the influence of transcription elongation on H-NS repression was analyzed. My results show that the transcription directed into the H-NS binding regions can relieve H-NS and H-NS/StpA repression. I showed that transcription directed from upstream promoter into the H-NS and H-NS/StpA binding region of *bgl, proU, pdeL* and *appY* abrogates their H-NS and H-NS/StpA repression. Moreover, in the native context, at low phosphate conditions, transcription from the upstream *pst-phoU* operon de-repressed the H-NS/StpA repressed promoter of *bgl*. However, the speed and the processivity of the RNA polymerase tested with slow and fast moving RNA polymerase mutants did not have influence on H-NS repression of bgl_{DRE} and *proU*. In the context of chromosomal organization, long range chromosomal interaction of the H-NS repressed genes and the intragenic looping of *bgl* mediated by H-NS could not be observed with chromosome capture confirmation (3C) assay.

3.1 How do transcription elongation and H-NS repression modulate each other?

My results support a model of transcription elongation interfering with H-NS repression. At high transcription rate, RNA polymerases will trail behind one another thereby displacing H-NS. RNA polymerase can also re-model the DNA which enables the displacement of H-NS complex. The continuous engagement of RNA polymerase may prevent re-formation of H-NS nucleoprotein complex. At low transcription rate, H-NS complex would be stable to act as road-block and induces RNA polymerase pausing and facilitate Rho-dependent transcription termination (Figure 21). This mutual interference between transcription and H-NS repression could indicate that poorly transcribed AT-rich DNA regions are prone to H-NS repression, whereas H-NS repression complex may not be formed in highly transcribed regions. Additionally, transcriptional read-through from the upstream genes could concomitantly

abrogate the H-NS repression of downstream genes thus influencing the transcription of the neighboring genes.

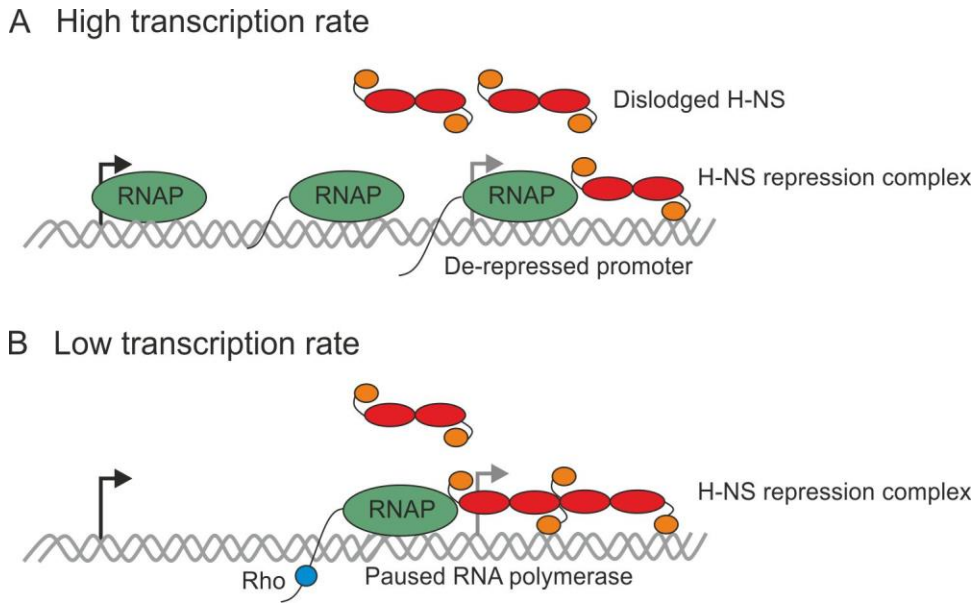

Figure 21: Model depicting mutual interference between transcription rate and H-NS repression (A) At high transcription rate RNA polymerase dislodges H-NS or modifies DNA complex to enable dislodging of H-NS causing de-repression of downstream promoter. At high transcription rate, because of the continuous engagement of RNA polymerase H-NS cannot re-bind to form stable nucleoprotein complex. (B) At low transcription rate H-NS road-block enables RNA polymerase to pause facilitating Rho mediated transcription termination.

My results show that transcription elongation can counteract H-NS repression. However, whether RNA polymerase reads through the H-NS road-blocks and dislodges the H-NS complex or whether transcription remodels the DNA to displace the H-NS is un-clear. H-NS dimer bound to DNA can be displaced with a relatively weak force of 7 pN per dimer (Dame *et al*., 2006). The elongating RNA polymerase during transcription generates a force of up to 25 pN (Wang *et al*., 1998). Thus, RNA polymerase exerts considerably higher force which could displace H-NS from DNA. Moreover, co-operation between elongating RNA polymerase molecules was shown to read through the transcriptional road-blocks *in vitro* and *in vivo* (Epshtein *et al*., 2003). Thus the elongating RNA polymerases could dislodge the bound H-NS. However, slow and fast moving RNA polymerase with varying processivity did not influence the H-NS repression of bgl_{DRE} and *proU* (Figure 17). Hence, H-NS de-repression could depend on the number of transcribing RNA polymerase with respect to the transcription rate rather than the processivity of the transcribing RNA polymerase. The

influence of transcription rate on H-NS repression could be tested using *in vitro* transcription assay. The transcription rate into the H-NS repressed promoter can be modulated using an active upstream promoter together with varying the concentration of RNA polymerase. Upon increasing the concentration of RNA polymerase enabling higher transcription rate, transcripts from the H-NS repressed downstream promoter might be detected.

The process of transcription elongation could also cause structural changes in DNA which in turn leads to displacing H-NS complex. Elongating RNA polymerase causes negative supercoiling upstream and positive supercoiling downstream of the elongating complex in DNA (Liu & Wang, 1987, Chong *et al.*, 2014). In eukaryotes it was shown that at high transcription rate multiple transcribing RNA polymerase complexes can displace histone complexes from DNA (Kulaeva *et al.*, 2013, Teves & Henikoff, 2014). Moreover, in eukaryotes it was shown that transcription induced supercoiling could dislodge histone complexes from DNA (Teves & Henikoff, 2014). Thus the transcription caused supercoiling could remodel the DNA's topology downstream and possibly dislodge the H-NS complex from DNA.

Like RNA polymerase complex dislodging H-NS, the H-NS complex can also interfere with the process of transcription elongation. H-NS repression of bgl_{DRE} requires Rho dependent termination (Dole *et al*., 2004b). *In vitro* experiments with inverse region of bgl_{DRE} have shown that H-NS bridging complexes act as a road block for the elongating RNA polymerase enabling RNA polymerase pausing thereby facilitating termination of transcription by termination factor Rho (Kotlajich *et al*., 2015). Contrarily, ChIP-seq analysis has shown that inhibiting Rho and therefore indirectly promoting transcription elongation decreased H-NS occupancy in the chromosome (Chandraprakash & Seshasayee, 2014). These experiments suggest a synergy between Rho mediated transcription termination and H-NS repression. H-NS complex by acting as road-block could increase the RNA polymerase dwelling time on the DNA at the pause site which is a prerequisite for Rho dependent termination (Ray-Soni *et al.*, 2016).

3.2 What is the role of StpA and Hha proteins interacting with H-NS?

StpA is a paralogue of H-NS possessing 59% sequence identity with H-NS (Zhang & Belfort, 1992). Similar to H-NS, StpA also binds to AT-rich DNA and forms stiffening and bridging complexes on DNA and causes transcriptional repression (Sonnenfield *et al*., 2001, Lim *et al*., 2012). Biochemical and genetic analysis have shown that StpA forms heteromeric complexes with H-NS, however the mechanism of how StpA modulates the H-NS complex is unknown

(Williams *et al*., 1996, Johansson *et al*., 2001). StpA levels are low in exponential phase since the *stpA* gene is negatively regulated by H-NS at the transcriptional level and post-translationally StpA protein is degraded by Lon protease when it is not associated with H-NS (Zhang *et al*., 1996, Wolf *et al*., 2006, Johansson *et al*., 2001). ChIP experiments have shown that there is significant overlap between the StpA binding sites with the H-NS (Uyar *et al*., 2009, Srinivasan *et al*., 2013). Further analysis of StpA binding sites by ChIP analysis showed StpA specifically binds to high affinity H-NS binding sites in the absence of H-NS. Moreover, these sites are enriched in highly expressed horizontally acquired genes (Srinivasan *et al*., 2013). Thus StpA might provide an additional back-up layer of transcriptional repression in a subset of H-NS repressed genes that are otherwise highly expressed in the absence of H-NS. Among the genes analyzed in this study, *proU, pdeL* and *yciF* were not affected by StpA but were repressed only by H-NS (Kavalchuk, 2011, Yilmaz, 2014) (Figure 18), whereas *appY* and *ycdT* were strongly repressed by StpA (Figure 9, Figure 18). The *appY, ycdT* genes might belong to horizontally acquired genes possessing high affinity H-NS binding sites. Moreover, my result shows that transcription into *appY* promoter which is strongly repressed by StpA enables de-repression of StpA (Figure 9). Thus StpA nucleoprotein complexes can be counteracted by transcription similar to H-NS complex.

Hha is a small basic protein, which forms heteromeric complexes with H-NS. Hha interacts with the N-terminal domain of H-NS and provides an additional binding surface with the positive charge to H-NS, thus enabling bridged H-NS/Hha complex formation (Ali et al., 2013, Wang et al., 2014, van der Valk et al., 2017). Moreover, bridged H-NS complex was shown to be more efficient in repression than linear H-NS complex (Kotlajich *et al*., 2015). Since, Hha facilitates bridged H-NS complex it could enable the formation of more stable repression complex. Hha may not be able to bind to DNA by itself since it lacks the C-terminal DNA binding domain. This is supported by the ChIP experiments showing complete loss of Hha binding upon deletion of H-NS. However, H-NS binding is not affected in the absence of Hha (Ueda *et al*., 2013). In *E. coli*, although ChIP analysis shows Hha binding regions along with H-NS in subset of H-NS regulated genes, transcriptome analysis shows no differences in transcriptome levels between wild-type and *hha* and between *hns* and *hns hha* mutant (Ueda *et al*., 2013, Srinivasan *et al*., 2013). This is consistent with my results showing merely 2 fold difference in relative expression of *ycdT, yciF and appY* genes between *hha* and isogenic wild-type background (Figure 18). Since, Hha provides an additional binding surface and enables bridging of H-NS protein, Hha was also speculated to be involved with H-NS in

chromosome compaction (Wang et al., 2014, Singh *et al.*, 2016). Thus Hha might play a significant role in chromosome structuring with H-NS rather than a regulatory role.

3.3 What are the consequences of interplay between transcription and H-NS repression on genome organization?

Organization of nucleoid is mediated by supercoiling, nucleoid associated proteins and macromolecular crowding but the precise role of each on the overall chromosome organization is unknown. On a broad scale, *E. coli* chromosome is divided into four major macrodomains; Ori, Ter, Right, left and two non-structured domains (Valens *et al.*, 2004). Certain proteins have defined macrodomain specificity to enable proper chromosomal replication and segregation. MatP protein binds specifically to Ter macrodomain enabling the separation of daughter chromosomes during cell division (Thiel *et al.*, 2012). SlmA proteins bind to the Ori macrodomain and play an important role in chromosome positioning (Tonthat *et al.*, 2011) (Figure 22).

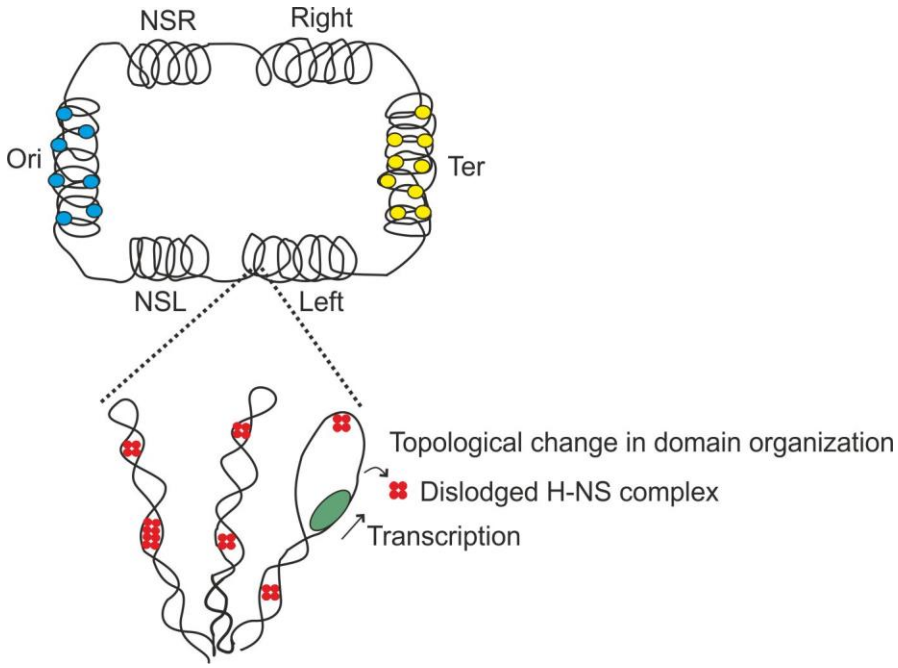

Figure 22: Transcription caused H-NS de-repression may involve in microdomain remodelling. *E. coli* chromosome contains four macrodomains. Ori, Non-structured domain right (NSR), Right, Ter, Left and Non-structured domain left (NSL). Ori and Ter macrodomains are bound by MatP (blue) and SlmA (yellow) proteins, respectively. Superimposed on macrodomains are microdomain loops which are presumambly stabilized by H-NS complex. Transcription enabling the dislodging of H-NS complex could cause topological change in domain organization. Figure adapted and modified from Valens *et al*., 2004.

Superimposed on the macrodomain structure, the nucleoid is organized into topologically isolated looped DNA microdomains. *E. coli* chromosome contains ~400 of looped microdomains with 10-12 Kb in length which are highly dynamic (Postow *et al*., 2004, Deng *et al*., 2005). H-NS was proposed to play a role in microdomain organization stabilizing the domain boundaries (Hardy & Cozzarelli, 2005, Noom *et al*., 2007). The bridging property of H-NS protein also supports the role of H-NS on microdomain organization (Dillon & Dorman, 2010, Dorman, 2014a). Transcriptionally silent Extended Protein Occupancy Domains (tsEPODs) present across the genome have low transcription activity and are presumably bound with nucleoid-associated proteins (Bryant *et al.*, 2014). The tsEPODs have been indicated as potential chromosomal organizational hubs that may insulate the topologically isolated microdomains and macrodomains (Vora *et al.*, 2009). Subsequent analysis of H-NS binding regions by ChIP analysis have shown significant correlation between the H-NS binding regions and the position of tSEPODs and horizontally acquired genes (Zarei *et al.*, 2013). Therefore H-NS might bind to tsEPODs and stabilize the loops in microdomains.

The phenomenon of DNA supercoiling was also indicated to be involved in the formation and maintenance of microdomain loops (Hardy & Cozzarelli, 2005, Travers & Muskhelishvili, 2005). Moreover, supercoiling was also shown to affect transcription and vice versa (Travers & Muskhelishvili, 2005, Ma *et al.*, 2013). My results show that transcription can dislodge H-NS complex. Thus, transcription into the H-NS stabilized loops in the microdomain could dislodge the H-NS complex, thereby changing the supercoiling state and local genome architecture (Figure 22). Organization of chromosome is the result of the interplay between several factors including transcription, supercoiling, H-NS and other nucleoid-associated proteins. How each of these factors influence each other thereby affecting the overall chromosome organization remain to be studied. Hi-C assays enabling high resolution mapping of chromosome organization can be exploited to understand the mechanistic interdependence of H-NS repression, supercoiling and transcription on nucleoid organization.

4. Materials and Methods

4.1 Bacterial strains, plasmids and oligonucleotides

E. coli strains used in this study are listed in Table 1, a list of plasmids is given in Table 2 and sequences of oligonucleotides are given in Table 3.

Table 1: *E. coli* strains

Strain	Genotype	Reference / Construction[a]
***E. coli* K12 strains**		
CY15014	W3110 *trp*^{R} *rpoB2*	(Yanofsky & Horn, 1981)
JW0449-5	*Δ(araD-araB)567 ΔlacZ4787(::rrnB-3) Δhha-745::kan λ-, rph-1, Δ(rhaD-rhaB)568 hsdR514* (CGSC#8608)	(Baba *et al.*, 2006)
M182 *stpA*	Δ(*lacIPOZYA*)*74 galU galK strA stpA*::TcR	(Zhang *et al*., 1996)
N4735	AB1157 *rpoB*35 arg*$^{+}$	(Trautinger & Lloyd, 2002)
SMMT8	KL226 *rpoB8 btuB::Tn10*	(Meenakshi & Munavar, 2015)
T1734	N4735 *rpoB*35 zja::*cmR	N4735 x PCR T919/T920 (pKD3)
T2142	KL226 *rpoB8 btuB::Tn10 zja*::cmR	SMMT8 x PCR T919/T920 (pKD3)
T2145	W3110 *trp*^{R} *rpoB2 zja*::cmR	CY15014 x PCR T919/T920 (pKD3)
CSH50	*bgl°* Δ(*lac-pro*) *ara thi*	(Miller, 1972)
S541	CSH50 Δ*bgl*-AC11 Δ*lacZ*-Y217	(Dole *et al.*, 2002)
S3077	S541 Δ$proU_{FRT}$	(Kavalchuk *et al.*, 2012)
MG1655 *fnr*$^{-}$	*E. coli* K-12 *fnr*$^{-}$ *ilvG*$^{-}$ *rph*$^{-}$ (CGSC#6300) Labarotory collection #S527	(Guyer *et al.*, 1981)
S3754	S527 (MG1655 *fnr*$^{-}$) Δhns_{kanR}	(Stratmann *et al*., 2012)
MG1655	*E. coli* K-12 wild-type *ilvG*$^{-}$ *rph*$^{-}$ (CGSC#6300) Laboratory collection #S3836	CGSC#6300
BW30270	MG1655 *rph*$^{+}$ Laboratory collection #S3839	CGSC #7925
S3974	BW30270^{+} *ilvG*$^{+}$ (=MG1655 *rph*$^{+}$ *ilvG*$^{+}$) (non-motile)	(Venkatesh *et al.*, 2010)
T208	S3974 *ilvG*$^{+}$ Δhns_{kanR} (non-motile)	(Stratmann *et al*., 2012)
S4084	S3974 Δ(*lacI-lacZYA*)$_{FRT}$ (non-motile)	Lab collection
T1241	BW30270 *ilvG*$^{+}$ (motile) (used as wild-type *E. coli* K-12 strain)	(Pannen *et al.*, 2016)
U65	T1241 Δ*ara*, Δ*lac*, Δ*araE*p-531$_{FRT}$, φP$_{cp8}$*araE*-535, Δ(*araH-araF*)572$_{FRT}$	(Breddermann & Schnetz, 2016)
U71	T1241 Δhns_{kanR}	T1241 x T4*GT7* (S3754)
U72	T1241 Δhns_{FRT}	U71 x pCP20
U73	T1241 Δhns_{FRT} *stpA*::TcR	U72 x T4*GT7* (M182 *stpA*::TcR)
U107	T1241 Δ*hha*-745$_{kanR}$	T1241 x P1 *vir* (JW0449-5)
U108	T1241 Δhns_{FRT} Δ*hha*-745$_{kanR}$	U72 x P1 *vir* (JW0449-5)
U109	T1241 Δhns_{FRT} *stpA*::TcR Δ*hha*-745$_{kanR}$	U73 x P1 *vir* (JW0449-5)
U110	T1241 Δ*hha*-745$_{FRT}$	U107 x pCP20
U111	T1241 Δhns_{FRT} Δ*hha*-745$_{FRT}$	U108 x pCP20
U112	T1241 Δhns_{FRT} *stpA*::TcR Δ*hha*-745$_{FRT}$	U109 x pCP20
***E. coli* K12 strains with *proU lacZ* fusions at *attB* integration site**		
S4066	S3077 *attB*::(Spec^{R} P_{proU} $proV_{HA}$ *lacZ*)	(Kavalchuk *et al*., 2012)
T1810	S3077 *attB*::(Spec^{R} P_{proU} $proV_{HA}$ *lacZ*) *rpoB*35 zja* $_{cmR}$	S4066 x P1*vir* (T1734)

T1815	S3077 *attB*::(Spec^R P_{proU} $proV_{HA}$ *lacZ*) *rpoB*35 zja* $_{FRT}$	T1810 x pCP20
T2154	S3077 *attB*::(Spec^R P_{proU} $proV_{HA}$ *lacZ*) *rpoB8 zja* ::cmR	S4066 x P1*vir* (T2142)
T2159	S3077 *attB*::(Spec^R P_{proU} $proV_{HA}$ *lacZ*) *rpoB2 zja* ::cmR	S4066 x P1*vir* (T2145)

***E. coli* K12 strains with bgl_{DRE} *lacZ* fusions at *attB* integration site**

T204	S4084 *attB*::(Spec^R P_{UV5} *λtR1* bgl_{DRE} *lacZ*)	Lab collection (attB::pKEIB14)
T233	S4084 *attB*::(Spec^R P_{UV5} *λtR1* bgl_{DRE} *lacZ*) Δ*hns*$_{FRT}$	Lab collection (derivative of T204)
T2148	S4084 *attB*::(Spec^R P_{UV5} *λtR1* bgl_{DRE} *lacZ*) *rpoB*35 zja* $_{cmR}$	T204 x P1*vir* (T1734)
T2149	S4084 *attB*::(Spec^R P_{UV5} *λtR1* bgl_{DRE} *lacZ*) *rpoB*35 zja* $_{FRT}$	T2148 x pCP20
T2162	S4084 *attB*::(Spec^R P_{UV5} *λtR1* bgl_{DRE} *lacZ*) *rpoB2 zja* ::cmR	T204 x P1*vir* (T2145)
T2165	S4084 *attB*::(Spec^R P_{UV5} *λtR1* bgl_{DRE} *lacZ*) *rpoB8 zja* ::cmR	T204 x P1*vir* (T2142)
T2255	S4084 *attB*::(Spec^R P_{UV5} *mVenus λtR1* bgl_{DRE} *lacZ*)	S4084/pLDR8 x pKEAR14
T2256	S4084 *attB*::(Spec^R P_{UV5} *mVenus* bgl_{DRE} *lacZ*)	S4084/pLDR8 x pKEAR15
T2259	S4084 *attB*::(Spec^R P_{UV5} *mVenus lacZ*)	S4084/pLDR8 x pKEAR18
T2260	S4084 *attB*::(Spec^R P_{UV5} *mVenus λtR1 lacZ*)	S4084/pLDR8 x pKEAR20
T2261	S4084 *attB*::(Spec^R P_{UV5} *lacZ*)	S4084/pLDR8 x pKES268
T2265	S4084 *attB*::(Spec^R P_{UV5} *mVenus λtR1* bgl_{DRE} *lacZ*) Δ*hns*$_{kanR}$	T2255 x T4*GT7* (T208)
T2266	S4084 *attB*::(Spec^R P_{UV5} *mVenus* bgl_{DRE} *lacZ*) Δ*hns*$_{kanR}$	T2256 x T4*GT7* (T208)
T2269	S4084 *attB*::(Spec^R P_{UV5} *mVenus lacZ*) Δ*hns*$_{kanR}$	T2259 x T4*GT7* (T208)
T2270	S4084 *attB*::(Spec^R P_{UV5} *mVenus λtR1 lacZ*) Δ*hns*$_{kanR}$	T2260 x T4*GT7* (T208)
T2271	S4084 *attB*::(Spec^R P_{UV5} *lacZ*) Δ*hns*$_{kanR}$	T2261 x T4*GT7* (T208)
T2273	S4084 *attB*::(Spec^R P_{UV5} *mVenus λtR1* bgl_{DRE} *lacZ*) Δ*hns*$_{FRT}$	T2265 x pCP20
T2274	S4084 *attB*::(Spec^R P_{UV5} *mVenus* bgl_{DRE} *lacZ*) Δ*hns*$_{FRT}$	T2266 x pCP20
T2277	S4084 *attB*::(Spec^R P_{UV5} *mVenus lacZ*) Δ*hns*$_{FRT}$	T2269 x pCP20
T2278	S4084 *attB*::(Spec^R P_{UV5} *mVenus λtR1 lacZ*) Δ*hns*$_{FRT}$	T2270 x pCP20
T2279	S4084 *attB*::(Spec^R P_{UV5} *lacZ*) Δ*hns*$_{FRT}$	T2271 x pCP20
T2316	S4084 *attB*::(Spec^R P_{UV5} *λtR1 lacZ*)	S4084/pLDR8 x pKES269
T2317	S4084 *attB*::(Spec^R P_{UV5} *λtR1 lacZ*) Δ*hns*$_{kanR}$	T2316 x T4*GT7* (T208)
T2318	S4084 *attB*::(Spec^R P_{UV5} *λtR1 lacZ*) Δ*hns*$_{FRT}$	T2317 x pCP20
T2346	S4084 *attB*::(Spec^R P_{UV5} *λtR1* bgl_{DRE} *lacZ*) *ΔbglGFBH-yieLK*$_{kanR}$	T204 x PCR OA459/OA460 (pKD4)
T2347	S4084 *attB*::(Spec^R P_{UV5} *mVenus λtR1* bgl_{DRE} *lacZ*) *ΔbglGFBH-yieLK*$_{kanR}$	T2349 x PCR OA459/OA460 (pKD4)
T2348	S4084 *attB*::(Spec^R P_{UV5} *λtR1* bgl_{DRE} *lacZ*) *ΔbglGFBH-yieLK*$_{FRT}$	T2346 x pCP20
T2349	S4084 *attB*::(Spec^R P_{UV5} *mVenus λtR1* bgl_{DRE} *lacZ*) *ΔbglGFBH-yieLK*$_{FRT}$	T2347 x pCP20
T2352	S4084 *attB*::(Spec^R P_{UV5} *λtR1* bgl_{DRE} *lacZ*) *ΔbglGFBH-yieLK*$_{FRT}$ Δ*hns*$_{kanR}$	T2348 x T4*GT7* (T208)
T2353	S4084 *attB*::(Spec^R P_{UV5} *mVenus λtR1* bgl_{DRE} *lacZ*) *ΔbglGFBH-yieLK*$_{FRT}$ Δ*hns*$_{kanR}$	T2349 x T4*GT7* (T208)
T2354	S4084 *attB*::(Spec^R P_{UV5} *λtR1* bgl_{DRE} *lacZ*) *ΔbglGFBH-yieLK*$_{FRT}$ Δ*hns*$_{FRT}$	T2352 x pCP20
T2355	S4084 *attB*::(Spec^R P_{UV5} *mVenus λtR1* bgl_{DRE} *lacZ*) *ΔbglGFBH-yieLK*$_{FRT}$ Δ*hns*$_{FRT}$	T2353 x pCP20
T2378	S4084 *attB*::(Spec^R P_{UV5} *mVenus 48 bp λtR1 lacZ*)	S4084/pLDR8 x pKEAR29
T2379	S4084 *attB*::(Spec^R P_{UV5} *mVenus 48 bp λtR1* bgl_{DRE} *lacZ*)	S4084/pLDR8 x pKEAR30
T2380	S4084 *attB*::(Spec^R P_{UV5} *mVenus 48 bp λtR1 lacZ*) Δ*hns*$_{kanR}$	T2378 x T4*GT7* (T208)
T2381	S4084 *attB*::(Spec^R P_{UV5} *mVenus 48 bp λtR1* bgl_{DRE} *lacZ*) Δ*hns*$_{kanR}$	T2379 x T4*GT7* (T208)
T2392	S4084 *attB*::(Spec^R P_{UV5} *mVenus 48 bp λtR1 lacZ*) Δ*hns*$_{FRT}$	T2380 x pCP20
T2393	S4084 *attB*::(Spec^R P_{UV5} *mVenus 48 bp λtR1* bgl_{DRE} *lacZ*) Δ*hns*$_{FRT}$	T2381 x pCP20
T2416	S4084 *attB*::(Spec^R P_{UV5} *λtR1 mVenus lacZ*)	S4084/pLDR8 x pKEAR31

T2417	S4084 *attB*::(Spec^R P_{UV5} *λtR1 mVenus* bgl_{DRE} *lacZ*)	S4084/pLDR8 x pKEAR32
T2418	S4084 *attB*::(Spec^R P_{UV5} *λtR1 mVenus lacZ*) Δhns_{kanR}	T2416 x T4*GT7* (T208)
T2419	S4084 *attB*::(Spec^R P_{UV5} *λtR1 mVenus* bgl_{DRE} *lacZ*) Δhns_{kanR}	T2417 x T4*GT7* (T208)
T2420	S4084 *attB*::(Spec^R P_{UV5} *λtR1 mVenus lacZ*) Δhns_{FRT}	T2418 x pCP20
T2421	S4084 *attB*::(Spec^R P_{UV5} *λtR1 mVenus* bgl_{DRE} *lacZ*) Δhns_{FRT}	T2419 x pCP20
U115	U65 *attB*::(Spec^R *araC* P_{BAD} *lacZ*)	U65/pLDR8 x pKEAR19
U123	U65 *attB*:: (Spec^R *araC* P_{BAD} *mVenus lacZ*)	U65/pLDR8 x pKEAR22
U124	U65 *attB*:: (Spec^R *araC* P_{BAD} bgl_{DRE} *lacZ*)	U65/pLDR8 x pKEAR23
U125	U65 *attB*:: (Spec^R *araC* P_{BAD} *lacZ*) Δhns_{kanR}	U115 x T4*GT7* (T208)
U126	U65 *attB*:: (Spec^R *araC* P_{BAD} *mVenus* bgl_{DRE} *lacZ*)	U65/pLDR8 x pKEAR25
U127	U65 *attB*:: (Spec^R *araC* P_{BAD} *lacZ*) Δhns_{FRT}	U125 x pCP20
U128	U65 *attB*:: (Spec^R *araC* P_{BAD} *mVenus lacZ*) Δhns_{kanR}	U123 x T4*GT7* (T208)
U129	U65 *attB*:: (Spec^R *araC* P_{BAD} bgl_{DRE} *lacZ*) Δhns_{kanR}	U124 x T4*GT7* (T208)
U130	U65 *attB*:: (Spec^R *araC* P_{BAD} *mVenus lacZ*) Δhns_{FRT}	U128 x pCP20
U131	U65 *attB*:: (Spec^R *araC* P_{BAD} bgl_{DRE} *lacZ*) Δhns_{FRT}	U129 x pCP20
U132	U65 *attB*:: (Spec^R *araC* P_{BAD} *mVenus* bgl_{DRE} *lacZ*) Δhns_{kanR}	U126 x T4*GT7* (T208)
U133	U65 *attB*:: (Spec^R *araC* P_{BAD} *mVenus* bgl_{DRE} *lacZ*) Δhns_{FRT}	U132 x pCP20
U134	U65 *attB*:: (Spec^R *araC* P_{BAD} $lacZ_{26}$)	U65/pLDR8 x pKEAR26
U135	U65 *attB*:: (Spec^R *araC* P_{BAD} *mVenus* bgl_{DRE} *lacZ*) *ΔbglGFBH-yieLK*$_{kanR}$	U126 x PCR OA459/OA460 (pKD4)
U136	U65 *attB*:: (Spec^R *araC* P_{BAD} $lacZ_{26}$) Δhns_{kanR}	U134 x T4*GT7* (T208)
U137	U65 *attB*:: (Spec^R *araC* P_{BAD} *mVenus* bgl_{DRE} *lacZ*) *ΔbglGFBH-yieLK*$_{FRT}$	U135 x pCP20
U138	U65 *attB*:: (Spec^R *araC* P_{BAD} $lacZ_{26}$) Δhns_{FRT}	U136 x pCP20
U139	U65 *attB*:: (Spec^R *araC* P_{BAD} *mVenus* bgl_{DRE} *lacZ*) *ΔbglGFBH-yieLK*$_{FRT}$ Δhns_{kanR}	U137 x T4*GT7* (T208)
U140	U65 *attB*:: (Spec^R *araC* P_{BAD} *mVenus* bgl_{DRE} *lacZ*) *ΔbglGFBH-yieLK*$_{FRT}$ Δhns_{FRT}	U139 x pCP20
U141	U65 *attB*:: (Spec^R *araC* P_{BAD} $lacZ_{27}$)	U65/pLDR8 x pKEAR27
U142	U65 *attB*:: (Spec^R *araC* P_{BAD} $lacZ_{28}$)	U65/pLDR8 x pKEAR28
U143	U65 *attB*:: (Spec^R *araC* P_{BAD} $lacZ_{27}$) Δhns_{kanR}	U141 x T4*GT7* (T208)
U144	U65 *attB*:: (Spec^R *araC* P_{BAD} $lacZ_{28}$) Δhns_{kanR}	U142 x T4*GT7* (T208)
U145	U65 *attB*:: (Spec^R *araC* P_{BAD} $lacZ_{27}$) Δhns_{FRT}	U143 x pCP20
U146	U65 *attB*:: (Spec^R *araC* P_{BAD} $lacZ_{28}$) Δhns_{FRT}	U144 x pCP20

***E. coli* K12 strains with promoter insertions upstream of H-NS repressed loci**

T1634	T1241 φ($_{kanR}$$P_{UV5}$ *λtR1 proU*)	T1241 x PCR T864/T865 (pKES305)
T1642	T1241 φ($_{FRT}$$P_{UV5}$ *λtR1 proU*)	T1634 x pCP20
T1641	T1241 φ($_{kanR}$$P_{UV5}$ *λtR1 pdeL*)	T1241 x PCR T866/T867 (pKES305)
T1647	T1241 φ($_{FRT}$$P_{UV5}$ *λtR1 pdeL*)	T1641 x pCP20
T1654	T1241 φ($_{FRT}$$P_{UV5}$ *λtR1 pdeL*) Δhns_{kanR}	T1647 x T4*GT7* (T208)
T1713	T1241 φ($_{FRT}$$P_{UV5}$ *λtR1 pdeL*) Δhns_{FRT}	T1654 x pCP20
T1637	T1241 φ($_{kanR}$$P_{UV5}$ *λtR1 appY*)	T1241 x PCR T858/T859 (pKES305)
T1646	T1241 φ($_{FRT}$$P_{UV5}$ *λtR1 appY*)	T1637 x pCP20
T1653	T1241 φ($_{FRT}$$P_{UV5}$ *λtR1 appY*) Δhns_{kanR}	T1646 x T4*GT7* (T208)
T1712	T1241 φ($_{FRT}$$P_{UV5}$ *λtR1 appY*) Δhns_{FRT}	T1653 x pCP20
T1949	T1241 φ($_{FRT}$$P_{UV5}$ *λtR1 appY*) Δhns_{FRT} *stpA*::Tc^R	T1712 x T4*GT7* (M182 *stpA*::Tc^R)

U80	T1241 φ(kanR*araC* P_{BAD} *proU*)	T1241 x PCR T864/OA79 (pKEAR3)
U83	U65 φ(kanR*araC* P_{BAD} *proU*)	U65 x P1*vir* (U80)
U86	U65 φ(FRT*araC* P_{BAD} *proU*)	U83 x pCP20

[a] Transductions were performed with phages T4*GT7* (Wilson *et al*., 1979) and P1*vir* (Miller, 1992), represented as "strain number of the recipient x phage (donor strain)''. Chromosomal deletions and insertions were constructed by λ-Red mediated recombination (Datsenko & Wanner, 2000). The parent strain, oligonucleotides and plasmids used for the generation of PCR fragment for λ-Red mediated recombination are represented as "parent strain x PCR oligonucleotides (plasmid)''. Flipping of the FRT (Flp recombinant target site) flanked resistance cassette by Flp recombinase was performed using plasmid pCP20 (x pCP20). Promoter *lacZ* fusions were integrated into phage λ attachment site *attB* by site-specific recombination, as described (Diederich *et al.*, 1992, Dole *et al*., 2002). All the constructed and transduced alleles were characterized by PCR using oligonucleotides given in Table 3.

Table 2: Plasmids

Plasmid No.	Relevant features[b]	Reference / Construction
pVs133	*mVenus* (*yfp* variant) in pTrc99a	Obtained from Surjik lab
pKD4	FRT kan^R FRT *oriRγ* amp^R	(Datsenko & Wanner, 2000)
pKD13	FRT kan^R FRT *tL3 oriRγ* amp^R	(Datsenko & Wanner, 2000)
pCP20	cI_{857} P_R *λ flp* in pSC101-*ori* rep_{ts} amp^R	(Cherepanov & Wackernagel, 1995)
pLDR8	cI_{857} P_R *λ int* in pSC101-*ori* rep_{ts} kan^R	(Diederich et al., 1992)
pBAD30	*araC* P_{BAD} *rrnB-T1* p15A-*ori* amp^R	(Guzman *et al.*, 1995)
pUC12	P_{lac} *lacZ'*(alpha) pMB1-*ori* amp^R	(Vieira & Messing, 1987)
pKK177-3	P_{tac} *rrnB-T1T2* in pBR amp^R	(Brosius & Holy, 1984)
pFDY400	P_{tac} *hns rrnB-T1 T2* pKK-*ori* amp^R	(Schnetz & Wang, 1996)
pKENV68	bgl_{URE} *PUV5* bgl_{DRE} *lacZ* in p15A kan^R *attP* spec^R	(Nagarajavel *et al*., 2007)
pKES268	P_{UV5} MCS *lacZ* in p15A kan^R *attP* spec^R	(Salscheider *et al*., 2014)
pKES269	P_{UV5} *λtR1 lacZ* in p15A kan^R *attP* spec^R	Lab collection
pFDY241	bgl_{URE} *PUV5 bglG bglF bglB* in p15A kan^R *attP* spec^R	Lab collection
pKEIB13	P_{UV5} bgl_{DRE} *lacZ* in p15A kan^R *attP* spec^R	Lab collection
pKEIB14	P_{UV5} bgl_{DRE} *λtR1 lacZ* in p15A kan^R *attP* spec^R	Lab collection
pKES214	bgl_{URE} P_{UV5} *t1 bglG rrnB-T1* in pUC amp^R	Lab collection
pKES215	bgl_{URE} P_{UV5} bgl_{DRE} *rrnB-T1* in pUC amp^R	Lab collection
pKES219	$lacI^q$ *tacOP λN* in p15A kan^R	Lab collection
pKES288	pKD4 with MCS	Lab collection
pKES305	P_{UV5} *λtR1* in pKD13	Lab collection
pKEAR3	*araC* P_{BAD} in pKD4	Cloning of *araC* P_{BAD} by PCR (pBAD30, primers OA75/OA76) in pKES288, *Eco*RI/*Sal*I
pKEAR6	bgl_{URE} P_{UV5} bgl_{DRE} *rrnB-T1 T2* in pBR amp^R	Cloning of bgl_{URE} P_{UV5} bgl_{DRE} by PCR (pKENV68, OA269/S726) in pKK177-3, *Bam*HI/*Pst*I
pKEAR7	bgl_{URE} P_{UV5} *λtR1* bgl_{DRE} *rrnB-T1 T2* in pBR amp^R	Cloning of bgl_{URE} P_{UV5} *λtR1* bgl_{DRE} by PCR (pKEIB14, OA236/S726+ pFDY241, OA269/S196) in pKK177-3, *Bam*HI/*Pst*I
pKEAR14	P_{UV5} *mVenus λtR1* bgl_{DRE} *lacZ* in p15A kan^R attP spec^R	Cloning of *mVenus* by PCR (pVs133, primers OA354/OA355) in pKEIB14, *Eco*RI/*Mun*I
pKEAR15	P_{UV5} *mVenus* bgl_{DRE} *lacZ* in p15A kan^R *attP* spec^R	Cloning of *mVenus* by PCR (pVs133, primers OA354/OA355) in pKEIB13, *Eco*RI/*Mun*I
pKEAR18	P_{UV5} *mVenus lacZ* in p15A kan^R *attP* spec^R	Cloning of *mVenus* by PCR (pVs133, primers OA354/OA355) in pKES268, *Mun*I
pKEAR19	*araC* P_{BAD} *lacZ* in p15A kan^R *attP* spec^R	Cloning of *araC* P_{BAD} by PCR (pBAD30, primers OA75/OA359) in pKES268, *Sal*I/*Xba*I
pKEAR20	P_{UV5} *mVenus λtR1 lacZ* in p15A kan^R *attP* spec^R	Cloning of *mVenus* by PCR (pVs133, primers OA354/OA355) in pKES269, *Mun*I
pKEAR22	*araC* P_{BAD} *mVenus lacZ* in p15A kan^R *attP* spec^R	Cloning of *mVenus* by PCR (pVs133, primers OA354/OA355) in pKEAR19, *Eco*RI/*Mun*I
pKEAR23	*araC* P_{BAD} bgl_{DRE} *lacZ* in p15A kan^R *attP* spec^R	Insertion of bgl_{DRE} from pKEIB13 into pKEAR19, *Eco81*I/*Spe*I

pKEAR25	*araC* P_{BAD} *mVenus* bgl_{DRE} *lacZ* in p15A kan^R *attP* $spec^R$	Insertion of bgl_{DRE} from pKEIB13 into pKEAR22, *Eco*81I/*Spe*I
pKEAR26	*araC* P_{BAD} $lacZ_{26}$ in p15A kan^R *attP* $spec^R$	Cloning of *araC* P_{BAD} by PCR (pBAD30, primers OA75/OA456) in pKES268, *Sal*I/*Xba*I
pKEAR27	*araC* P_{BAD} $lacZ_{27}$ in p15A kan^R *attP* $spec^R$	Deletion of linker between *Nhe*I and *Xba*I in pKEAR19
pKEAR28	*araC* P_{BAD} $lacZ_{28}$ in p15A kan^R *attP* $spec^R$	5'end mutations of *lacZ* by PCR in pKEAR19 (primers OA478/OA429)
pKEAR29	P_{UV5} *mVenus 48bp λtR1 lacZ* in p15A kan^R *attP* $spec^R$	Cloning of *λtR1* with 48 bp upstream sequence by PCR (*λdv*1, primers OA497/T244) in pKEAR20, *Mun*I/*Spe*I
pKEAR30	P_{UV5} *mVenus 48bp λtR1* bgl_{DRE} *lacZ* in p15A kan^R *attP* $spec^R$	Cloning of *λtR1* with 48 bp upstream sequence by PCR (*λdv*1, primers OA497/T244) in pKEAR14, *Mun*I/*Spe*I
pKEAR31	P_{UV5} *λtR1 mVenus lacZ* in p15A kan^R *attP* $spec^R$	Cloning of *mVenus* by PCR (pVs133, primers OA538/OA539) in pKES269, *Spe*I
pKEAR32	P_{UV5} *λtR1 mVenus* bgl_{DRE} *lacZ* in p15A kan^R *attP* $spec^R$	Cloning of *mVenus* by PCR (pVs133, primers OA538/OA539) in pKEIB14, *Spe*I

[b] The following abbreviations are used FRT = Flp recombinase target site; MCS = multiple cloning site. Genes encoding antibiotic resistance are designated as $spec^R$ = spectinomycin resistance, kan^R = kanamycin resistance amp^R = ampicillin resistance, cm^R = chloramphenicol resistance. ori represents origin of replication.
bgl_{DRE} represents regions including $t1_{RAT}$ and +1 to +964 relative to the transcription start site of *bgl* operon. $t1_{RAT}$ indicates AA to T mutation at position +67 and +68 in *bglt1* making the expression independent of BglG mediated anti-termination(Nagarajavel *et al*., 2007).
λtR1 region consists of *nutR* and *λtR1* terminator sequence. CGCTCTTACACATTCCAGCCCTG AAAAAGGGCATCAAATTAAACCACACCTATGGTGTATGCATTTATTTGCATACAT. The *nutR* sequence is underlined.
The sequence of $lacZ_n$ alleles from the transcription start site (+1) of P_{BAD} to first eight codons of *lacZ* are as follows:
pKEAR19 (*lacZ*) atacccgttttttgggctagcgaattcactactagtagcatctagagcttcacaggaaacagctATGaccatgattacggattcactg
pKEAR26 ($lacZ_{26}$) atacccgttttttgggctagcgaattctagagcttcaccttcacaggaaacagctATGaccatgattacggattcactg
pKEAR27 ($lacZ_{27}$) atacccgttttttgggctagagcttcacaggaaacagctATGaccatgattacggattcactg
pKEAR28 ($lacZ_{28}$) atacccgttttttgggctagagcttcacaggaaacagctATGacAatgattacAgattcactT
ATG represents start codon of *lacZ*. Mutated nucleotides are underlined.

Table 3: Oligonucleotides

Number	Sequence[c]	Description and use
OA9	gcgcaagcttTCCTGTAGAACGAACACTAGAAG	5' RACE RNA adapter specific primer with *Hind*III site
OA24	cagttctagaAGGCAGCTCATTATTCACGTCG	*appY*, 5'RACE
OA75	ctgagtcgacTTATGACAACTTGACGGCTACATCATTC	Cloning of *araC* P_{BAD}
OA76	tacggaattcGCTAGCCCAAAAAAACGGG	Cloning of *araC* P_{BAD}
OA79	ATTTCCCTGCTGCGGGTAGTGATATTTTTGAAAATAACA CCgccatggtccataggatccatactag	*araC*-P_{BAD} insertion at *proU*
OA94	GTTGCATTATTCGCCTGAAACCAC	Upstream region of P_{proU} in P_{BAD} *proU*, qRT-PCR
OA95	TCCCGTGATATAAGGGCTGAGAGC	Upstream region of P_{proU} in P_{BAD} *proU*, qRT-PCR
OA98	CCCGACTTCACCAGTATTCTCTGG	*bgl*, qRT-PCR
OA99	AATGACTGGATTGTTACTGCATTCG	*bgl*, qRT-PCR
OA104	ATGCCGCATTTGCCAGAAAACAAC	*gltF*, 3C
OA106	AGTACTGAGCGGAGTTTCTTACAGCT	*ydeO*, 3C
OA107	GCAGCTTGAGTAGCAGTCGTTCTTTC	*pdeL*, 3C
OA108	AACAGCAACTGATGGAAACCAGCC	*lacZ*, 3C
OA151	AGCCAGACGCATAACTTCTTCATCGC	*rpoB*, 3C
OA152	AATGCTCACCGTTAAGTCTGATGACG	*rpoB*, 3C
OA153	TCGTCTTCCAGTTCGATGTTGATACC	*rpoB*, 3C
OA154	AGGCGGTATGACCAACCTGGAACG	*rpoB*, 3C
OA157	TTTCTGTGCTCATTACTGACCTCCG	Analysis of Δ*hha*-745$_{FRT}$
OA158	AGAAATGGCGGAAGTCAGGTAATCG	Analysis of Δ*hha*-745$_{FRT}$
OA161	CGTAACTGGCAATCTCATAATGCTCG	*yciF*, qPCR
OA162	CATGAAATGTGTGGCAATGGAAGG	*yciF*, qPCR
OA163	AAGCATACGACCAGATGACCTTTTAGC	*ycdT*, qPCR
OA164	CTCAACATTTTCCCGAATCCTTTCC	*ycdT*, qPCR
OA178	ACCATTGCCAGTTTGCGATTAAACG	*bgl*, 3C
OA179	TCCTTGCTATGAACATGCAAATCACC	*bgl*, 3C
OA180	GGGAAAGATAGCGACAAATAATTCACCA	*bgl*, 3C
OA181	GAAATCCTGCCCCTTCACGTAGTAGAAG	*bgl*, 3C
OA236	GCTTTACACTTTATGCTTCCGGCTCGTA	Cloning of bgl_{URE} P_{UV5} $\lambda tR1$ bgl_{DRE}
OA269	ccgggatccgtcgacGCGTTCGCGCGGATGGACATTGACGAAG C	Cloning of bgl_{URE} P_{UV5} bgl_{DRE}
OA354	acgtgaattcGAGCTCAGGAGTGTGAAATG	Cloning of *mVenus*
OA355	cagcaggcctgttattcaattgTTACTTGTACAGCTCGTCCATGCC	Cloning of *mVenus*
OA359	ctagtctagaTGCTACTAGTAGTGAATTCGCTAGCCCAAAAA AACG	Cloning of *araC* P_{BAD}
OA429	TAACCGTGCATCTGCCAGTTTG	Cloning of *lacZ* fragment
OA442	actgggatccCCCGACTTCACCAGTATTCTCTGG	bgl_{DRE}, 5'RACE
OA443	TATCACCGCCGACAAGCAGAAGAAC	*mVenus*, qRT-PCR
OA444	TGTTCTGCTGGTAGTGGTCGGCG	*mVenus*, qRT-PCR
OA456	ctagtctagaattcGCTAGCCCAAAAAAACG	Cloning of *araC* P_{BAD}
OA457	ACGCGCTGGCGAAAGAATTAAC	bgl_{DRE}, qRT-PCR
OA458	TAATACGATCACAGGTTGCCATCACC	bgl_{DRE}, qRT-PCR
OA459	CAGGCCGGAGCGTAATTCACACATCCGGCCTTATTTCTT AAGCgtgtaggctggagctgcttcg	Deletion of *bgl* operon
OA460	AATCCCAATAACTTAATTATTGGGATTTGTTATATATAA	Deletion of *bgl* operon

	CTTTATcatatgaatatcctccttagttcctattcc	
OA478	agcatctagaGCTTCACAGGAAACAGCTATGACAATGATTAC AGATTCACTTGCCGTCGTTTTACAACGTCG	Cloning of mutated *lacZ* fragment
OA489	actgggatccTAATACGATCACAGGTTGCCATCACC	bgl_{DRE}, 5'RACE
OA493	ctgagtcgacTGTTCTGCTGGTAGTGGTCGGCG	*mVenus*, 5'RACE
OA497	acgtcaattgAGGTAAAGCCCTTCCCGAGTAAC	Cloning of $\lambda tR1$with 48 bp upstream sequence
OA538	acgtactagtGAGCTCAGGAGTGTGAAATGGTG	Cloning of *mVenus*
OA539	acgttctagaTTACTTGTACAGCTCGTCCATG	Cloning of *mVenus*
S93	CCGGGCCGACAACAAAGTCA	Analysis of *attB* integration
S95	CATATGGGGATTGGTGGCGA	Analysis of *attB* integration
S118	TGCGGGCCTCTTCGCTATTA	Analysis of *attB* integration
S126	GGTTTTTATAACGAACATCCAGGTTC	*bgl*, 3C
S164	GAGCAGGGGAATTGATCCGGTGGA	Analysis of *attB* integration
S182	ATAAGATGCCGTGGAACCAA	Analysis of *stpA*::TcR
S183	CGCTTACACTACGCGACGAA	Analysis of *stpA*::TcR
S196	ATTATACGAGCCGGAAGCATAAAGTGTAAAGCC	Cloning of bgl_{URE} P_{UV5} $\lambda tR1$ bgl_{DRE}
S487	AAAGCCCACTTCATCTTTCGGTAACT	*bgl*, 3C
S726	ccgctgcagtctagaTTTCAGTGTTCTTTGCGCACG	Cloning of bgl_{URE} P_{UV5} bgl_{DRE}
S728	tttctagaTCCTTGTTCGATATATTTGAACGC	*proU* 5' RACE
T123	AGCGCAACGCAATTAATGTGAGTTAGCTCA	Analysis of clones in pUC12
T124	TCGCTATTACGCCAGCTGGCGAAAG	Analysis of clones in pUC12
T244	cagtactagtAATTGATTGAATGTATGCAAATAAATGCA	Cloning of $\lambda tR1$
T247	GACGAAGAAGATGGCGATGACGAC	*rpoD*, qRT-PCR
T248	TTCCTGAGCGGTAGCGTGACTG	*rpoD*, qRT-PCR
T265	GCGCGAATTCCTGTAGAACGA	5' RACE RNA adapter specific primer with *Eco*RI site
T268	AUAUGCGCGAAUUCCUGUAGAACGAACACUAGAAGAAA	5' RACE RNA Adapter
T334	TGGCGAAGTAATCGCAACATCC	Analysis of *attB* integration
T520	AACTGGGCTATCGCTTGGCGTA	*proU*, qRT-PCR
T521	CGAAATGATGCCGACATACTGTTGG	*proU*, qRT-PCR
T528	GGTGTAGCGGTGAAATGCGTAGAG	16srRNA, qRT-PCR
T529	CTCAAGGGCACAACCTCCAAGTC	16srRNA, qRT-PCR
T858	TCGGTGTGTTATTTGTTTGTTTGATGTTATGCTTTTGCGC Cgtgtaggctggagctgcttcg	P_{UV5} $\lambda tR1$ insertion at *appY*
T859	GAAAATCAATTGATAAAATACATCTAAACAACCTTTTG Ggggatccgaattctactagtaattgattg	P_{UV5} $\lambda tR1$ insertion at *appY*
T864	GAAAGCGGTTGAAACAGAAGATGAAGACTGGAATTTCT GAGgtgtaggctggagctgcttcg	P_{UV5} $\lambda tR1$ insertion at *proU*
T865	ATTTCCCTGCTGCGGGTAGTGATATTTTTGAAAATAACA CCgggatccgaattctactagtaattgattg	P_{UV5} $\lambda tR1$ insertion at *proU*
T866	TGATTGTTATTGCATAAAACCGCGCCATGTCTGCATATG gtgtaggctggagctgcttcg	P_{UV5} $\lambda tR1$ insertion at *pdeL*
T867	CCGTATAGATATAACGTATCAAGAGGTAGGAGAAACAG CGCgggatccgaattctactagtaattgattg	P_{UV5} $\lambda tR1$ insertion at *pdeL*
T892	TGACGGGCTGTGAGGTGCTTG	*pdeL*, qRT-PCR
T893	TCATCAGTTGGCGGGTCATTATG	*pdeL*, qRT-PCR
T910	TCAATGTCGTAGCCCAGAAATGTG	*appY*, qRT-PCR
T911	CCATCTGTGACGCCGATTATTTTC	*appY*, qRT-PCR
T912	GCTGGTGGCACTGGGTAGTTGTTA	Analysis of *attB* integration
T919	TTCGCCCTGGACAACATTCCTGCTGACGGCACTACCATA	Analysis of cmR insertion at *zja*

	AAgtgtaggctggagctgcttcg	
T920	GGAAGATGAAAAACGCAAGGTTGTTGAAAGCGTTGTGT TTTcatatgaatatcctccttagttcctattcc	Analysis of cmR insertion at *zja*
T921	CTTCAGTCTGCTGCATCCTGG	Analysis of *zja::*cmR insertion
T922	TTCTCACCGCACGACGATCG	Analysis of *zja::*cmR insertion
T930	cagttctagaGAACTCTTGCAGAAAAACACGAAAATC	*pdeL,* 5'RACE

[c] Oligonucleotide sequences are given in 5' to 3' direction. Homologous sequences to the indicated target are shown in capital letters and the sites for restriction endonucleases are underlined.

4.2 Media and antibiotics

Compositions of media and concentrations of antibiotics used are given below.

LB Medium: 10 g of Bacto Tryptone, 5 g of Yeast extract, 5 g of NaCl per 1000 ml.

LB Agar Plates: 10 g of Bacto Tryptone, 5 g of Yeast extract, 5 g of NaCl, 15 g of Bacto Agar per 1000 ml.

SOB Medium: 20 g of Bacto Tryptone, 5 g of Yeast extract, 0.5 g of NaCl, 1.25 ml of 2 M KCl per 1000 ml. pH was adjusted to 7.0 with NaOH. After autoclaving 10 ml of 1 M $MgCl_2$ was added.

SOC Medium: 19.8 ml of 20% glucose was added to 1000 ml of SOB medium.

20 x M9: 140 g Na_2HPO_4, 60 g KH_2PO_4, 20 g NH_4Cl per 1000 ml.

M9 Minimal Medium: 50 ml of 20x M9, 1 ml of 0.1 M $CaCl_2$, 1 ml of 1 M $MgSO_4$, 0.5 ml of 1 mM $FeCl_3$ per 1000 ml. 15 g of Bacto Agar was added for plates.

MOPS Minimal Medium: MOPS minimal medium was prepared according to the procedure described previously (Neidhardt *et al.*, 1974).

Stock solutions: Freshly prepared 1 M MOPS (pH 7.4 with 10 M KOH), freshly prepared 1 M Tricine (pH 7.4 with 10 M KOH), freshly prepared 10 mM $FeSO_4.7\ H_2O$, 1.9 M NH_4Cl, 0.276 M K_2SO_4, 5 mM $CaCl_2$, 0.528 M $MgCl_2$, 5 M NaCl, 0.132 M K_2HPO_4, 10 M KOH, 10 M NaOH, micronutrient stock, 20% glucose, 80% glycerol, 10% salicin.

Micronutrient stock: 3 mg of $(NH_4)_6Mo_7O_{24}.4H_2O$, 24 mg of H_3BO_3, 7 mg of $CoCl_2$, 2.5 mg of $CuSO_4$, 16 mg of $MnCl_2$, 2.8 mg of $ZnSO_4$. The components were dissolved in 80 ml of Milli-Q H_2O and the total volume was brought to 100 ml. The micronutrient stock solution was further filter sterilized and stored at room temperature.

10x MOPS Mixture: 1 litre of 10x MOPS mixture was prepared by mixing the following components in the order given to prevent precipitation of salts. 400 ml of 1 M MOPS (pH 7.4), 40 ml of 1 M Tricine, 10 ml of 10 mM $FeSO_4.7\ H_2O$, 50 ml of 1.9 M NH_4Cl, 10 ml of 0.276 M K_2SO_4, 10 ml of 5 mM $CaCl_2$, 10 ml of 0.528 M $MgCl_2$, 100 ml of 5 M NaCl, 10 ml of micronutrient stock and 360 ml of Milli-Q H_2O. This mixture was

filter sterilized with a 1 litre capacity 0.2 micron filter and aliquoted into 100 or 200 ml plastic bottles and frozen at -20°C.

MOPS Minimal Medium: 100 ml of 10x MOPS mixture and 880 ml of Milli-Q H_2O were mixed. 0.132 M K_2HPO_4 was added to the final concentration of 0.1 mM (phosphate limiting condition) or 2 mM (phosphate sufficient condition) and brought to the final volume of 990 ml. The pH was adjusted to 7.2 with 10 M NaOH and filter sterilized. Final concentration of 0.5% glucose or 2% glycerol or 0.2 % salicin was used as a carbon source. Before use, required carbon source was added and the volume was adjusted to 1000 ml.

T4 Top Agar: 6 g of Bacto Agar, 10 g of Bacto Tryptone, 8 g of NaCl, 2 g of Tri-sodium citrate dihydrate, 3 g of Glucose per 1000 ml

Antibiotics: Antibiotics were used at the following concentrations: ampicillin 50 µg/ml, chloramphenicol 15 µg/ml, kanamycin 25 µg/ml, spectinomycin 50µg/ml, tetracyclin 12 µg/ml, rifampicin 100 µg/ml.

4.3 Standard molecular techniques

Standard molecular biology techniques such as cloning, PCR, agarose gel electrophoresis were performed according to published protocols (Ausubel *et al.*, 2005). Sequencing was done by GATC Biotech AG, Konstanz, Germany. Sequences were analyzed using VNTI 11 software (Thermo Fisher Scientific, USA).

4.4 $CaCl_2$ competent cells and transformation

TEN Buffer: 20 mM Tris-HCl (pH 7.5), 1 mM EDTA, 50 mM NaCl

For transformation with plasmids and ligation samples $CaCl_2$ competent cells were prepared. For preparing $CaCl_2$ competent cells, 200 µl of fresh overnight culture was inoculated in 25 ml of LB medium and incubated at 37°C. The culture was grown to OD_{600} 0.3, harvested on ice and centrifuged at 3000 rpm (A-4-62, 5810R Eppendorf) for 10 minutes at 4°C. Pellets were resuspended in 12.5 ml of ice cold 0.1 M $CaCl_2$ and incubated on ice for 20 minutes, followed by centrifugation at 3000 rpm (A-4-62, 5810R Eppendorf) for 10 minutes at 4°C. Pellets were resuspended in 1 ml of ice cold 0.1 M $CaCl_2$. These cells were directly used for transformation or glycerol (15% final concentration) was added and kept on ice for one hour and stored at -80°C. For transformation, 1 to 100 ng of plasmid DNA or 10 µl of ligation samples was added to TEN buffer to a final volume of 50 µl. To this ligation samples, 100 µl of competent cells were added on ice and samples were incubated in ice for 20 minutes and incubated at 42°C for 2 minutes for heat shock treatment. Samples were immediately placed on ice for 5 minutes and 1 ml of LB medium was added and samples were transferred to culture tube and incubated for 1 hour at appropriate temperature in shaker. 100 µl was plated on plates with appropriate antibiotics. The rest of the sample was pelleted by centrifugation, resuspended in 100 µl LB medium and plated on plates with appropriate antibiotics and incubated at appropriate temperature.

4.5 Electrocompetent cells and electroporation

Electrocompetent cells were used for gene deletion or insertion using λ-Red Gam mediated recombination (Datsenko & Wanner, 2000). For the preparation of electrocompetent cells cultures were grown in 3 ml SOB medium with appropriate antibiotics at appropriate temperature. 50 ml of SOB medium was inoculated with 200 µl of overnight culture with appropriate antibiotics and grown to OD_{600} 0.6. The culture was kept on ice for an hour, transferred to pre-chilled tubes and centrifuged for 15 minutes at 3000 rpm (A-4-62, 5810R Eppendorf) at 4°C. The pellet was re-suspended in 50 ml ice-cold sterile H_2O and centrifuged for 15 minutes at 3000 rpm (A-4-62, 5810R Eppendorf) at 4°C. The supernatant was

discarded and the cell pellet was resuspended in 25 ml ice-cold sterile H_2O and centrifuged for 15 minutes at 3000 rpm (A-4-62, 5810R Eppendorf) at 4°C. The pellets were resuspended in 2 ml of ice-cold 10% glycerol and pelleted by centrifugation at 6000 rpm (F-45-24-11, 5415R Eppendorf) for 15 minutes at 4°C. The cell pellet was resuspended in 200 µl sterile ice-cold 10% glycerol. The cells were either used immediately for electroporation or incubated in ice for an additional hour and 40 µl aliquots were made and stored at -80°C. For electroporation, 40 µl of electrocompetent cells were mixed with PCR fragment (100 ng/µl in H_2O) or 0.1 ng of plasmid and incubated on ice for 10 minutes. The mixture was transferred to a pre-chilled electroporation cuvette (Bio-Rad) and placed in an electroporator (Gene pulser, Bio-Rad). Electroshock was given 1.8 kV for 3 milliseconds. 1 ml of SOC medium was immediately added to cuvettes and cells were transferred to culture tubes and incubated for 1 hour at 37°C. After incubation, 100 µl was plated on plates with appropriate antibiotics. The remaining culture was incubated at room temperature overnight and spun down at 5000 rpm (F-45-24-11, 5415R Eppendorf) for 5 min. The pellet was resuspended in 100 µl SOC medium and plated on plates with appropriate antibiotics.

4.6 Chromosomal integration into *attB* sites

Integration of *lacZ* reporter fusions into the chromosomal λ attachment site *attB* was performed according to the method described previously (Diederich *et al*., 1992, Dole *et al*., 2002). The desired strain was transformed with temperature-sensitive helper plasmid pLDR8 which encodes λ integrase. The transformants carrying pLDR8 were selected on LB kanamycin plates at 28°C and used for preparing $CaCl_2$ competent cells. Overnight culture of pLDR8 was setup in LB with kanamycin at 28°C, and the culture was diluted 20-fold in LB with kanamycin and grown at 37°C for 90 minutes. This temperature shift allows the expression of integrase and arrests the replication of pLDR8, since it has a temperature sensitive origin of replication. The culture was harvested on ice and was made chemically competent. The desired plasmid with the reporter fusion was digested with *Bam*HI or *Bgl*II to create origin less fragments having spectinomycin resistance gene. These fragments were gel purified, 10 ng was re-ligated and used to transform competent cells. Since these competent cells express integrase, it allows the integration of *attP* site in the plasmid into the *attB* site of the chromosome. For selection of integrants, 200 µl was plated on premwarmed LB plates with spectinomycin and incubated at 42°C overnight. The transformants were restreaked on LB plates with spectinomycin and analyzed for kanamycin sensitivity (loss of pLDR8). The transformants were further analyzed by PCR using primers S93/S164, S95/T912, S95/S164,

and T334/S118 to verify proper integration and to exclude dimers. Two independent clones were selected and stored for further expression analyses.

4.7 Gene deletion and insertion using λ-Red mediated recombination

Gene deletion and insertion was carried out according to the method described (Datsenko & Wanner, 2000). This method is based on homologous recombination between linear DNA fragments and the chromosomal locus using λ-Red mediated recombination. Linear DNA containing antibiotic resistance gene flanked by FRT (Flp Recombination Target sites) was amplified from plasmid pKD3/pKD4/pKD13 or its derivatives. The oligonucleotides used for PCR were designed to have 36 to 50 nucleotide homology to the chromosomal locus. The PCR products were further gel purified and eluted in H_2O. Briefly, the cells were transformed with the temperature sensitive plasmid pKD46, which encodes the λ-Red system under the control of an arabinose inducible promoter. Electrocompetent cells were prepared from cultures grown at 28°C in SOB medium supplemented with 10 mM L-arabinose for induction of λ-Red recombinase. 100 ng of the gel purified PCR product was electroporated into the cells harboring pKD46. The recombinants were selected at 37°C and restreaked on LB plates supplemented with suitable antibiotics. The loss of pKD46 was confirmed by ampicillin sensitivity and the insertion of the target gene was confirmed by PCR using primers flanking the inserted region. The antibiotic resistance genes are flanked by FRT (Flp recombinase target sites). The antibiotic resistance markers were removed by transforming the strains with helper plasmid pCP20 encoding the site specific Flp recombinase gene which is under temperature sensitive promoter. The transformants were selected on LB ampicillin plates at 28°C. Selected transformants were restreaked on LB plates and incubated at 42°C which induces the Flp recombinase and loss of pCP20 plasmid. The removal of the antibiotic resistant cassette was confirmed by antibiotic sensitivity of the clones and by PCR.

4.8 β-galactosidase assay

Z-Buffer (pH 7.0): 60 mM Na_2HPO_4, 40 mM NaH_2PO_4, 10 mM KCl, 1 mM $MgSO_4$, 100 µg/ml of chloramphenicol

β-galactosidase assay was performed as described (Miller, 1992). Briefly, cultures were grown overnight in LB medium or tryptone medium with antibiotics, if necessary. 8 ml cultures were inoculated to an OD_{600} of 0.05 and grown to an OD_{600} of approximately 0.5. For induction, IPTG (isopropyl-β-D-thiogalactopyranoside, final concentration of 1mM) or arabinose (varying concentrations) was added, to the exponential culture where indicated. The bacteria were harvested and β-galactosidase activities were determined. The assays were

performed in Z-buffer with dilutions of bacterial cultures. β-galatosidase acitivity was detected using ONPG (o-nirophenyl-β-galoctoside) as substrate and activity was determined with the following formula: 1 unit = [OD_{420} x dilution factor x 1000]/ [OD_{600} x time (minutes)]. The assays were performed with at-least three independent biological replicates.

4.9 Transduction using T4*GT7* phage

Generalized transduction by using T4*GT7* phage was carried out as described (Wilson *et al*., 1979). For the preparation of a lysate, 100 µl of overnight culture of the donor strain was incubated with serially diluted 100 µl of wildtype T4*GT7* lysate and was incubated at room temperature for 20 minutes. 1ml of LB was added and the mixture was transferred to a culture tube containing 3 ml of T4 top agar at 44°C. The warm top agar mix was plated on fresh LB plates and incubated overnight at 37°C. Plates that showed confluent lysis were taken and lysate was prepared by chloroform extraction. For transduction of the allele of interest, 100 µl of the overnight culture of the recipient strain was incubated with 0.1 to 10 µl of the lysate prepared from the donor strain. The mixture was incubated at room temperature for 15 minutes and was plated on plates containing appropriate antibiotics. The transductants were restreaked three to four times to get rid of contaminating phages. The transfer of the desired allele was confirmed by PCR and the lysate was stored for further use.

4.10 Transduction using P1*vir* phage

Transduction using P1*vir* phage was performed as described (Miller, 1992). Freshly prepared wild-type P1 *vir* lysates with 10^9 to 10^{10} pfu/ml is used for lysate preparation. For the preparation of P1*vir* lysate from donor strain, 100 µl overnight culture of the donor strain was added to 5 ml LB medium supplemented with 2.5 mM $CaCl_2$ and grown to OD_{600} 0.2. Then, 100 µl of P1*vir* lysate (10^9 to 10^{10} pfu/ml) was added to and the cells are allowed to grow for 3 to 4 hours until the culture lyses. 20-40 µl chloroform was added to the lysed cultures and vortexed well. The samples were then centrifuged at 4500 rpm (A-4-62, 5810R Eppendorf) for 10 minutes to clear the lysate from cell debris. The supernatant was transferred to a fresh tube and stored with few drops of chloroform at 4°C. For transduction, the recipient strain was grown in LB medium supplemented with 2.5 mM $CaCl_2$ to OD_{600} 0.5. 1 ml of the recipient cells was centrifuged, supernatant was discarded and the pellet was resuspended in 1 ml LB medium with 2.5 mM $CaCl_2$. 100 µl of P1*vir* lysate prepared from the donor strain was added. The mixture was vortexed and incubated for 30 min at 37°C for phage adsorption. After incubation, 100 µl of 1 M Trisodium citrate was added and the mixture was vortexed vigorously to prevent further adsorption of phages. The infected cells are pelleted by

centrifugation, resuspended in LB containing 50 mM Trisodium citrate and incubated for 45 minutes in shaker at appropriate temperature. After incubation, cells are pelleted by centrifugation and washed with 1 ml Mg-saline three times. The pellet was resuspended in 100 µl of Mg-saline and plated on LB plates with appropriate antibiotics. Transductants were restreaked, analyzed by PCR and stored for further use.

4.11 RNA extraction

For RNA extraction, fresh overnight cultures were used to inoculate 8 ml of medium with antibiotics if necessary, to OD_{600} 0.05. IPTG (1 mM) or arabinose (varying concentrations) was added and grown till OD_{600} 0.5. 1 ml or 2 ml of culture was mixed with twice the volume of RNA Protect Bacteria Reagent (Qiagen) and RNA was isolated using RNeasy Mini Kit (Qiagen) according to manufacturer's instructions with on-column DNase I (Qiagen) digestion. RNA was eluted in RNase free H_2O and the RNA concentration was determined by measuring absorbance at 260 nm and the quality of RNA was checked by denaturing urea PAGE. RNA samples were stored at -80°C for further use.

4.12 Urea PAGE

10 x TBE Buffer (1000 ml): 108 g of Tris base, 55 g of boric acid, 40 ml of 0.5 M EDTA (pH 8.0)

The quality of RNA sample was tested using denaturing urea polyacrylamide gel electrophoresis. 1 µg of RNA sample was mixed with equal volume of 2 x RNA loading dye (95% formamide, 0.025% bromophenol blue, 0.025% xylene cyanol, 0.025% SDS, 0.025% EtBR, 0.5 mM EDTA) (Thermo Fisher Scientific), heated at 70°C for 10 minutes and spun down. Samples were loaded onto denaturing urea polyacrylamide gel (5% acrylamide (19:1), 7 M Urea, 0.5 x TBE) and run with 0.5x TBE buffer at 200V for 1.5 hours. As a marker, 5 µl of RiboRuler low range RNA ladder (Thermo Fisher Scientific) was used. The gel was stained in 0.5 x TBE containing ethidium bromide (10 µg/ml final concentration) for 15 minutes. The gel was checked for intact 2904 nt (23S rRNA) and 1542 nt (16S rRNA) RNA bands without degradation for each sample, which is an indication for good quality RNA sample preparation (Sambrook and Russel, 2001).

4.13 cDNA synthesis

cDNA synthesis was performed using Superscript III First Strand Synthesis kit (Thermo Fisher Scientific) according to manufacturer's instruction. Briefly, 1 µg of RNA was mixed with 4 µl of random hexamers (50 ng/µl) and 2 µl of dNTPs (10 mM) to the final volume of 10 µl. The sample was incubated at 65°C for 5 minutes and placed on ice. To this, 2 µl of 10 x

Reverse Transcription Buffer (Thermo Fisher Scientific), 4 µl of 25 mM $MgCl_2$, 2 µl of 0.1 M DTT, 1 µl of RNaseOUT (40 U/µl) and 1 µl of Superscript III reverse transcriptase (200 U) was added to the final volume of 20 µl. The mixture was incubated at 25°C for 10 minutes, 50°C for 1 hour and the reaction was terminated by incubating at 85°C for 5 minutes and placed on ice. RNA was removed by adding 1 µl of RNase H and incubated at 37°C for 20 minutes. The cDNA samples were stored at -20°C.

4.14 qRT-PCR

Relative expression levels of mRNA was determined by qRT-PCR using SYBR green dye in C1000 touch thermal cycler with optical reaction module CFX96 (Bio-Rad). RNA isolation and cDNA synthesis was done as described. For one assay, 4 µl of dNTPs (1 mM each), 4 µl of 5 x GoTaq buffer (Promega), 6.8 µl of DEPC treated H_2O, 0.8 ml of DMSO, 0.2 µl of SYBR green (1:1000 in DMSO), 0.2 µl of GoTaq DNA Polymerase (Promega) or 10 µl of qPCR master mix (Promega) and 6 µl of DEPC treated H_2O with 1 µl of each primer (10 pmol/µl) were used. 2 µl of appropriately diluted cDNA was added as template. For the internal control 16S rRNA and rpoD 1:10000 and 1:10 dilutions were used, respectively. The reagents and the template was pipetted onto 96 well plate (Bio-Rad) and sealed with optical quality adhesive film (Bio-Rad) and spun down briefly. The plate was placed on the C1000 touch thermocycler and the following PCR program was used: 94°C for 3 min, 40 x (94°C for 10 s, 58°C for 30 s, 72°C for 30 s), 72°C for 10 min. A melting curve analysis was performed from 50°C leading to 95°C in steps of 0.5°C. Each sample was analyzed in triplicates and pooled cDNA with appropriate dilutions were used as standards to determine the efficiency of PCR. 16S rRNA or rpoD gene was used as a reference gene for normalization. The relative expression was determined using the $2^{-\Delta\Delta CT}$ method (Livak & Schmittgen, 2001).

4.15 5'RACE

5'RACE (Rapid Amplification of cDNA Ends) was used to determine the 5' nucleotide of the RNA which represents the transcription start site of the transcript. 5'RACE analysis was performed according to the published protocol (Wagner & Vogel, 2005). RNA was isolated as described above. 12 µg of RNA was brought to the final volume of 86.5 µl with DEPC treated H_2O. To this 10 µl of 10 x Tobacco Acid Pyrophosphatase buffer (for Tobacco Acid Pyrophosphatase enzyme) or 10 µl of NEB buffer 2 (for RppH enzyme), 0.5 µl of RNase Inhibitor (SUPERase IN, Ambion) were added and the contents were spilt equally into two tubes. To one tube, 1 µl of Tobacco Acid Pyrophosphatase (10U/µl) (Epicentre Biotechnologies) or 2 µl of RNA 5' pyrophosphohydrolase (5U/µl) (RppH, NEB) was added.

The samples were incubated at 37°C for 30 min. After incubation, 5 µl of RNA Adapter (100 pmol/µl) and 100 µl of H_2O was added. Enzyme was removed by phenol:chloroform:isoamylalcohol (25:24:1) extraction followed by ethanol precipitation. The RNA pellet was resuspended in 12 µl H_2O, heated to 90°C for 5 min and placed on ice for 5 min. For adapter ligation, 2 µl of 10x RNA ligation buffer (NEB), 2 µl of 10 mM ATP stock (NEB), 2 µl DMSO, 1.8 µl T4 RNA ligase (20U) (NEB) pre-mixed with 0.2 µl RNase inhibitor was added and the samples were incubated at 17°C overnight. After incubation, 4 µl of Random hexamers (50 ng/µl) and 128 µl of H_2O were added. Enzyme and buffer was removed by phenol:chloroform:isoamylalcohol (25:24:1) extraction followed by ethanol precipitation. The RNA pellet was dissolved in 20 µl of DEPC treated H_2O and 10 µl of RNA was used for cDNA synthesis as described. For PCR amplification, Platinum Taq DNA Polymerase (Thermo Fisher Scientific) was used according to the manufacturer's instructions with adapter specific and gene specific primer and 2 µl of cDNA as template in a 50 µl reaction. 25 µl of PCR products were run on 2% agarose gel. The bands indicated were purified, restriction digested, ligated and cloned in pUC12 and sequenced.

5. References

Ali Azam, T., A. Iwata, A. Nishimura, S. Ueda & A. Ishihama, (1999) Growth phase-dependent variation in protein composition of the Escherichia coli nucleoid. *J Bacteriol* **181**: 6361-6370.

Ali, S. S., J. C. Whitney, J. Stevenson, H. Robinson, P. L. Howell & W. W. Navarre, (2013) Structural insights into the regulation of foreign genes in Salmonella by the Hha/H-NS complex. *J Biol Chem* **288**: 13356-13369.

Amit, R., A. B. Oppenheim & J. Stavans, (2003) Increased bending rigidity of single DNA molecules by H-NS, a temperature and osmolarity sensor. *Biophys J* **84**: 2467-2473.

Arold, S. T., P. G. Leonard, G. N. Parkinson & J. E. Ladbury, (2010) H-NS forms a superhelical protein scaffold for DNA condensation. *Proc Natl Acad Sci U S A* **107**: 15728-15732.

Atlung, T. & L. Brondsted, (1994) Role of the transcriptional activator AppY in regulation of the cyx appA operon of Escherichia coli by anaerobiosis, phosphate starvation, and growth phase. *J Bacteriol* **176**: 5414-5422.

Atlung, T., S. Sund, K. Olesen & L. Brondsted, (1996) The histone-like protein H-NS acts as a transcriptional repressor for expression of the anaerobic and growth phase activator AppY of Escherichia coli. *J Bacteriol* **178**: 3418-3425.

Ausubel, F. M., R. Brent, R. E. Kingston, D. D. Moore, J. G. Seidman, A. J. Smith & K. Struhl, (2005) *Current Protocols in Molcular Biology*. John Wiley & Sons, Inc.

Baba, T., T. Ara, M. Hasegawa, Y. Takai, Y. Okumura, M. Baba, K. A. Datsenko, M. Tomita, B. L. Wanner & H. Mori, (2006) Construction of Escherichia coli K-12 in-frame, single-gene knockout mutants: the Keio collection. *Mol Syst Biol* **2**: 2006 0008.

Badaut, C., R. Williams, V. Arluison, E. Bouffartigues, B. Robert, H. Buc & S. Rimsky, (2002) The degree of oligomerization of the H-NS nucleoid structuring protein is related to specific binding to DNA. *J Biol Chem* **277**: 41657-41666.

Badrinarayanan, A., T. B. Le & M. T. Laub, (2015) Bacterial chromosome organization and segregation. *Annu Rev Cell Dev Biol* **31**: 171-199.

Balsalobre, C., J. Johansson, B. E. Uhlin, A. Juarez & F. J. Munoa, (1999) Alterations in protein expression caused by the hha mutation in Escherichia coli: influence of growth medium osmolarity. *J Bacteriol* **181**: 3018-3024.

Banos, R. C., A. Vivero, S. Aznar, J. Garcia, M. Pons, C. Madrid & A. Juarez, (2009) Differential regulation of horizontally acquired and core genome genes by the bacterial modulator H-NS. *PLoS Genet* **5**: e1000513.

Bouchara, D., (2009) Zur Transkriptionsregulation durch den globalen Regulator H-NS in Escherichia coli. *Institute for Genetics, University of Cologne*.

Bouffartigues, E., M. Buckle, C. Badaut, A. Travers & S. Rimsky, (2007) H-NS cooperative binding to high-affinity sites in a regulatory element results in transcriptional silencing. *Nat Struct Mol Biol* **14**: 441-448.

Brandi, A., C. L. Pon & C. O. Gualerzi, (1994) Interaction of the main cold shock protein CS7.4 (CspA) of Escherichia coli with the promoter region of hns. *Biochimie* **76**: 1090-1098.

Breddermann, H. & K. Schnetz, (2016) Correlation of Antagonistic Regulation of leuO Transcription with the Cellular Levels of BglJ-RcsB and LeuO in Escherichia coli. *Front Cell Infect Microbiol* **6**: 106.

Brescia, C. C., M. K. Kaw & D. D. Sledjeski, (2004) The DNA binding protein H-NS binds to and alters the stability of RNA in vitro and in vivo. *J Mol Biol* **339**: 505-514.

Brondsted, L. & T. Atlung, (1996) Effect of growth conditions on expression of the acid phosphatase (cyx-appA) operon and the appY gene, which encodes a transcriptional activator of Escherichia coli. *J Bacteriol* **178**: 1556-1564.

Brosius, J. & A. Holy, (1984) Regulation of ribosomal RNA promoters with a synthetic lac operator. *Proc Natl Acad Sci U S A* **81**: 6929-6933.

Brühl, N., (2011) Transcription and Repression by H-NS (Laboratory Module). *Institute for Genetics, University of Cologne*.

Bryant, J. A., L. E. Sellars, S. J. Busby & D. J. Lee, (2014) Chromosome position effects on gene expression in Escherichia coli K-12. *Nucleic Acids Res* **42**: 11383-11392.

Caramel, A. & K. Schnetz, (1998) Lac and lambda repressors relieve silencing of the Escherichia coli bgl promoter. Activation by alteration of a repressing nucleoprotein complex. *J Mol Biol* **284**: 875-883.

Chandraprakash, D. & A. S. Seshasayee, (2014) Inhibition of factor-dependent transcription termination in Escherichia coli might relieve xenogene silencing by abrogating H-NS-DNA interactions in vivo. *J Biosci* **39**: 53-61.

Chenchik, A. A., R. Bibilashvili, A. D. Mirzabekov & V. V. Shik, (1982) [Contacts of Escherichia coli RNA polymerase subunits with nucleotides of lacUV5 promoter]. *Mol Biol (Mosk)* **16**: 35-46.

Cherepanov, P. P. & W. Wackernagel, (1995) Gene disruption in *Escherichia coli*: TcR and KmR cassettes with the option of Flp-catalyzed excision of the antibiotic-resistance determinant. *Gene* **158**: 9-14.

Chong, S., C. Chen, H. Ge & X. S. Xie, (2014) Mechanism of transcriptional bursting in bacteria. *Cell* **158**: 314-326.

Coombes, B. K., M. E. Wickham, M. J. Lowden, N. F. Brown & B. B. Finlay, (2005) Negative regulation of Salmonella pathogenicity island 2 is required for contextual control of virulence during typhoid. *Proc Natl Acad Sci U S A* **102**: 17460-17465.

Dame, R. T., M. S. Luijsterburg, E. Krin, P. N. Bertin, R. Wagner & G. J. Wuite, (2005) DNA bridging: a property shared among H-NS-like proteins. *J Bacteriol* **187**: 1845-1848.

Dame, R. T., M. C. Noom & G. J. Wuite, (2006) Bacterial chromatin organization by H-NS protein unravelled using dual DNA manipulation. *Nature* **444**: 387-390.

Dame, R. T., C. Wyman & N. Goosen, (2000) H-NS mediated compaction of DNA visualised by atomic force microscopy. *Nucleic Acids Res* **28**: 3504-3510.

Dame, R. T., C. Wyman, R. Wurm, R. Wagner & N. Goosen, (2002) Structural basis for H-NS-mediated trapping of RNA polymerase in the open initiation complex at the rrnB P1. *J Biol Chem* **277**: 2146-2150.

Datsenko, K. A. & B. L. Wanner, (2000) One-step inactivation of chromosomal genes in Escherichia coli K-12 using PCR products. *Proc Natl Acad Sci U S A* **97**: 6640-6645.

Dattananda, C. S., K. Rajkumari & J. Gowrishankar, (1991) Multiple mechanisms contribute to osmotic inducibility of proU operon expression in Escherichia coli: demonstration of two osmoresponsive promoters and of a negative regulatory element within the first structural gene. *J Bacteriol* **173**: 7481-7490.

Deng, S., R. A. Stein & N. P. Higgins, (2005) Organization of supercoil domains and their reorganization by transcription. *Mol Microbiol* **57**: 1511-1521.

Desai, S. K., R. S. Winardhi, S. Periasamy, M. M. Dykas, Y. Jie & L. J. Kenney, (2016) The horizontally-acquired response regulator SsrB drives a Salmonella lifestyle switch by relieving biofilm silencing. *Elife* **5**.

Di Martino, M. L., M. Falconi, G. Micheli, B. Colonna & G. Prosseda, (2016) The Multifaceted Activity of the VirF Regulatory Protein in the Shigella Lifestyle. *Front Mol Biosci* **3**: 61.

Diederich, L., L. J. Rasmussen & W. Messer, (1992) New cloning vectors for integration in the lambda attachment site *attB* of the *Escherichia coli* chromosome. *Plasmid* **28**: 14-24.

Dillon, S. C. & C. J. Dorman, (2010) Bacterial nucleoid-associated proteins, nucleoid structure and gene expression. *Nat Rev Microbiol* **8**: 185-195.

Dole, S., Y. Klingen, V. Nagarajavel & K. Schnetz, (2004a) The protease Lon and the RNA-binding protein Hfq reduce silencing of the Escherichia coli bgl operon by H-NS. *J Bacteriol* **186**: 2708-2716.

Dole, S., S. Kuhn & K. Schnetz, (2002) Post-transcriptional enhancement of Escherichia coli bgl operon silencing by limitation of BglG-mediated antitermination at low transcription rates. *Mol Microbiol* **43**: 217-226.

Dole, S., V. Nagarajavel & K. Schnetz, (2004b) The histone-like nucleoid structuring protein H-NS represses the Escherichia coli bgl operon downstream of the promoter. *Mol Microbiol* **52**: 589-600.

Dorman, C. J., (2004) H-NS: a universal regulator for a dynamic genome. *Nat Rev Microbiol* **2**: 391-400.

Dorman, C. J., (2014a) Function of nucleoid-associated proteins in chromosome structuring and transcriptional regulation. *J Mol Microbiol Biotechnol* **24**: 316-331.

Dorman, C. J., (2014b) H-NS-like nucleoid-associated proteins, mobile genetic elements and horizontal gene transfer in bacteria. *Plasmid* **75C**: 1-11.

Epshtein, V., F. Toulme, A. R. Rahmouni, S. Borukhov & E. Nudler, (2003) Transcription through the roadblocks: the role of RNA polymerase cooperation. *EMBO J* **22**: 4719-4727.

Esposito, D., A. Petrovic, R. Harris, S. Ono, J. F. Eccleston, A. Mbabaali, I. Haq, C. F. Higgins, J. C. Hinton, P. C. Driscoll & J. E. Ladbury, (2002) H-NS oligomerization domain structure reveals the mechanism for high order self-association of the intact protein. *J Mol Biol* **324**: 841-850.

Falconi, M., A. Brandi, A. La Teana, C. O. Gualerzi & C. L. Pon, (1996) Antagonistic involvement of FIS and H-NS proteins in the transcriptional control of hns expression. *Mol Microbiol* **19**: 965-975.

Falconi, M., M. T. Gualtieri, A. La Teana, M. A. Losso & C. L. Pon, (1988) Proteins from the prokaryotic nucleoid: primary and quaternary structure of the 15-kD Escherichia coli DNA binding protein H-NS. *Mol Microbiol* **2**: 323-329.

Falconi, M., N. P. Higgins, R. Spurio, C. L. Pon & C. O. Gualerzi, (1993) Expression of the gene encoding the major bacterial nucleoid protein H-NS is subject to transcriptional auto-repression. *Mol Microbiol* **10**: 273-282.

Forns, N., A. Juarez & C. Madrid, (2005) Osmoregulation of the HtrA (DegP) protease of Escherichia coli: an Hha-H-NS complex represses HtrA expression at low osmolarity. *FEMS Microbiol Lett* **251**: 75-80.

Free, A. & C. J. Dorman, (1995) Coupling of Escherichia coli hns mRNA levels to DNA synthesis by autoregulation: implications for growth phase control. *Mol Microbiol* **18**: 101-113.

Gao, X., T. Zou, Z. Mu, B. Qin, J. Yang, S. Waltersperger, M. Wang, S. Cui & Q. Jin, (2013) Structural insights into VirB-DNA complexes reveal mechanism of transcriptional activation of virulence genes. *Nucleic Acids Res* **41**: 10529-10541.

Gordon, B. R., Y. Li, A. Cote, M. T. Weirauch, P. Ding, T. R. Hughes, W. W. Navarre, B. Xia & J. Liu, (2011) Structural basis for recognition of AT-rich DNA by unrelated xenogeneic silencing proteins. *Proc Natl Acad Sci U S A* **108**: 10690-10695.

Gowrishankar, J., (1985) Identification of osmoresponsive genes in Escherichia coli: evidence for participation of potassium and proline transport systems in osmoregulation. *J Bacteriol* **164**: 434-445.

Gowrishankar, J. & D. Manna, (1996) How is osmotic regulation of transcription of the Escherichia coli proU operon achieved? A review and a model. *Genetica* **97**: 363-378.

Grainger, D. C., (2016) Structure and function of bacterial H-NS protein. *Biochem Soc Trans* **44**: 1561-1569.

Grainger, D. C., M. D. Goldberg, D. J. Lee & S. J. Busby, (2008) Selective repression by Fis and H-NS at the Escherichia coli dps promoter. *Mol Microbiol* **68**: 1366-1377.

Grainger, D. C., D. Hurd, M. D. Goldberg & S. J. Busby, (2006) Association of nucleoid proteins with coding and non-coding segments of the Escherichia coli genome. *Nucleic Acids Res* **34**: 4642-4652.

Guyer, M. S., R. R. Reed, J. A. Steitz & K. B. Low, (1981) Identification of a sex-factor-affinity site in E. coli as gamma delta. *Cold Spring Harb Symp Quant Biol* **45 Pt 1**: 135-140.

Guzman, L. M., D. Belin, M. J. Carson & J. Beckwith, (1995) Tight regulation, modulation, and high-level expression by vectors containing the arabinose PBAD promoter. *J Bacteriol* **177**: 4121-4130.

Hardy, C. D. & N. R. Cozzarelli, (2005) A genetic selection for supercoiling mutants of Escherichia coli reveals proteins implicated in chromosome structure. *Mol Microbiol* **57**: 1636-1652.

Helgesen, E., S. Fossum-Raunehaug & K. Skarstad, (2016) Lack of the H-NS Protein Results in Extended and Aberrantly Positioned DNA during Chromosome Replication and Segregation in Escherichia coli. *J Bacteriol* **198**: 1305-1316.

Hommais, F., E. Krin, C. Laurent-Winter, O. Soutourina, A. Malpertuy, J. P. Le Caer, A. Danchin & P. Bertin, (2001) Large-scale monitoring of pleiotropic regulation of gene expression by the prokaryotic nucleoid-associated protein, H-NS. *Mol Microbiol* **40**: 20-36.

Hsieh, Y. J. & B. L. Wanner, (2010) Global regulation by the seven-component Pi signaling system. *Curr Opin Microbiol* **13**: 198-203.

Jin, D. J., R. R. Burgess, J. P. Richardson & C. A. Gross, (1992) Termination efficiency at rho-dependent terminators depends on kinetic coupling between RNA polymerase and rho. *Proc Natl Acad Sci U S A* **89**: 1453-1457.

Jin, D. J. & C. A. Gross, (1991) RpoB8, a rifampicin-resistant termination-proficient RNA polymerase, has an increased Km for purine nucleotides during transcription elongation. *J Biol Chem* **266**: 14478-14485.

Jin, D. J., W. A. Walter & C. A. Gross, (1988) Characterization of the termination phenotypes of rifampicin-resistant mutants. *J Mol Biol* **202**: 245-253.

Johansson, J., S. Eriksson, B. Sonden, S. N. Wai & B. E. Uhlin, (2001) Heteromeric interactions among nucleoid-associated bacterial proteins: localization of StpA-stabilizing regions in H-NS of Escherichia coli. *J Bacteriol* **183**: 2343-2347.

Kahramanoglou, C., A. S. Seshasayee, A. I. Prieto, D. Ibberson, S. Schmidt, J. Zimmermann, V. Benes, G. M. Fraser & N. M. Luscombe, (2011) Direct and indirect effects of H-NS and Fis on global gene expression control in Escherichia coli. *Nucleic Acids Res* **39**: 2073-2091.

Kavalchuk, K., (2011) Osmoregulation of the proU operon at a post-transcriptional level in Escherichia coli (PhD Thesis). *Institute for Genetics, University of Cologne*.

Kavalchuk, K., S. Madhusudan & K. Schnetz, (2012) RNase III initiates rapid degradation of proU mRNA upon hypo-osmotic stress in Escherichia coli. *RNA Biol* **9**: 98-109.

Kogenaru, M. & S. J. Tans, (2014) An improved Escherichia coli strain to host gene regulatory networks involving both the AraC and LacI inducible transcription factors. *J Biol Eng* **8**: 2.

Kogoma, T., (1994) Escherichia coli RNA polymerase mutants that enhance or diminish the SOS response constitutively expressed in the absence of RNase HI activity. *J Bacteriol* **176**: 1521-1523.

Kotlajich, M. V., D. R. Hron, B. A. Boudreau, Z. Sun, Y. L. Lyubchenko & R. Landick, (2015) Bridged filaments of histone-like nucleoid structuring protein pause RNA polymerase and aid termination in bacteria. *Elife* **4**.

Kulaeva, O. I., F. K. Hsieh, H. W. Chang, D. S. Luse & V. M. Studitsky, (2013) Mechanism of transcription through a nucleosome by RNA polymerase II. *Biochim Biophys Acta* **1829**: 76-83.

Landick, R., J. T. Wade & D. C. Grainger, (2015) H-NS and RNA polymerase: a love-hate relationship? *Curr Opin Microbiol* **24**: 53-59.

Lang, B., N. Blot, E. Bouffartigues, M. Buckle, M. Geertz, C. O. Gualerzi, R. Mavathur, G. Muskhelishvili, C. L. Pon, S. Rimsky, S. Stella, M. M. Babu & A. Travers, (2007) High-affinity DNA binding sites for H-NS provide a molecular basis for selective silencing within proteobacterial genomes. *Nucleic Acids Res* **35**: 6330-6337.

Lee, N. & J. Carbon, (1977) Nucleotide sequence of the 5' end of araBAD operon messenger RNA in Escherichia coli B/r. *Proc Natl Acad Sci U S A* **74**: 49-53.

Levine, J. A., A. M. Hansen, J. M. Michalski, T. H. Hazen, D. A. Rasko & J. B. Kaper, (2014) H-NST induces LEE expression and the formation of attaching and effacing lesions in enterohemorrhagic Escherichia coli. *PLoS One* **9**: e86618.

Lim, C. J., Y. R. Whang, L. J. Kenney & J. Yan, (2012) Gene silencing H-NS paralogue StpA forms a rigid protein filament along DNA that blocks DNA accessibility. *Nucleic Acids Res* **40**: 3316-3328.

Lithgow, J. K., F. Haider, I. S. Roberts & J. Green, (2007) Alternate SlyA and H-NS nucleoprotein complexes control hlyE expression in Escherichia coli K-12. *Mol Microbiol* **66**: 685-698.

Liu, L. F. & J. C. Wang, (1987) Supercoiling of the DNA template during transcription. *Proc Natl Acad Sci U S A* **84**: 7024-7027.

Liu, Q. & C. C. Richardson, (1993) Gene 5.5 protein of bacteriophage T7 inhibits the nucleoid protein H-NS of Escherichia coli. *Proc Natl Acad Sci U S A* **90**: 1761-1765.

Liu, Y., H. Chen, L. J. Kenney & J. Yan, (2010) A divalent switch drives H-NS/DNA-binding conformations between stiffening and bridging modes. *Genes Dev* **24**: 339-344.

Livak, K. J. & T. D. Schmittgen, (2001) Analysis of relative gene expression data using real-time quantitative PCR and the 2(-Delta Delta C(T)) Method. *Methods* **25**: 402-408.

Lucchini, S., G. Rowley, M. D. Goldberg, D. Hurd, M. Harrison & J. C. Hinton, (2006) H-NS mediates the silencing of laterally acquired genes in bacteria. *PLoS Pathog* **2**: e81.

Lucht, J. M. & E. Bremer, (1994) Adaptation of Escherichia coli to high osmolarity environments: osmoregulation of the high-affinity glycine betaine transport system proU. *FEMS Microbiol Rev* **14**: 3-20.

Lucht, J. M., P. Dersch, B. Kempf & E. Bremer, (1994) Interactions of the nucleoid-associated DNA-binding protein H-NS with the regulatory region of the osmotically controlled proU operon of Escherichia coli. *J Biol Chem* **269**: 6578-6578.

Luijsterburg, M. S., M. C. Noom, G. J. Wuite & R. T. Dame, (2006) The architectural role of nucleoid-associated proteins in the organization of bacterial chromatin: a molecular perspective. *J Struct Biol* **156**: 262-272.

Ma, J., L. Bai & M. D. Wang, (2013) Transcription under torsion. *Science* **340**: 1580-1583.

Madhusudan, S., A. Paukner, Y. Klingen & K. Schnetz, (2005) Independent regulation of H-NS-mediated silencing of the bgl operon at two levels: upstream by BglJ and LeuO and downstream by DnaKJ. *Microbiology* **151**: 3349-3359.

Mahadevan, S., A. E. Reynolds & A. Wright, (1987) Positive and negative regulation of the bgl operon in Escherichia coli. *J Bacteriol* **169**: 2570-2578.

Maurer, S., J. Fritz & G. Muskhelishvili, (2009) A systematic in vitro study of nucleoprotein complexes formed by bacterial nucleoid-associated proteins revealing novel types of DNA organization. *J Mol Biol* **387**: 1261-1276.

McDowell, J. C., J. W. Roberts, D. J. Jin & C. Gross, (1994) Determination of intrinsic transcription termination efficiency by RNA polymerase elongation rate. *Science* **266**: 822-825.

McGovern, V., N. P. Higgins, R. S. Chiz & A. Jaworski, (1994) H-NS over-expression induces an artificial stationary phase by silencing global transcription. *Biochimie* **76**: 1019-1029.

Meenakshi, S. & M. H. Munavar, (2015) Suppression of capsule expression in Deltalon strains of Escherichia coli by two novel rpoB mutations in concert with HNS: possible role for DNA bending at rcsA promoter. *Microbiologyopen* **4**: 712-729.

Megerle, J. A., G. Fritz, U. Gerland, K. Jung & J. O. Radler, (2008) Timing and dynamics of single cell gene expression in the arabinose utilization system. *Biophys J* **95**: 2103-2115.

Miller, J. H., (1972) *Experimets in Molecular Genetics* Cold Spring Harbor Laboratory Press.

Miller, J. H., (1992) *A short course in bacterial genetics : a laboratory manual and handbook for Escherichia coli and related bacteria*. Cold Spring Harbor Laboratory Press, Plainview, N.Y.

Muhr, M., (2008) Analysis of repression by binding of H-NS within the transcription unit (Bachelor Thesis). *Institute for Genetics, University of Cologne*.

Mukerji, M. & S. Mahadevan, (1997) Characterization of the negative elements involved in silencing the bgl operon of Escherichia coli: possible roles for DNA gyrase, H-NS, and CRP-cAMP in regulation. *Mol Microbiol* **24**: 617-627.

Muller, C. M., U. Dobrindt, G. Nagy, L. Emody, B. E. Uhlin & J. Hacker, (2006) Role of histone-like proteins H-NS and StpA in expression of virulence determinants of uropathogenic Escherichia coli. *J Bacteriol* **188**: 5428-5438.

Nagarajavel, V., S. Madhusudan, S. Dole, A. R. Rahmouni & K. Schnetz, (2007) Repression by binding of H-NS within the transcription unit. *J Biol Chem* **282**: 23622-23630.

Navarre, W. W., M. McClelland, S. J. Libby & F. C. Fang, (2007) Silencing of xenogeneic DNA by H-NS-facilitation of lateral gene transfer in bacteria by a defense system that recognizes foreign DNA. *Genes Dev* **21**: 1456-1471.

Neidhardt, F. C., P. L. Bloch & D. F. Smith, (1974) Culture medium for enterobacteria. *J Bacteriol* **119**: 736-747.

Nieto, J. M., C. Madrid, A. Prenafeta, E. Miquelay, C. Balsalobre, M. Carrascal & A. Juarez, (2000) Expression of the hemolysin operon in Escherichia coli is modulated by a nucleoid-protein complex that includes the proteins Hha and H-NS. *Mol Gen Genet* **263**: 349-358.

Noom, M. C., W. W. Navarre, T. Oshima, G. J. Wuite & R. T. Dame, (2007) H-NS promotes looped domain formation in the bacterial chromosome. *Curr Biol* **17**: R913-914.

Nudler, E. & M. E. Gottesman, (2002) Transcription termination and anti-termination in E. coli. *Genes Cells* **7**: 755-768.

Ohniwa, R. L., H. Muchaku, S. Saito, C. Wada & K. Morikawa, (2013) Atomic force microscopy analysis of the role of major DNA-binding proteins in organization of the nucleoid in Escherichia coli. *PLoS One* **8**: e72954.

Olekhnovich, I. N. & R. J. Kadner, (2006) Crucial roles of both flanking sequences in silencing of the hilA promoter in Salmonella enterica. *J Mol Biol* **357**: 373-386.

Ono, S., M. D. Goldberg, T. Olsson, D. Esposito, J. C. Hinton & J. E. Ladbury, (2005) H-NS is a part of a thermally controlled mechanism for bacterial gene regulation. *Biochem J* **391**: 203-213.

Overdier, D. G. & L. N. Csonka, (1992) A transcriptional silencer downstream of the promoter in the osmotically controlled proU operon of Salmonella typhimurium. *Proc Natl Acad Sci U S A* **89**: 3140-3144.

Pannen, D., M. Fabisch, L. Gausling & K. Schnetz, (2016) Interaction of the RcsB Response Regulator with Auxiliary Transcription Regulators in Escherichia coli. *J Biol Chem* **291**: 2357-2370.

Panyukov, V. V. & O. N. Ozoline, (2013) Promoters of Escherichia coli versus promoter islands: function and structure comparison. *PLoS One* **8**: e62601.

Parks, A. R., C. Court, L. Lubkowska, D. J. Jin, M. Kashlev & D. L. Court, (2014) Bacteriophage lambda N protein inhibits transcription slippage by Escherichia coli RNA polymerase. *Nucleic Acids Res* **42**: 5823-5829.

Peters, J. M., R. A. Mooney, J. A. Grass, E. D. Jessen, F. Tran & R. Landick, (2012) Rho and NusG suppress pervasive antisense transcription in Escherichia coli. *Genes Dev* **26**: 2621-2633.

Postow, L., C. D. Hardy, J. Arsuaga & N. R. Cozzarelli, (2004) Topological domain structure of the Escherichia coli chromosome. *Genes Dev* **18**: 1766-1779.

Prosseda, G., M. Falconi, M. Giangrossi, C. O. Gualerzi, G. Micheli & B. Colonna, (2004) The virF promoter in Shigella: more than just a curved DNA stretch. *Mol Microbiol* **51**: 523-537.

Ray-Soni, A., M. J. Bellecourt & R. Landick, (2016) Mechanisms of Bacterial Transcription Termination: All Good Things Must End. *Annu Rev Biochem* **85**: 319-347.

Rimsky, S., F. Zuber, M. Buckle & H. Buc, (2001) A molecular mechanism for the repression of transcription by the H-NS protein. *Mol Microbiol* **42**: 1311-1323.

Roberts, J. W., S. Shankar & J. J. Filter, (2008) RNA polymerase elongation factors. *Annu Rev Microbiol* **62**: 211-233.

Rosenberg, M., D. Court, H. Shimatake, C. Brady & D. L. Wulff, (1978) The relationship between function and DNA sequence in an intercistronic regulatory region in phage lambda. *Nature* **272**: 414-423.

Salscheider, S. L., A. Jahn & K. Schnetz, (2014) Transcriptional regulation by BglJ-RcsB, a pleiotropic heteromeric activator in Escherichia coli. *Nucleic Acids Res* **42**: 2999-3008.

Schmidt, A. J., D. A. Ryjenkov & M. Gomelsky, (2005) The ubiquitous protein domain EAL is a cyclic diguanylate-specific phosphodiesterase: enzymatically active and inactive EAL domains. *J Bacteriol* **187**: 4774-4781.

Schnetz, K., (1995) Silencing of Escherichia coli bgl promoter by flanking sequence elements. *EMBO J* **14**: 2545-2550.

Schnetz, K. & B. Rak, (1988) Regulation of the bgl operon of Escherichia coli by transcriptional antitermination. *EMBO J* **7**: 3271-3277.

Schnetz, K. & B. Rak, (1992) IS5: a mobile enhancer of transcription in Escherichia coli. *Proc Natl Acad Sci U S A* **89**: 1244-1248.

Schnetz, K., C. Toloczyki & B. Rak, (1987) Beta-glucoside (bgl) operon of Escherichia coli K-12: nucleotide sequence, genetic organization, and possible evolutionary relationship to regulatory components of two Bacillus subtilis genes. *J Bacteriol* **169**: 2579-2590.

Schnetz, K. & J. C. Wang, (1996) Silencing of the Escherichia coli bgl promoter: effects of template supercoiling and cell extracts on promoter activity in vitro. *Nucleic Acids Res* **24**: 2422-2428.

Sharma, V. K. & R. L. Zuerner, (2004) Role of hha and ler in transcriptional regulation of the esp operon of enterohemorrhagic Escherichia coli O157:H7. *J Bacteriol* **186**: 7290-7301.

Shimada, T., N. Fujita, M. Maeda & A. Ishihama, (2005) Systematic search for the Cra-binding promoters using genomic SELEX system. *Genes Cells* **10**: 907-918.

Shin, M., A. C. Lagda, J. W. Lee, A. Bhat, J. H. Rhee, J. S. Kim, K. Takeyasu & H. E. Choy, (2012) Gene silencing by H-NS from distal DNA site. *Mol Microbiol* **86**: 707-719.

Shin, M., M. Song, J. H. Rhee, Y. Hong, Y. J. Kim, Y. J. Seok, K. S. Ha, S. H. Jung & H. E. Choy, (2005) DNA looping-mediated repression by histone-like protein H-NS: specific requirement of Esigma70 as a cofactor for looping. *Genes Dev* **19**: 2388-2398.

Siegele, D. A. & J. C. Hu, (1997) Gene expression from plasmids containing the araBAD promoter at subsaturating inducer concentrations represents mixed populations. *Proc Natl Acad Sci U S A* **94**: 8168-8172.

Silphaduang, U., M. Mascarenhas, M. Karmali & B. K. Coombes, (2007) Repression of intracellular virulence factors in Salmonella by the Hha and YdgT nucleoid-associated proteins. *J Bacteriol* **189**: 3669-3673.

Sinden, R. R., C. E. Pearson, V. N. Potaman & D. W. Ussery, (1998) DNA: structure and function. *Adv Gen Biol* **5A**: 1-141.

Singh, K., J. N. Milstein & W. W. Navarre, (2016) Xenogeneic Silencing and Its Impact on Bacterial Genomes. *Annu Rev Microbiol* **70**: 199-213.

Singh, S. S., N. Singh, R. P. Bonocora, D. M. Fitzgerald, J. T. Wade & D. C. Grainger, (2014) Widespread suppression of intragenic transcription initiation by H-NS. *Genes Dev* **28**: 214-219.

Sonnenfield, J. M., C. M. Burns, C. F. Higgins & J. C. Hinton, (2001) The nucleoid-associated protein StpA binds curved DNA, has a greater DNA-binding affinity than H-NS and is present in significant levels in hns mutants. *Biochimie* **83**: 243-249.

Spurio, R., M. Durrenberger, M. Falconi, A. La Teana, C. L. Pon & C. O. Gualerzi, (1992) Lethal overproduction of the Escherichia coli nucleoid protein H-NS: ultramicroscopic and molecular autopsy. *Mol Gen Genet* **231**: 201-211.

Srinivasan, R., D. Chandraprakash, R. Krishnamurthi, P. Singh, V. F. Scolari, S. Krishna & A. S. Seshasayee, (2013) Genomic analysis reveals epistatic silencing of "expensive" genes in Escherichia coli K-12. *Mol Biosyst* **9**: 2021-2033.

Stoebel, D. M., A. Free & C. J. Dorman, (2008) Anti-silencing: overcoming H-NS-mediated repression of transcription in Gram-negative enteric bacteria. *Microbiology* **154**: 2533-2545.

Stratmann, T., U. Pul, R. Wurm, R. Wagner & K. Schnetz, (2012) RcsB-BglJ activates the Escherichia coli leuO gene, encoding an H-NS antagonist and pleiotropic regulator of virulence determinants. *Mol Microbiol* **83**: 1109-1123.

Sundriyal, A., C. Massa, D. Samoray, F. Zehender, T. Sharpe, U. Jenal & T. Schirmer, (2014) Inherent regulation of EAL domain-catalyzed hydrolysis of second messenger cyclic di-GMP. *J Biol Chem* **289**: 6978-6990.

Tendeng, C. & P. N. Bertin, (2003) H-NS in Gram-negative bacteria: a family of multifaceted proteins. *Trends Microbiol* **11**: 511-518.

Teves, S. S. & S. Henikoff, (2014) Transcription-generated torsional stress destabilizes nucleosomes. *Nat Struct Mol Biol* **21**: 88-94.

Thacker, V. V., K. Bromek, B. Meijer, J. Kotar, B. Sclavi, M. C. Lagomarsino, U. F. Keyser & P. Cicuta, (2014) Bacterial nucleoid structure probed by active drag and resistive pulse sensing. *Integr Biol (Camb)* **6**: 184-191.

Thiel, A., M. Valens, I. Vallet-Gely, O. Espeli & F. Boccard, (2012) Long-range chromosome organization in E. coli: a site-specific system isolates the Ter macrodomain. *PLoS Genet* **8**: e1002672.

Tonthat, N. K., S. T. Arold, B. F. Pickering, M. W. Van Dyke, S. Liang, Y. Lu, T. K. Beuria, W. Margolin & M. A. Schumacher, (2011) Molecular mechanism by which the nucleoid occlusion factor, SlmA, keeps cytokinesis in check. *EMBO J* **30**: 154-164.

Trachman, J. D. & M. Yasmin, (2004) Thermo-osmoregulation of heat-labile enterotoxin expression by Escherichia coli. *Curr Microbiol* **49**: 353-360.

Trautinger, B. W. & R. G. Lloyd, (2002) Modulation of DNA repair by mutations flanking the DNA channel through RNA polymerase. *EMBO J* **21**: 6944-6953.

Travers, A. & G. Muskhelishvili, (2005) DNA supercoiling - a global transcriptional regulator for enterobacterial growth? *Nat Rev Microbiol* **3**: 157-169.

Troxell, B., M. L. Sikes, R. C. Fink, A. Vazquez-Torres, J. Jones-Carson & H. M. Hassan, (2011) Fur negatively regulates hns and is required for the expression of HilA and virulence in Salmonella enterica serovar Typhimurium. *J Bacteriol* **193**: 497-505.

Ueda, T., H. Takahashi, E. Uyar, S. Ishikawa, N. Ogasawara & T. Oshima, (2013) Functions of the Hha and YdgT proteins in transcriptional silencing by the nucleoid proteins, H-NS and StpA, in Escherichia coli. *DNA Res* **20**: 263-271.

Ueguchi, C. & T. Mizuno, (1993) The Escherichia coli nucleoid protein H-NS functions directly as a transcriptional repressor. *EMBO J* **12**: 1039-1046.

Uyar, E., K. Kurokawa, M. Yoshimura, S. Ishikawa, N. Ogasawara & T. Oshima, (2009) Differential binding profiles of StpA in wild-type and h-ns mutant cells: a comparative analysis of cooperative partners by chromatin immunoprecipitation-microarray analysis. *J Bacteriol* **191**: 2388-2391.

Valens, M., S. Penaud, M. Rossignol, F. Cornet & F. Boccard, (2004) Macrodomain organization of the Escherichia coli chromosome. *EMBO J* **23**: 4330-4341.

van der Valk, R. A., J. Vreede, L. Qin, G. F. Moolenaar, A. Hofmann, N. Goosen & R. T. Dame, (2017) Mechanism of environmentally driven conformational changes that modulate H-NS DNA-bridging activity. *Elife* **6**.

Venkatesh, G. R., F. C. Kembou Koungni, A. Paukner, T. Stratmann, B. Blissenbach & K. Schnetz, (2010) BglJ-RcsB heterodimers relieve repression of the Escherichia coli *bgl* operon by H-NS. *The Journal of Bacteriology* **192**: 6456–6464.

Vieira, J. & J. Messing, (1987) Production of single-stranded Plasmid DNA. *Methods Enzymol.* **153**: 3-11.

Vivero, A., R. C. Banos, J. F. Mariscotti, J. C. Oliveros, F. Garcia-del Portillo, A. Juarez & C. Madrid, (2008) Modulation of horizontally acquired genes by the Hha-YdgT proteins in Salmonella enterica serovar Typhimurium. *J Bacteriol* **190**: 1152-1156.

Vora, T., A. K. Hottes & S. Tavazoie, (2009) Protein occupancy landscape of a bacterial genome. *Mol Cell* **35**: 247-253.

Wagner, E. G. H. & J. Vogel, (2005) *Approaches to identify novel non-messenger RNAs in bacteria and to investigate their biological functions: functional analysis of identified non-mRNAs*. In Handbook of RNA Biochemistry. Hartmann, R.K., Bindereif, A., Schön, A., and Westhof, E. (eds). Weinheim: Wiley-VCH.

Walthers, D., Y. Li, Y. Liu, G. Anand, J. Yan & L. J. Kenney, (2011) Salmonella enterica response regulator SsrB relieves H-NS silencing by displacing H-NS bound in polymerization mode and directly activates transcription. *J Biol Chem* **286**: 1895-1902.

Wang, H., S. Yehoshua, S. S. Ali, W. W. Navarre & J. N. Milstein, (2014) A biomechanical mechanism for initiating DNA packaging. *Nucleic Acids Res* **42**: 11921-11927.

Wang, M. D., M. J. Schnitzer, H. Yin, R. Landick, J. Gelles & S. M. Block, (1998) Force and velocity measured for single molecules of RNA polymerase. *Science* **282**: 902-907.

Wang, W., G. W. Li, C. Chen, X. S. Xie & X. Zhuang, (2011) Chromosome organization by a nucleoid-associated protein in live bacteria. *Science* **333**: 1445-1449.

Will, W. R., W. W. Navarre & F. C. Fang, (2015) Integrated circuits: how transcriptional silencing and counter-silencing facilitate bacterial evolution. *Curr Opin Microbiol* **23C**: 8-13.

Williams, R. M., S. Rimsky & H. Buc, (1996) Probing the structure, function, and interactions of the Escherichia coli H-NS and StpA proteins by using dominant negative derivatives. *J Bacteriol* **178**: 4335-4343.

Williamson, H. S. & A. Free, (2005) A truncated H-NS-like protein from enteropathogenic Escherichia coli acts as an H-NS antagonist. *Mol Microbiol* **55**: 808-827.

Wilson, G. G., K. Y. Young, G. J. Edlin & W. Konigsberg, (1979) High-frequency generalised transduction by bacteriophage T4. *Nature* **280**: 80-82.

Winardhi, R. S., R. Gulvady, J. L. Mellies & J. Yan, (2014) Locus of Enterocyte Effacement-Encoded Regulator (Ler) of pathogenic Escherichia coli Competes Off Nucleoid Structuring Protein H-NS through Non-Cooperative DNA Binding. *J Biol Chem*.

Winardhi, R. S., J. Yan & L. J. Kenney, (2015) H-NS Regulates Gene Expression and Compacts the Nucleoid: Insights from Single-Molecule Experiments. *Biophys J* **109**: 1321-1329.

Wolf, T., W. Janzen, C. Blum & K. Schnetz, (2006) Differential dependence of StpA on H-NS in autoregulation of stpA and in regulation of bgl. *J Bacteriol* **188**: 6728-6738.

Yang, J., M. Tauschek, R. Strugnell & R. M. Robins-Browne, (2005) The H-NS protein represses transcription of the eltAB operon, which encodes heat-labile enterotoxin in enterotoxigenic Escherichia coli, by binding to regions downstream of the promoter. *Microbiology* **151**: 1199-1208.

Yanofsky, C. & V. Horn, (1981) Rifampin resistance mutations that alter the efficiency of transcription termination at the tryptophan operon attenuator. *J Bacteriol* **145**: 1334-1341.

Yarnell, W. S. & J. W. Roberts, (1999) Mechanism of intrinsic transcription termination and antitermination. *Science* **284**: 611-615.

Yilmaz, C., (2014) Transcriptional regulation of yahA and the effect of the cyclic-di-GMP phosphodiesterase YahA on the osmoregulation of proU (Bachelor thesis). *Institute for Genetics, University of Cologne*.

Yoshida, T., C. Ueguchi, H. Yamada & T. Mizuno, (1993) Function of the Escherichia coli nucleoid protein, H-NS: molecular analysis of a subset of proteins whose expression is enhanced in a hns deletion mutant. *Mol Gen Genet* **237**: 113-122.

Zarei, M., B. Sclavi & M. Cosentino Lagomarsino, (2013) Gene silencing and large-scale domain structure of the E. coli genome. *Mol Biosyst* **9**: 758-767.

Zhang, A. & M. Belfort, (1992) Nucleotide sequence of a newly-identified Escherichia coli gene, stpA, encoding an H-NS-like protein. *Nucleic Acids Res* **20**: 6735.

Zhang, A., S. Rimsky, M. E. Reaban, H. Buc & M. Belfort, (1996) Escherichia coli protein analogs StpA and H-NS: regulatory loops, similar and disparate effects on nucleic acid dynamics. *EMBO J* **15**: 1340-1349.

Zuker, M., (2003) Mfold web server for nucleic acid folding and hybridization prediction. *Nucleic Acids Res* **31**: 3406-3415.

Abbreviations

5' RACE	rapid amplification of cDNA 5' ends
amp	ampicillin
bp	base pairs
cam	chloramphenicol
DMSO	dimethyl sulfoxide
dNTP	deoxynucleoside triphosphate
DRE	downstream regulatory element
EDTA	ethylenediaminetetraacetic acid
FRT (FRT site)	Flp recombinase target site
IPTG	isopropyl-β-D-thiogalactopyranoside
kan	kanamycin
kDa	kilo dalton
nt	nucleotide
ORF	open reading frame
OD_X	optical density at X nm wavelength
PAGE	polyacrylamide gel electrophoresis
PCR	polymerase chain reaction
qRT-PCR	quantitative real-time polymerase chain reaction
rpm	revolutions per minute
spec	spectinomycin
tet	tetracycline
URE	upstream regulators element
wt	wild-type

Acknowledgement

Foremost, I would like to express my deepest gratitude to Prof. Dr. Karin Schnetz for her discerning guidance and support. I thank her for the insightful scientific discussions and constructive criticisms which molded my scientific temper. I am indebted to her for making me a better organized person and showing that even the best can still be made better.

I thank my thesis committee members Prof. Dr. Jürgen Dohmen and Prof. Dr. Jan Riemer for their valuable time.

I am eternally grateful to my mentor Prof. Hussain Munavar of Madurai Kamaraj University, for introducing me to the fascinating facet of molecular genetics through his thought provoking lectures which were instrumental in developing the passion for me to pursue *E. coli* genetics. I also thank him for sending *rpoB8* and *rpoB87* mutants used in this study.

I thank Prof. Irina Artsimovitch of Ohio University for kindly sending the *rpoB2* and *rpoB8* mutants used in this study.

I thank the International Graduate School for Development Health and Disease for funding. I thank Dr. Isabell Witt and Kathy Joergens for their help and support in making my stay in Germany comfortable and also for organizing various courses.

I thank all former and current Schnetz lab members for providing a great lab atmosphere. My special thanks to Derk, Hannes, Susann and Cihan for being very helpful and supportive throughout my PhD journey. I especially thank Susann for helping with purification of H-NS protein. I also thank Cihan for helping me out with ‘major computer problems’ which are usually a click away for him.

I would like to thank all other colleagues on the third floor of Genetics, for memorable times during Monday cakes, Carnival, Christmas party and Excursions.

I thank all my Indian friends in Cologne for providing me a home away from home filled with great fun. I specially thank Arun, Ruchika, Hemal, Venkatesh, Vimal, Ranu, Roshini, Gaurav, Kusum, Sravya, Udhaya and Arti for their help and support during my good and bad days.

I am grateful to Deepak who has been extremely helpful, understanding and always supporting and encouraging me in all my endeavours.

I am thankful to Srinivasan, Akshaya, Snehal, Vibhuti and Direndra for being great friends and for providing me regular dose of much needed encouragement and advice at the right time.

I would like to express the biggest thanks to my entire family for nurturing and encouraging my dream. I am truly indebted to them for bestowing me with undying love and support.

Saving the best for the last, I thank the wondorous *E. coli* for continuing to be a source of enigma and fascination.

Lebenslauf

Name:	Aathmaja Anandhi Rangarajan
Geburtsdatum:	03.06.1990
Geburtsort:	Arakkonam, Indien
Staatsangehörigkeit:	Indisch
Anschrift:	Am Sportpark Müngersdorf 1 50933 Köln
2004-2005	Gymnasium (Matrikulation), Tamil Nadu, Indien
2005-2007	Abitur (HSc), Tamil Nadu, Indien
2007-2010	Bachelor of Science (BSc), Madras University, Indien
2010-2012	Master of Science (MSc), Madurai Kamaraj University, Indien
seit July 2013	Doktorand an der Universität zu Köln Institut für Genetik, Abteilung für Bakteriengenetik Prof. Dr. Karin Schnetz

Aathmaja Anandhi Rangarajan

Erklärung

Ich versichere, dass ich die von mir abgegebene Dissertation selbstständig angefertigt habe, die benutzten Quellen und Hilfsmittel vollständig angegeben und die Stellen der Arbeit - einschließlich Tabellen, Karten und Abbildungen -, die anderen Werken im Wortlaut oder dem Sinn nach entnommen sind, in jedem Einzelfall als Entlehnung kenntlich gemacht habe; dass diese Dissertation noch keiner anderen Fakultät oder Universität zur Prüfung vorgelegen hat; dass sie - abgesehen von unten angegebenen Teilpublikationen - noch nicht veröffentlicht worden ist sowie, dass ich eine solche Veröffentlichung vor Abschluss des Promotionsverfahrens nicht vornehmen werde.
Die Bestimmungen der Promotionsordnung sind mir bekannt. Die von mir vorgelegte Dissertation ist von Prof. Dr. Karin Schnetz, Institut für Genetik, betreut worden.

Aathmaja Anandhi Rangarajan

Teilpublikation im Rahmen dieser Arbeit

Rangarajan, A. A. & K. Schnetz, (2018) Interference of transcription across H-NS binding sites and repression by H-NS. *Mol Microbiol* doi:10.1111/mmi.13926.